Midwest Pooled Fund Program
Fiscal Year FY2021
Research Project Number TPF-5(430) Supplement #17
NDOT Sponsoring Agency Code RPFP-21-CONC-3

DESIGN OF AN ADVANCED MASH TL-3 PORTABLE BARRIER

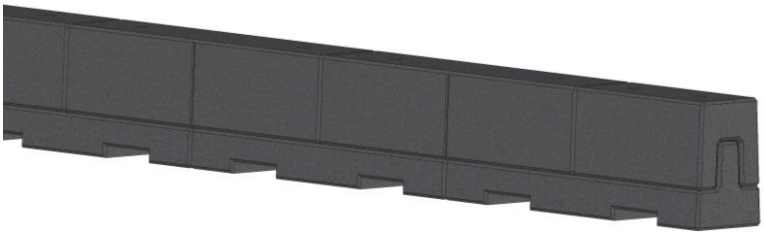

Submitted by

Robert W. Bielenberg, M.S.M.E.
Research Engineer

Ronald K. Faller, Ph.D., P.E.
Research Professor and MwRSF Director

Scott K. Rosenbaugh, M.S.C.E.
Research Engineer

Andrew E. Loken, Ph.D.
Research Assistant Professor

MIDWEST ROADSIDE SAFETY FACILITY
Nebraska Transportation Center
University of Nebraska-Lincoln

Main Office
Prem S. Paul Research Center at Whittier School
Suite 130, 2200 Vine Street
Lincoln, Nebraska 68583-0853
(402)472-0965

Outdoor Test Site
4630 N.W. 36th Street
Lincoln, Nebraska 68524

Submitted to

MIDWEST POOLED FUND PROGRAM
Nebraska Department of Transportation
1500 Nebraska Parkway
Lincoln, Nebraska 68502

MwRSF Research Report No. TRP-03-500-25

December 17, 2025

TECHNICAL REPORT DOCUMENTATION PAGE

1. Report No.	2. Government Accession No.	3. Recipient's Catalog No.
TRP-03-500-25		

4. Title And Subtitle	5. Report Date
Design of an Advanced MASH TL-3 Portable Barrier	December 17, 2025
	6. Performing Organization Code

7. Author(s)	8. Performing Organization Report No.
Bielenberg, R.W., Faller, R.K., Rosenbaugh, S.K., and Loken, A.E.	TRP-03-500-25

9. Performing Organization Name and Address	10. Work Unit No.
Midwest Roadside Safety Facility (MwRSF) Nebraska Transportation Center University of Nebraska-Lincoln Main Office: Prem S. Paul Research Center at Whittier School Suite 130, 2200 Vine Street Lincoln, Nebraska 68583-0853 Outdoor Test Site: 4630 N.W. 36th Street Lincoln, Nebraska 68524	**11. Contract** TPF-5(430) Supplement 17

12. Sponsoring Agency Name and Address	13. Type of Report and Period Covered
Midwest Pooled Fund Program Nebraska Department of Transportation 1500 Nebraska Parkway Lincoln, Nebraska 68502	Final Report: 2021-2025
	14. Sponsoring Agency Code RPFP – 21-CONC-3

15. Supplementary Notes

Prepared in cooperation with U.S. Department of Transportation, Federal Highway Administration

16. Abstract

This research effort focused on developing a new MASH Test Level 3 (TL-3) portable barrier system to address limitations of existing designs, including excessive dynamic deflection and compromised vehicle stability. The objective was to create a barrier that improved safety performance while simplifying installation, reducing reliance on connection hardware, and providing durability suitable for long-term service.

The project began with a review of concepts from an initial feasibility study and relevant design criteria. After criteria were established, project sponsors identified a near-vertical portable concrete barrier (PCB) composed of staggered, interlocking segments as the preferred option. This concept was selected for its ease of installation and potential to substantially reduce dynamic deflection during impacts.

An initial design was developed and evaluated using LS-DYNA simulation to estimate safety performance and guide refinements. Analyses examined reinforcement configurations, barrier segment length, and the effect of longitudinal gaps between segments. Results indicated that the interlocking PCB concept could meet MASH TL-3 requirements while reducing dynamic deflection below 24 in. An optimal reinforcement layout was identified to provide adequate strength, limit damage, and enhance durability. An 8-ft segment length was selected as a balance between deflection control and horizontal curvature needs, and end gaps up to 1 in were found to pose no safety concerns.

Additional refinements incorporated drainage features, lifting hardware, anchorage options, and improved constructability based on fabricator input. Full design details were completed, and prototype segments were fabricated. A follow-on study will conduct full-scale MASH Tests 3-10 and 3-11, with results to be reported separately.

17. Key Words	18. Distribution Statement
Highway Safety, Roadside Appurtenances, MASH, Portable Barrier, LS-DYNA	No restrictions. This document is available through the National Technical Information Service. 5285 Port Royal Road Springfield, VA 22161

19. Security Classification (of this report)	20. Security Classification (of this page)	21. No. of Pages	22. Price
Unclassified	Unclassified	108	

Form DOT F 1700.7 (8-72) Reproduction of completed page authorized

DISCLAIMER STATEMENT

This material is based upon work supported by the Federal Highway Administration, U.S. Department of Transportation and the Midwest Pooled Fund Program under TPF-5(430) Supplement #17. The contents of this report reflect the views and opinions of the authors who are responsible for the facts and the accuracy of the data presented herein. The contents do not necessarily reflect the official views or policies of the University of Nebraska-Lincoln, state highway departments participating in the Midwest Pooled Fund Program nor the Federal Highway Administration, U.S. Department of Transportation. This report does not constitute a standard, specification, or regulation. Trade or manufacturers' names, which may appear in this report, are cited only because they are considered essential to the objectives of the report. The United States (U.S.) government and the State of Nebraska do not endorse products or manufacturers.

ACKNOWLEDGEMENTS

The authors wish to acknowledge several sources that made a contribution to this project: (1) the Midwest Pooled Fund Program funded by the California Department of Transportation, Florida Department of Transportation, Georgia Department of Transportation, Hawaii Department of Transportation, Illinois Department of Transportation, Indiana Department of Transportation, Iowa Department of Transportation, Kansas Department of Transportation, Kentucky Department of Transportation, Minnesota Department of Transportation, Missouri Department of Transportation, Nebraska Department of Transportation, New Jersey Department of Transportation, North Carolina Department of Transportation, Ohio Department of Transportation, South Carolina Department of Transportation, South Dakota Department of Transportation, Utah Department of Transportation, Virginia Department of Transportation, Wisconsin Department of Transportation, and Wyoming Department of Transportation for sponsoring this project; and (2) the Holland Computing Center at the University of Nebraska, which receives support from the Nebraska Research Initiative, for providing computational resources.

The authors would also like to acknowledge Mark Wieser, Adam Wiser, and Wieser Concrete for their valuable feedback and expertise in the fabrication of the design prototypes.

Acknowledgement is also given to the following individuals who contributed to the completion of this research project.

Midwest Roadside Safety Facility
J.C. Holloway, M.S.C.E., Research Engineer & Assistant Director –Physical Testing Division
K.A. Lechtenberg, M.S.M.E., Research Engineer
C.S. Stolle, Ph.D., Research Associate Professor
J.S. Steelman, Ph.D., P.E., Associate Professor
B.J. Perry, M.E.M.E., Research Engineer
T.Y. Yosef, Ph.D., Research Assistant Professor
Q.A. Alomari, Ph.D., Research Assistant Professor
A.T. Russell, B.S.B.A., Testing and Maintenance Technician II
E.W. Krier, B.S., Former Engineering Testing Technician II
D.S. Charroin, Engineering Testing Technician II
R.M. Novak, Engineering Testing Technician II
T.C. Donahoo, Engineering Testing Technician I
J.T. Jones, Engineering Testing Technician II
E.L. Urbank, Research Communication Specialist
Z.Z. Jabr, Engineering Technician
J.J. Oliver, Solidworks Drafting Coordinator
Undergraduate and Graduate Research Assistants

California Department of Transportation
David Whitesel, P.E., Transportation Engineer
Thomas Mar, P.E., Transportation Engineer

Florida Department of Transportation
Derwood Sheppard, P.E., State Roadway Design Engineer
Richard Stepp, P.E., Senior Standard Plans Engineer
Rick Jenkins, P.E., State Standards Plans Engineer

Georgia Department of Transportation
Christopher Rudd, P.E., State Design Policy Engineer
Frank Flanders IV, P.E., Assistant State Design Policy Engineer
Doug Franks, P.E., Bridge Design Group Leader, Sr.

Hawaii Department of Transportation
Brent Ching, Structural Engineer
Keith Kalani, Structural Engineer
Kimberly Okamura, Engineer

Illinois Department of Transportation
Martha Brown, P.E., Safety Policy & Initiatives Engineer
Edgar Galofre, P.E., Safety Design Engineer
Kelli Erickson, Safety Design Evaluation Engineer

Indiana Department of Transportation
Katherine Smutzer, P.E., Standards Engineer
Andrew Blackburn, P.E., Engineer
Elizabeth Mouser, P.E., Standards & Policy Director

Iowa Department of Transportation
Daniel Harness, P.E., Transportation Engineer Specialist
Brian Smith, P.E., Methods Engineer
Mike Thiel, P.E., Transportation Engineer Specialist
Stuart Nielsen, P.E., Methods Engineer

Kansas Department of Transportation
Scott King, P.E., Road Design Bureau Chief
August Zuno, Engineer
Jackie Austin, Engineer
Jeff Sims, P.E., Road Design Leader

Kentucky Transportation Cabinet
Jason J. Siwula, P.E., Assistant State Highway Engineer
Jeff Jasper, Program Leader, University of Kentucky Transportation Center
Matthew Sipes, Transportation Engineer Branch Manager
Tim Layson, Transportation Engineer Director

Minnesota Department of Transportation
Khamsai Yang, P.E., State Design Standards Engineer
Michelle Moser, P.E., Assistant Design Standards Engineer
Braden Cyr, P.E., Bridge Engineer
Brian Tang, P.E., Assistant State Design Standards Engineer
Arielle Ehrlich, P.E., State Bridge Design Engineer

Missouri Department of Transportation
Gidget Koestner, P.E., Policy & Innovations Engineer
Kirby Woods, Jr., Roadside Design Engineer

Nebraska Department of Transportation
Jim Knott, P.E., Construction Engineer
Mick Syslo, P.E., Deputy Director – Operations
Mark Fischer, P.E., PMP, Research Program Manager
Austin White, P.E., Plan Quality & Standards Engineer
Brandie Neemann, P.E., Roadway Design Engineer
Fouad Jaber, Assistant State Bridge Engineer
Todd Hill, P.E., Assistant Roadway Design Engineer

New Jersey Department of Transportation
Hung Tang, P.E., Principal Engineer, Transportation
Joseph Warren, Assistant Engineer, Transportation
Xiaohua "Hannah" Cheng, P.E., Ph.D., Supervising Engineer, Structures
Binyamin Abu Haltam, Engineer
Sowatta Seng Eap, Engineer
Madhavi Andey, Principal Engineer
Vipul J. Shah, Engineer
Manar Alsharaa, Supervising Engineer

North Carolina Department of Transportation
Jordan Woodard, P.E., Design Development & Support Group Lead
Nicole Hackler, P.E., State Plans and Standards Engineer
Shawn Troy, P.E., State Traffic Safety Engineer

Ohio Department of Transportation
Don Fisher, P.E., Roadway Standards Engineer
Andrew Holloway, P.E., Transportation Engineer

South Carolina Department of Transportation
Mark H. Anthony, P.E., Letting Preparation Engineer
Jason Hall, P.E., Engineer

South Dakota Department of Transportation
Sam Weisgram, Engineering Manager
Drew Miller, Standards Engineer

Utah Department of Transportation
Shawn Debenham, Traffic and Safety Specialist
Kelly Ash, Traffic Operations Engineer
Clinton McCleery, Barrier & Attenuation Specialist

Virginia Department of Transportation
Charles Patterson, P.E., Standards/Special Design Section Manager
Andrew Zickler, P.E., Complex Bridge Design and ABC Support Program Manager
Bangfei Han, P.E., Senior Engineer
Junyi Meng, P.E., Senior Structural Engineer

Wisconsin Department of Transportation
Erik Emerson, P.E., Standards Development Engineer
Rodney Taylor, P.E., Roadway Design Standards Unit Supervisor

Wyoming Department of Transportation
William Wilson, P.E., Architectural and Highway Standards Engineer

Federal Highway Administration
David Mraz, Division Bridge Engineer, Nebraska Division Office

SI* (MODERN METRIC) CONVERSION FACTORS

APPROXIMATE CONVERSIONS TO SI UNITS

Symbol	When You Know	Multiply By	To Find	Symbol
		LENGTH		
in.	inches	25.4	millimeters	mm
ft	feet	0.305	meters	m
yd	yards	0.914	meters	m
mi	miles	1.61	kilometers	km
		AREA		
in^2	square inches	645.2	square millimeters	mm^2
ft^2	square feet	0.093	square meters	m^2
yd^2	square yard	0.836	square meters	m^2
ac	acres	0.405	hectares	ha
mi^2	square miles	2.59	square kilometers	km^2
		VOLUME		
fl oz	fluid ounces	29.57	milliliters	mL
gal	gallons	3.785	liters	L
ft^3	cubic feet	0.028	cubic meters	m^3
yd^3	cubic yards	0.765	cubic meters	m^3
		NOTE: volumes greater than 1,000 L shall be shown in m^3		
		MASS		
oz	ounces	28.35	grams	g
lb	pounds	0.454	kilograms	kg
T	short ton (2,000 lb)	0.907	megagrams (or “metric ton”)	Mg (or "t")
		TEMPERATURE (exact degrees)		
°F	Fahrenheit	5(F-32)/9 or (F-32)/1.8	Celsius	°C
		ILLUMINATION		
fc	foot-candles	10.76	lux	lx
fl	foot-Lamberts	3.426	candela per square meter	cd/m^2
		FORCE & PRESSURE or STRESS		
lbf	poundforce	4.45	newtons	N
lbf/in^2	poundforce per square inch	6.89	kilopascals	kPa

APPROXIMATE CONVERSIONS FROM SI UNITS

Symbol	When You Know	Multiply By	To Find	Symbol
		LENGTH		
mm	millimeters	0.039	inches	in.
m	meters	3.28	feet	ft
m	meters	1.09	yards	yd
km	kilometers	0.621	miles	mi
		AREA		
mm^2	square millimeters	0.0016	square inches	in^2
m^2	square meters	10.764	square feet	ft^2
m^2	square meters	1.195	square yard	yd^2
ha	hectares	2.47	acres	ac
km^2	square kilometers	0.386	square miles	mi^2
		VOLUME		
mL	milliliter	0.034	fluid ounces	fl oz
L	liters	0.264	gallons	gal
m^3	cubic meters	35.314	cubic feet	ft^3
m^3	cubic meters	1.307	cubic yards	yd^3
		MASS		
g	grams	0.035	ounces	oz
kg	kilograms	2.202	pounds	lb
Mg (or "t")	megagrams (or “metric ton”)	1.103	short ton (2,000 lb)	T
		TEMPERATURE (exact degrees)		
°C	Celsius	1.8C+32	Fahrenheit	°F
		ILLUMINATION		
lx	lux	0.0929	foot-candles	fc
cd/m^2	candela per square meter	0.2919	foot-Lamberts	fl
		FORCE & PRESSURE or STRESS		
N	newtons	0.225	poundforce	lbf
kPa	kilopascals	0.145	poundforce per square inch	lbf/in^2

*SI is the symbol for the International System of Units. Appropriate rounding should be made to comply with Section 4 of ASTM E380.

TABLE OF CONTENTS

LIST OF FIGURES

LIST OF TABLES

1 INTRODUCTION

The basic design of portable work-zone barriers has changed little in recent years. Most non-proprietary portable barrier systems on our nation's highways consist of safety-shape or single-slope barrier segments fabricated from reinforced concrete materials. These segments are attached by simple connections that allow the barriers to be easily installed or moved in work zones and for other portable barrier applications. Two general concerns exist with most current portable designs:

1. The segment connections allow high lateral barrier deflections upon vehicle impact, ranging from 19 in. to over 80 in. Where deflections must be limited, anchoring or pinning of the barrier segments into the pavement is required, which impedes installation and removal, exposes workers to traffic hazards, and causes pavement damage.

2. The sloped face of the barrier often allows vehicles to climb and roll as they impact the barrier, causing unstable behavior that can result in rollover.

Thus, an opportunity existed to develop a high-performance portable barrier system that met *Manual for Assessing Safety Hardware* (MASH) [1] safety criteria as well as address the deflection and stability concerns of most current portable barrier designs.

A high-performance portable barrier system with a vertical or near-vertical front face would reduce and/or eliminate the potential for vehicle instability, while a modified connection detail could reduce dynamic barrier deflections. In addition, a high-performance portable barrier could be made easier to transport and install as well as offer improved durability through modifications to the barrier geometry, materials, end-to-end connection, and structure.

1.1 Background

Portable barrier systems are used to redirect errant vehicles through a combination of inertial resistance, lateral friction loads, and tensile loads developed from the mass and friction of the barrier segments. While plastic, steel, and reinforced concrete barrier systems have been developed, state departments of transportation (DOTs) have primarily used portable concrete barriers (PCBs). PCB systems are typically comprised of safety-shape, reinforced concrete bodies with various end-to-end barrier connections to transfer load between the barrier segments. Currently, only a limited number of non-proprietary PCB designs have met MASH Test Level 3 (TL-3) requirements. These barriers include the non-proprietary Midwest Pooled Fund F-shape PCB, the New York PCB, New Jersey PCB, Oregon F-shape PCB, and the Texas X-bolt PCB. No non-proprietary steel or plastic portable barrier systems have been developed and evaluated to MASH TL-3.

A concern with many portable barriers is the large dynamic deflections associated with these systems. Table 1 shows free-standing portable barrier deflections for plastic, steel, and reinforced concrete barrier systems under National Cooperative Highway Research Program (NCHRP) Report 350 [2] and MASH TL-3 test criteria. Note that most systems have deflections over 5 ft and that deflections have increased significantly under MASH impact conditions. The current systems with reduced deflections utilize long, heavy barrier segments (20 ft to 30 ft long

concrete barrier segments), bolted connections such as the X-bolt connection, and/or some form of anchoring.

Table 1. Free-Standing Portable Barrier System Deflection Ranges

Test Criteria	Free-Standing Portable Barrier Dynamic Deflection Range (in.)		
	Concrete	Steel	Plastic
NCHRP 350 TL-3	27.0 – 148.8	37.4 – 157.5	107.87 – 271.7
MASH TL-3	19.0 – 84.6	66.5 – 77.4	114

Methods to reduce barrier deflections by pinning, staking, or otherwise tying the barrier to the deck, pavement, or soil have been developed in the past. However, this practice is labor intensive, expensive, and increases worker exposure. Other research has attempted to reduce deflections without anchoring barrier segments, but the effectiveness of this approach is limited without modifications to the barrier segment. Limiting free-standing barrier deflections would allow the barriers to be used more effectively when separating lanes of traffic or vehicles from the work zone because they would not require as much clear area behind the device. Thus, a new PCB design could provide reduced deflection without the use of anchors or other attachments to the road surface as well as allow for more economical and efficient installation of portable barriers.

Research has also shown that the sloped face of safety shape barriers causes increased vehicle instability and rollover, especially with regard to small passenger cars [3]. These studies have shown that 8.5 percent of safety-shape barrier accidents result in rollover, and that safety shape median barriers pose over twice the rollover rate of other median barriers. The increased rollover potential with these barrier shapes becomes critical because rollover accidents double the risk of incapacitating and fatal injuries [4].

Full-scale crash testing of safety-shape portable concrete barrier systems has indicated significant vehicle climb when these barriers are struck by light-truck test vehicles, as shown in Figure 1. Vertical face or near-vertical face, single-slope barriers have been shown to provide the largest reduction in vehicle rollover when compared with safety-shape barriers through both computer simulation and full-scale vehicle crash testing. However, the use of vertical shapes has not been widely implemented due to the concerns that vertical shapes might increase the lateral loads on impacting vehicles. A review of crash test data has demonstrated that vertical-shape barriers do tend to increase lateral vehicle accelerations, but the increased lateral decelerations do not exceed current safety guidelines for occupant risk [5]. These decelerations should be significantly less for portable barrier systems where moderate barrier deflection is allowed. Vertical-shape or near-vertical shape barriers would be easier to transport and store, thus increasing the functionality of the barrier.

Figure 1. Vehicle Climb, Roll, and Pitch Motions with Safety-Shape Portable Concrete Barrier

Other issues with available safety-shape PCBs include installation difficulties due to the design of the barrier connections and reduced durability. Many current barrier designs have connection hardware that extends from the barrier end, thus making vertical and/or horizontal placement impossible, which limits installation flexibility and efficiency. Additionally, barrier connections that are inefficient to install or require tools are not desired. Finally, the stepped region of safety-shape PCBs concentrates loads to the toes during impact loading and moving operations. However, barrier toes are difficult to reinforce, which promotes damage. A vertical face or near-vertical face, single-slope barrier could utilize more consistent barrier reinforcement and provide improved load distribution, which would limit damage and extend barrier life. Thus, a new portable barrier system could address barrier installation, connection, and durability issues and provide an improved user experience.

Portable barriers have traditionally been designed using reinforced concrete as the main structural material. Reinforced concrete is relatively inexpensive and easy to construct. In addition, its relatively high mass aids in vehicle redirection due to inertia transfer between the impacting vehicle and the barrier. However, there are some issues with reinforced concrete as a barrier material. First, reinforced concrete barriers tend to become damaged over time, which requires that barriers be replaced on average intervals of seven to ten years. While the mass of the barrier aids in vehicle redirection, the weight of the reinforced concrete sections can make them challenging to ship and move around in the work zone. Finally, the nature of reinforced concrete structures has limited the type of connection joints that can be utilized.

A research effort was conducted with the Wisconsin Department of Transportation (WisDOT) to develop a non-proprietary, high-performance portable barrier capable of meeting the MASH TL-3 safety requirements and with reduced free-standing barrier deflections and increased vehicle stability as compared to existing, widely used PCB systems [6]. This high-performance portable barrier could be widely implemented in most applications, and future research could be conducted to further reduce deflections from the baseline design. The potential for future anchoring of the barrier to further limit deflections was to be considered during the high-performance portable barrier development. Note that the barrier system was not limited to any certain material or shape, and the barrier system was focused on utilizing a practical length and weight such that typical construction equipment could be used for placement, repositioning, etc.

The WisDOT research project completed a review of existing portable barrier technology, developed design criteria that was ranked using an online survey, investigated alternative materials to reinforced concrete, and developed initial design concepts. A selection of the initial concepts from that study are shown in Figure 2 through Figure 5. While this preliminary research provided a strong start to the research and development of a new, MASH TL-3 portable barrier system,

further research was needed to analyze and develop preferred design concepts, fabricate prototypes, and conduct full-scale crash testing for evaluation of the barrier system to MASH TL-3 criteria.

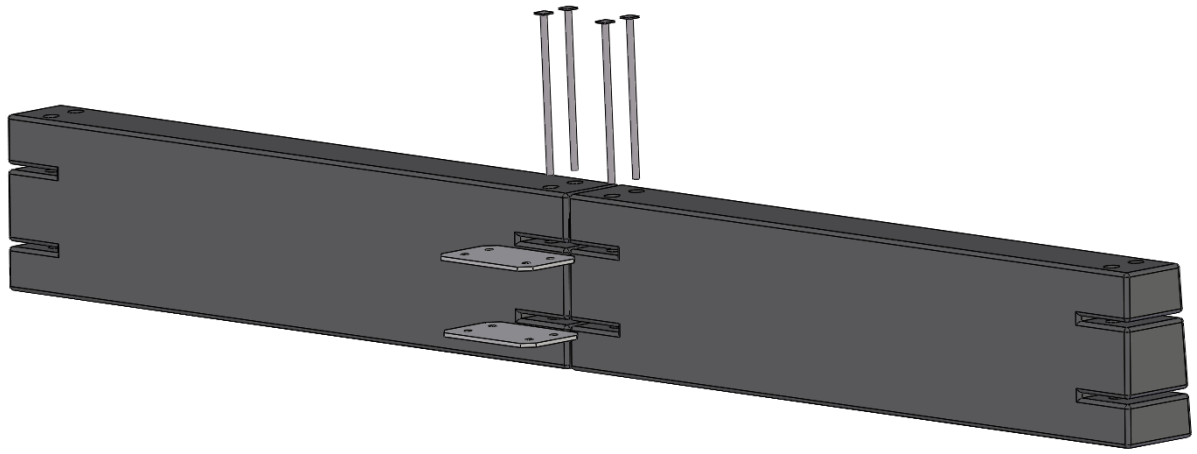

Figure 2. Near Vertical PCB with Pin and Plate Connection Concept

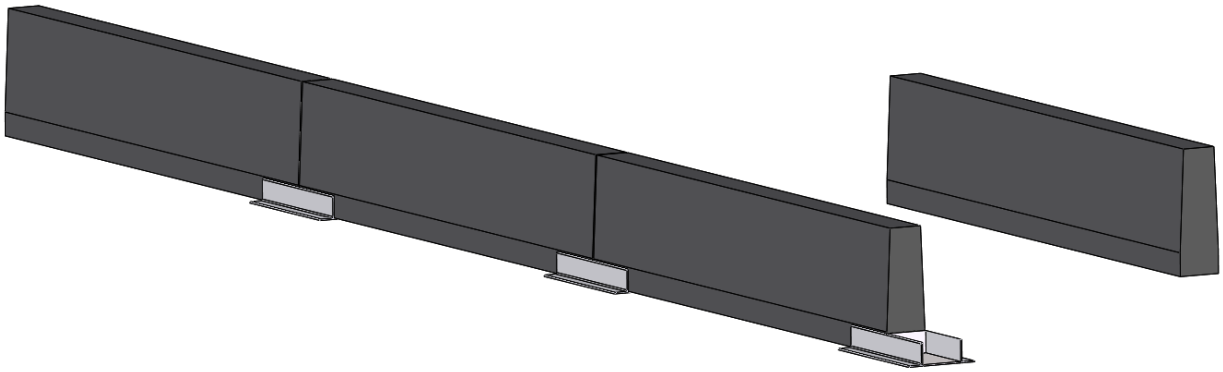

Figure 3. Near Vertical PCB with Drop-In Base Concept

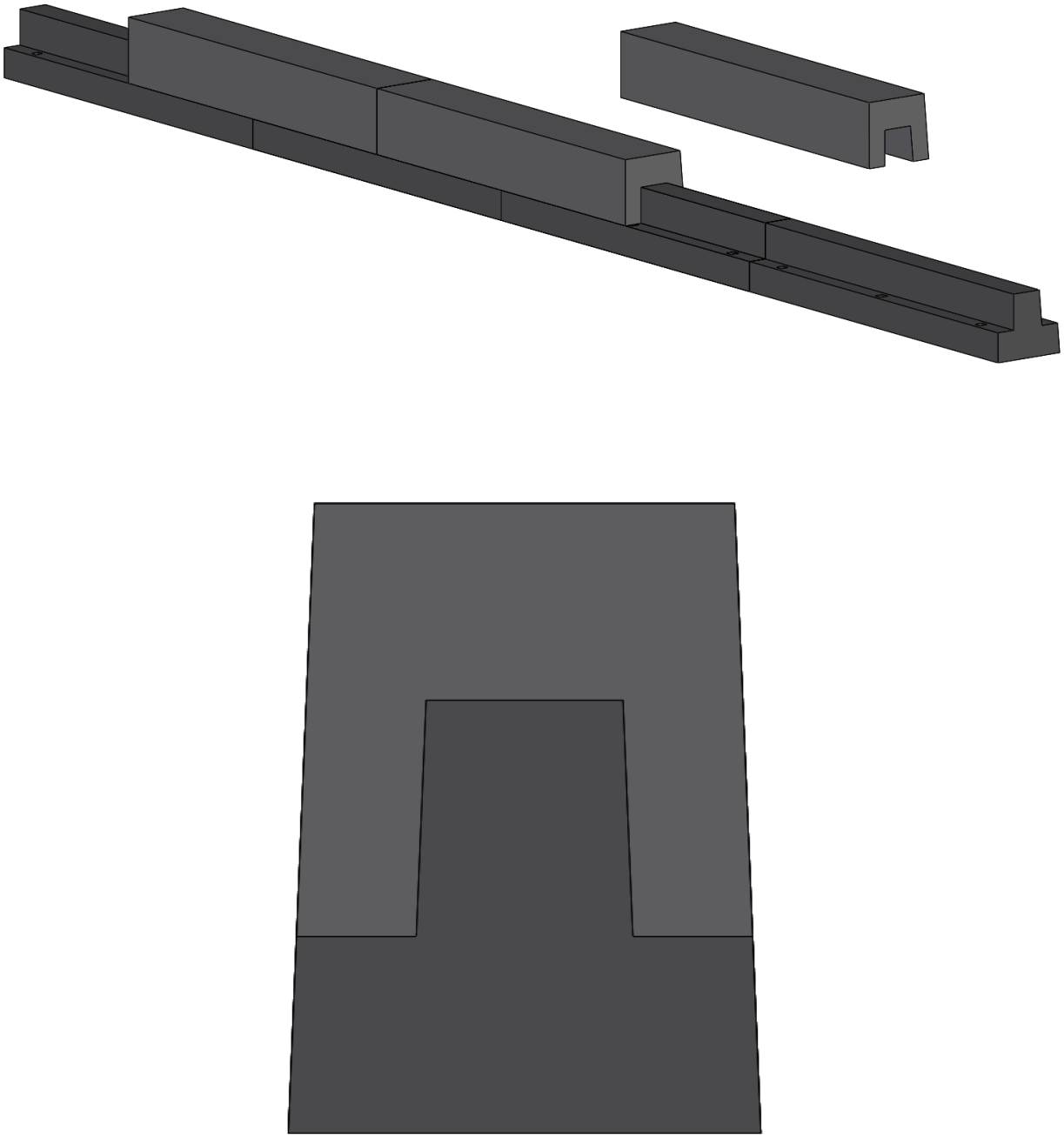

Figure 4. Staggered, Interlocking Near Vertical PCB Concept

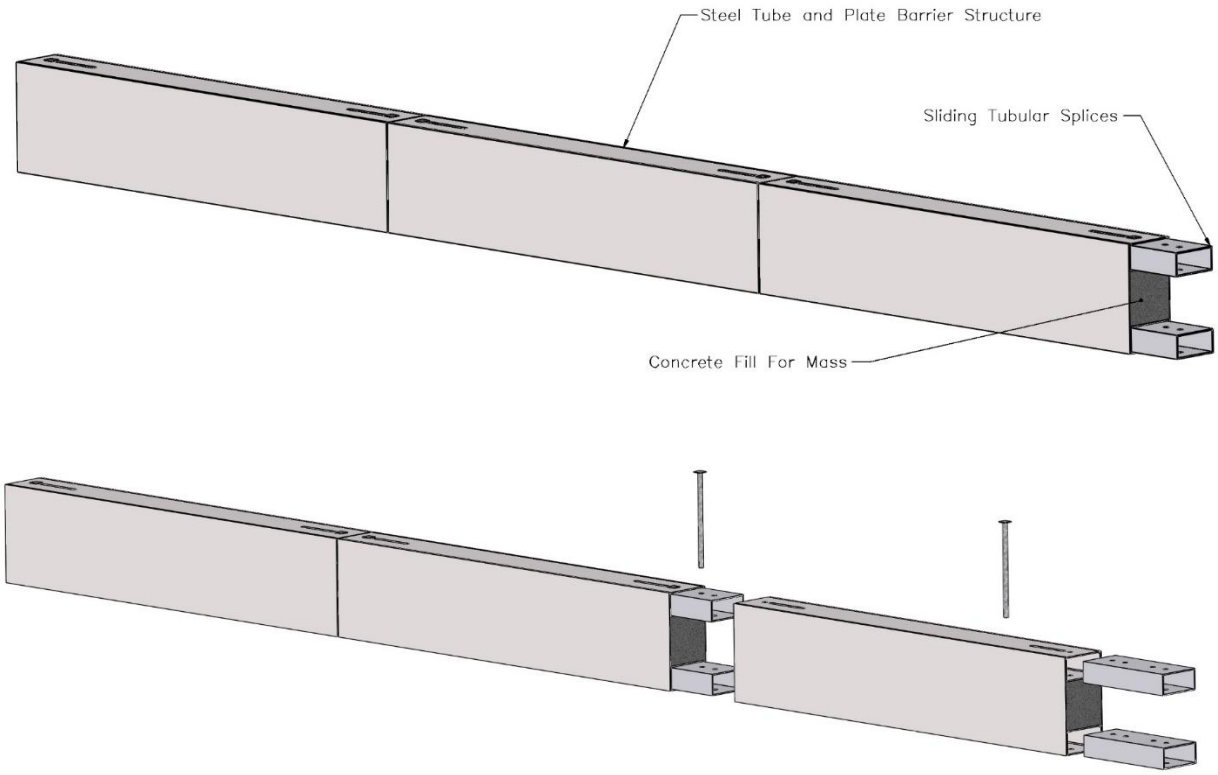

Figure 5. Steel Barrier Concept

1.2 Objective

The objective of this research project was to develop a non-proprietary, high-performance portable barrier capable of meeting MASH TL-3 safety requirements and with reduced free-standing barrier deflections and increased vehicle stability as compared to existing, widely used PCB systems. The design focused on a free-standing barrier initially, but considerations were also made for future anchoring of the portable barrier. Other design criteria included in barrier development were cost, durability, transportability, and ease of installation. A feasible portable barrier design developed in this research would be considered for full-scale crash testing in future research.

1.3 Scope

The research effort focused on further refinement and development of the preferred concepts from the existing WisDOT study in order to develop a prototype barrier system for full-scale crash testing. The research team contacted Midwest Pooled Fund Program member states with a review and summary of the design concepts developed in the preliminary study to obtain feedback on preferred designs and review design criteria. Design concepts most preferred by the member states were selected for further development through analysis and design of the barrier geometry, structural reinforcement, and connection details to meet the design criteria. LS-DYNA was used to determine the effectiveness of the preferred barrier concepts and estimate the structural

performance and deflection under MASH TL-3 impact conditions. Following these analyses, the researchers reviewed the portable barrier design and provided recommendations related to their expected performance.

A portable barrier design that demonstrated potential for meeting the MASH TL-3 impact criteria was developed and prototype CAD details were developed for fabrication. The prototype details were reviewed with portable barrier fabricators to garner feedback, and final design details for future full-scale crash testing were developed.

Finally, a summary research report was completed detailing the portable barrier design process, computer simulation modeling, and recommendations for full-scale crash testing.

2 PORTABLE BARRIER DESIGN CRITERIA

Development of the new, MASH TL-3 portable barrier system required the research team to revisit and refine the design criteria for portable barriers defined in the initial concept development effort. The concept development effort identified several basic design criteria for the portable barrier system that were relevant to the current effort in terms of further development of the preferred concepts into a prototype for full-scale testing. These design criteria were determined through surveying state DOTs, portable barrier fabricators, installers, and consultants [6]. The design criteria outlined in the original study are described below.

1. Cost – The cost of portable barrier was ranked as mid-level design criteria in the original study. It was preferred to keep costs similar to existing portable barrier systems, but the majority of respondents noted that a cost in the range of $100 per linear foot was acceptable if the barrier provided improved service life and/or performance.

2. Material – Concrete and steel were identified as the most desirable portable barrier materials. Concrete was preferred by approximately 75 percent of respondents.

3. Durability – Durability of the portable barrier design was ranked with medium to high importance. Thus, durability of the new portable barrier system was expected to be similar or better than current non-proprietary PCB systems in terms of transportation, installation, and post vehicle impact.

4. Overall Dimensions – It was desired that the new portable barrier use a 32-in. tall height that was consistent with the majority of MASH TL-3 PCB and permanent concrete barrier systems. The majority of respondents also desired a barrier segment length less than 14 ft for ease of transport and installation. Barrier width was to be kept 24 in. or less.

5. Barrier Weight – Weight criteria for the design were established to limit the lifting weight of the barrier segments to less than 7,000 lb based on typically available installation equipment.

6. Barrier Shape – A vertical or near vertical shape was preferred to improve vehicle stability and reduce vehicle climb during impact. According to precast concrete industry representatives, for manufacturing purposes, a draft of 0.5 in. per foot would need to be incorporated into the barrier sides for PCBs, resulting in a near-vertical shaped barrier with a draft of 2.4 degrees. This draft would allow the cured concrete barrier to strip out of the form without moving the sides.

7. Connection Design – Barrier connections which required no hardware or tools were desired as they tend to have short installation times and require no additional pieces that could be lost or stolen. Additionally, the efficiency of the portable barrier connections (shear transfer and moment continuity) significantly affects the barrier performance in terms of dynamic barrier deflections and vehicle snag. Based on these factors, the connection design for the new portable barrier was targeted to be simple to install without tools while providing improved shear transfer and moment continuity across the joint.

8. Deflection - Survey respondents were asked to provide an acceptable dynamic deflection for free-standing MASH TL-3 impacts. The majority of respondents desired barrier deflections below 3 ft. As such, the design of the new portable barrier system focused on limiting deflections below 3 ft and would attempt to reduce deflections further if possible.

9. Anchorage - The new portable barrier was to achieve reduced deflections without anchorage. However, some situations may exist where anchorage to the pavement is required. Survey respondents noted multiple road surfaces on which these barriers may be anchored, including asphalt, concrete, concrete with asphalt overlay, graded shoulder or gravel, and bridge decks. While the current research effort could not develop and evaluate anchorage for the new portable barrier, design concepts would consider anchorage compatibility in the design.

2.1 Additional Design Criteria Survey

The design criteria defined in the conceptual research effort provided the basis for the design prototypes. However, some additional clarification regarding design parameters was needed to better understand requirements for horizontal curvature, drainage, and lifting hardware. In order to determine appropriate design criteria for those items, an updated survey was sent to the Midwest Pooled Fund Program member states to attain more information.

2.1.1 Curvature

Determining the required minimum horizontal curvature was important as increased compliance must be designed into the barrier joints, and this compliance increases the barrier deflection. For example, the current Midwest F-shape PCB has a curvature radius around 40-50 ft and a deflection of 80 in. The Oregon F-shape barrier has a curvature radius around 110 ft and a deflection of 63.4 in. The barrier concepts proposed herein were intended to have drastically reduced deflections, but that may reduce the potential horizontal curve radius that could be achieved.

Respondents were asked to provide their desired minimum horizontal curvature radius from the ranges below.

a. 100-200 feet
b. 200-300 feet
c. 300-400 feet
d. 500-600 feet
e. > 700 ft

The results from the survey responses are shown in Figure 6. A curvature radius of 200 ft-300 ft would accommodate the majority of end users. However, it was noted that accommodation of increased curvature would require a corresponding increase in barrier deflection. It was decided to move forward with the barrier design by analyzing the compromise between barrier deflection and the accommodation of horizontal curvature through computer simulation.

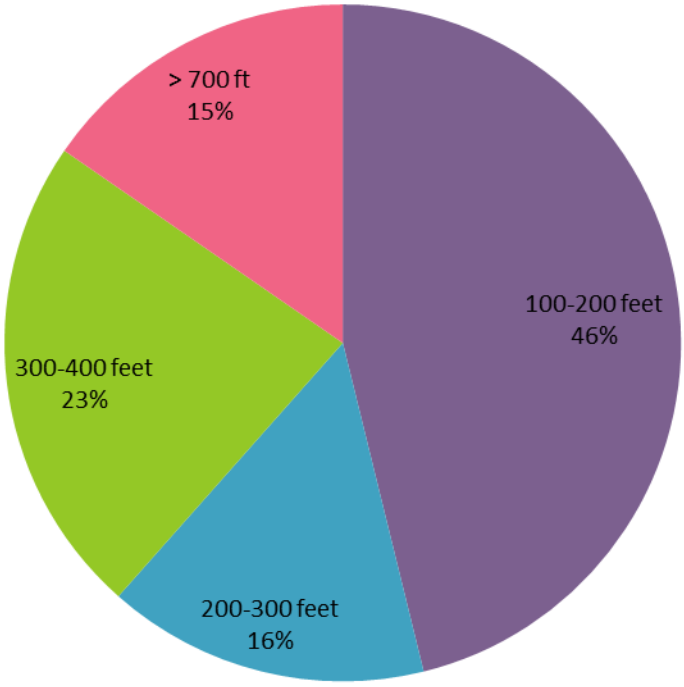

Figure 6. Survey Reponses on Horizontal Curvature

2.1.2 Drainage

Drainage or water flow through barrier segments is a need for portable barriers. However, the amount of drainage required may vary between users. For example, the Midwest F-shape PCB used by many Midwest Pooled Fund Program member states are configured with two or four 12-in. long slots for drainage.

Respondents were asked to provide their desired drainage from the ranges below.

a. 1-2 ft of drainage slot per 12.5 ft long barrier segment
b. 2-4 ft of drainage slot per 12.5 ft long barrier segment
c. Other – Please Specify

The results from the survey response are shown in Figure 7. All of the responses regarding drainage required 4 ft or less of drainage per 12.5 ft of barrier length. As such, drainage length along the barrier was selected to be 0.32 ft of drainage per foot of barrier length.

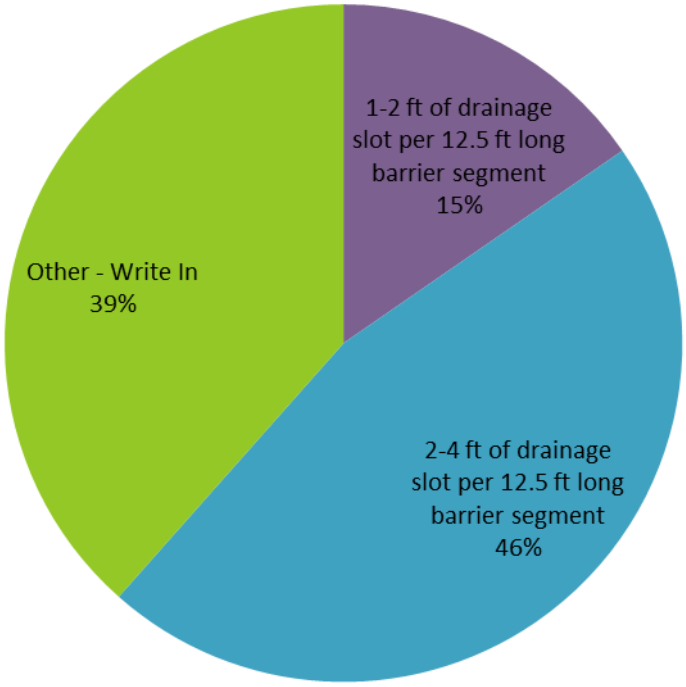

Figure 7. Survey Reponses on Drainage

2.1.3 Lifting Equipment

The previous study noted that contractors typically have equipment capable of moving barrier segments up to 7,000 lb in weight. However, appropriate lifting points needed to be designed into the barrier segments to allow barrier placement. As such, the state DOTs were surveyed to identify what types of equipment are typically available for lifting and moving portable barrier segments in their state from the following options.

a. Forklift
b. Crane
c. Front-end loader
d. Other – Please Specify

Responses regarding available portable barrier lifting equipment were distributed evenly across a number of possible options, as shown in Figure 8. In addition to forklifts, cranes, and front-end loaders, respondents noted the use of excavators, boom trucks, skid loaders, and backhoes. Thus, a wide variety of lifting options would need to be accommodated in the final design.

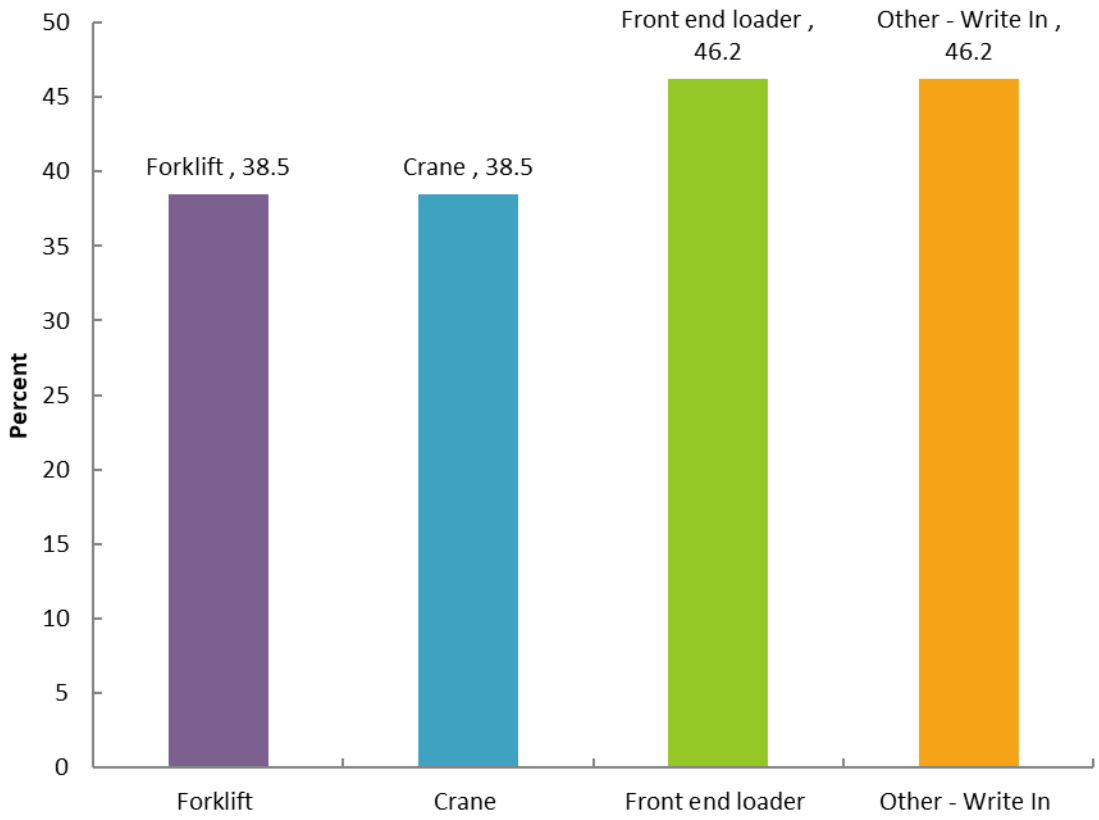

Figure 8. Survey Reponses on Lifting Equipment

2.2 Portable Barrier Deck Loading Considerations

A final design consideration that was identified in the research dealt with the effect of the dead weight of portable barriers installed adjacent to bridge deck edges on bridge deck capacity. The American Association of State Highway and Transportation Officials (AASHTO) *LRFD Bridge Design Specifications* [7] provide procedures for evaluating the loading and capacity of bridge decks under various load conditions. Design Case 3 addresses the strength limit state and evaluates the operational loads on bridge decks. Design Case 3 considers the deck configuration and overhang distance, the distance of the barrier segments relative to the overhand and deck edge, the weight of the barrier segments, and wheel loads from vehicular traffic.

For a structurally continuous barrier system, the wheel loads are defined as a 1-kip/ft line load 1 ft in front of the face of the barrier system. However, portable barriers are not considered a structurally continuous barrier segment due to their joint connections and lack of direct connection to the deck itself. For a non-continuous barrier system, wheel loads are defined as a 16-kip point load 1 ft in front of the face of the barrier system resisted by a finite deck length.

A Design Case 3 analysis was performed to investigate the potential concerns regarding decking loading of portable barriers adjacent to the deck edge. The analysis was conducted using both the Midwest F-shape PCB currently used by many state DOTs and two preliminary versions of a staggered, interlocking PCB concept. The Midwest F-shape PCB consists of a 12.5-ft long by

32-in. tall F-shape PCB that weighs 0.399 kip/ft. The two staggered, interlocking PCB concepts consisted of 12.5-ft long by 32-in. tall near-vertical barrier segments in 18-in. wide and 24-in. wide configurations that weighed 0.520 kip/ft and 0.716 kip/ft, respectively. The offset of the barrier segments from the edge of the bridge deck varied. For the Midwest F-shape PCB, the barrier was assumed to be in its anchored configuration, which placed the back of the barrier 6 in. from the deck edge. The staggered, interlocking PCB concepts were offset with the back of the barrier 12 in. from the edge of the deck. The bridge deck used in the analysis consisted of an 8-in. thick deck with a top rebar mat consisting of no. 6 bars at 8-in. spacing. No bottom steel was used in the calculations to be conservative, and the cantilever overhang length varied between 3 ft to 5 ft. The analysis setup is shown schematically in Figure 9.

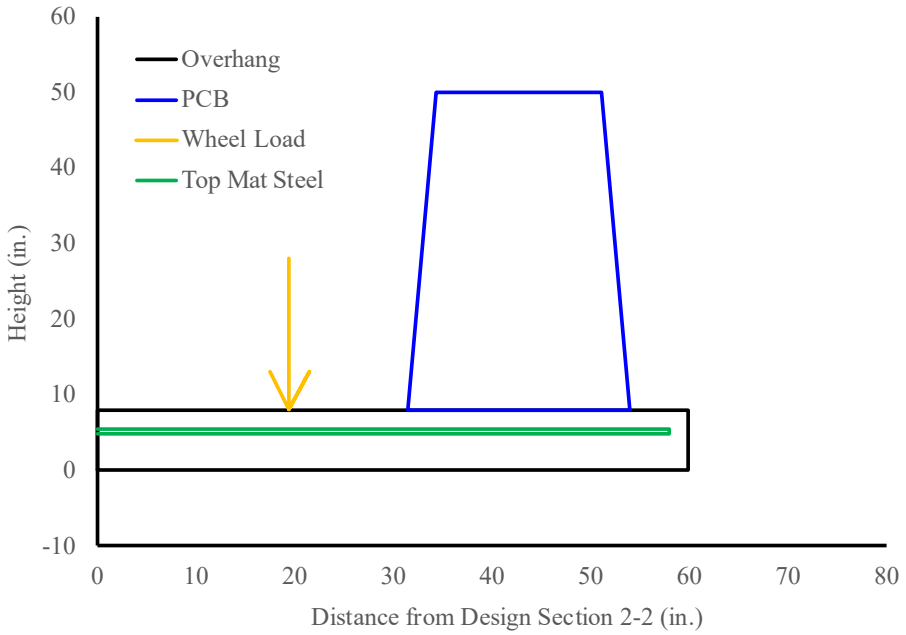

Figure 9. Design Case 3 Analysis Schematic

Results from that basic analysis are summarized in Table 2. The analysis found that portable barrier dead loads on bridge decks may be a concern, but only for extreme cases where the barriers are very close to the deck edge and the cantilever overhang is large. For example, the portable barrier configuration that exceeded capacity was the Midwest F-shape PCB installed 6 in. from the deck edge on a 5 ft overhang. The staggered, interlocking PCB concepts met deck capacity limits at a slightly larger 12-in. offset from the deck edge while being significantly heavier. Cantilever overhangs of 4 ft or less demonstrated no capacity issues. This analysis would suggest that end users should consider portable barrier loading on bridge decks, but the concerns may be limited to barriers installed on large overhangs very close to the deck edge. This would be consistent with existing concrete bridge rail and deck design which places concrete parapets directly adjacent to the deck edge in many instances, which would indicate that most bridge decks may already be designed to deal with this type of loading. Thus, the issue of portable barrier loading of bridge decks may largely be limited to construction efforts on older bridges with reduced deck capacity.

Table 2. Design Case 3 Analysis of Portable Barrier Deck Demands

Deck Overhang (ft)	Portable Barrier	PCB Width (in.)	PCB Weight (kip/ft)	Distance from Edge (in.)	Moment Demand (kip*ft/ft)	Demand to Capacity Ratio
4	Staggered, Interlocked PCB (24 in. wide)	24	0.716	12	3.2	0.232
	Staggered, Interlocked PCB (18 in. wide)	18	0.520	12	2.6	0.197
	Anchored F-Shape PCB	22.5	0.399	6	8.1	0.589
5	Staggered, Interlocked PCB (24 in. wide)	24	0.716	12	13	0.942
	Staggered, Interlocked PCB (18 in. wide)	18	0.520	12	12.1	0.889
	Anchored F-Shape PCB	22.5	0.399	6	15.9	1.146

3 SELECTION OF PREFERRED BARRIER DESIGN

After establishing and refining the design criteria for the new MASH TL-3 portable barrier system, the researchers reviewed the design concepts from the initial research phase and assessed them with the sponsors to select a preferred design concept for further development into a prototype for full-scale crash testing.

3.1 Recommended Design Concepts

The previous research study performed preliminary simulation analysis of several design concepts. Three concepts were identified as having potential for further development. The three recommended concepts consisted of the following.

1. A near-vertical PCB with a pin and plate joint was denoted as Concept 1 in the original study, as shown in Figure 10. This design featured two plates and four pins per joint connection. The plates slid horizontally into slots in the face of the barrier and four pins (two in each barrier end) were dropped through the barriers and plates. The use of dual pins and plates in this concept would provide increased moment continuity and reduced rotation at the barrier joint. The design also allowed for a minimal gap between barrier segments, which would further aid in reducing barrier deflections. This PCB design required pin and plate hardware but required no tools and could be placed vertically or horizontally.

2. A near-vertical PCB comprised of staggered, stackable rectangular segments was denoted as Concept 16 in the original study, as shown in Figure 11. This concept utilized short, stackable barrier segment sections which were staggered longitudinally with a ½ barrier length offset. One connection pin hole was located at each end of the barrier segment, and two connection pin holes were located near the midpoint of the barrier length. Connection pins were dropped through the holes in the barrier segments to connect the longitudinally staggered barrier elements. This connection allowed barriers to be placed vertically or horizontally. This connection design was simple and would provide a high degree of moment continuity throughout the barrier. Special end sections may also be required for this barrier concept due to its irregular barrier end geometry.

3. A near-vertical PCB comprised of staggered, interlocking barrier segments was denoted as Concept 19 in the original study, as shown in Figure 12. This concept consisted of a segmented concrete barrier system utilizing interlocking top and bottom segments that were stacked in an offset or staggered configuration to provide continuity in the barrier without discrete barrier connections or connection hardware between the barrier segments. The barrier design concept utilized upper and lower barrier segments with a fixed length. The lower base segment had a protrusion that extended into an interior cavity in the upper segment of the barrier. The upper and lower segments of the barrier were offset longitudinally ½ of the barrier segment length. The combination of the lower segment inserting into the upper segment and the longitudinal offset effectively interlocked the barrier segments to provide moment continuity throughout the barrier system without separate barrier connections. Special end sections may be required for this barrier concept due to its irregular barrier end geometry. It is also believed that this design could be anchored to further reduce deflections using pockets in the lower segment of the barrier for the installation of anchor rods.

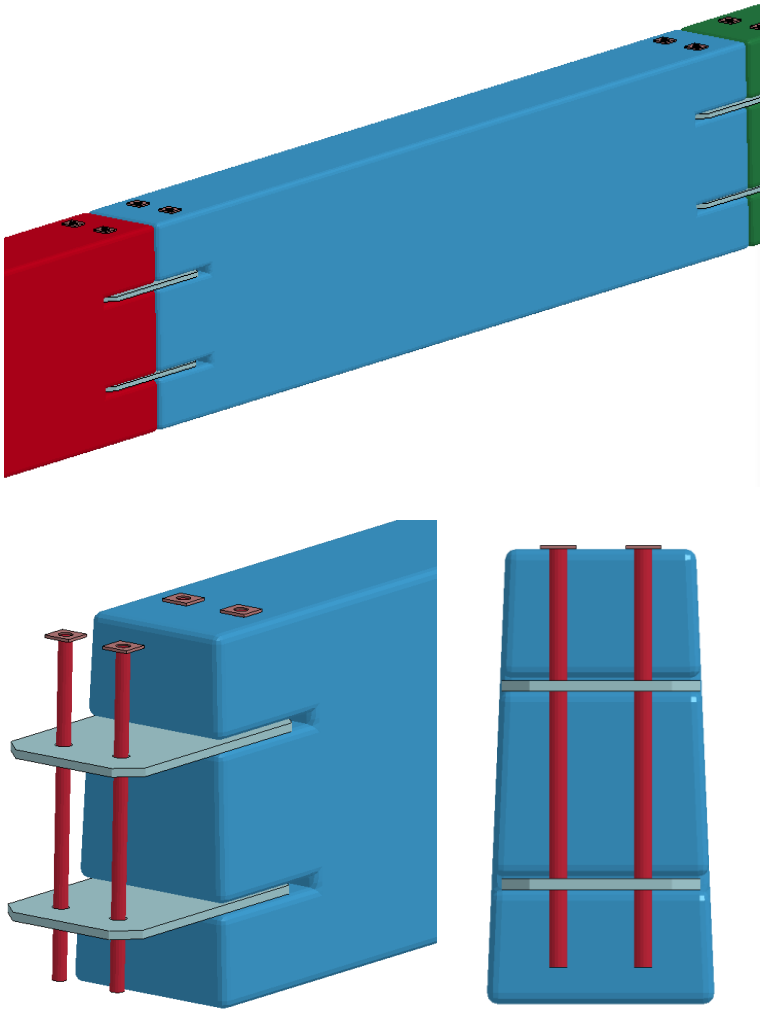

Figure 10. Concept 1: Near-Vertical PCB with Pin and Plate Joint

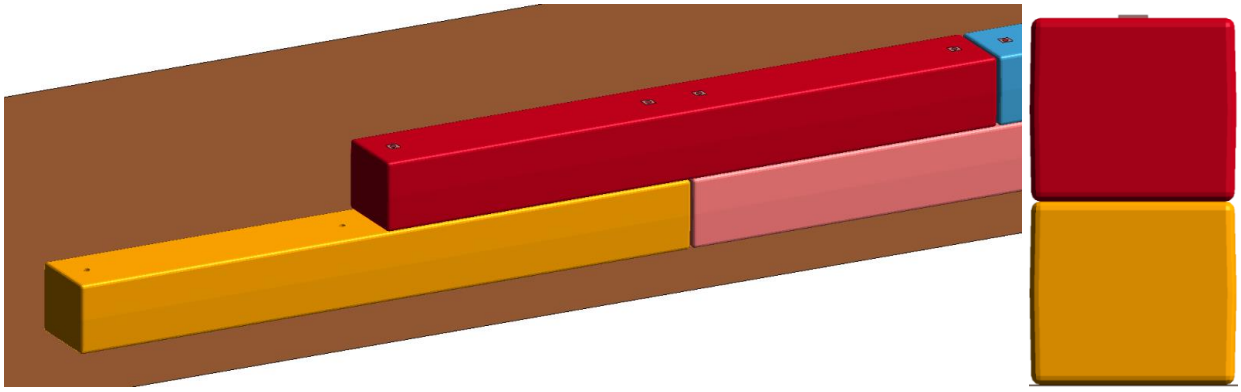

Figure 11. Concept 16: Near-Vertical PCB Comprised of Staggered, Stackable Rectangular Segments

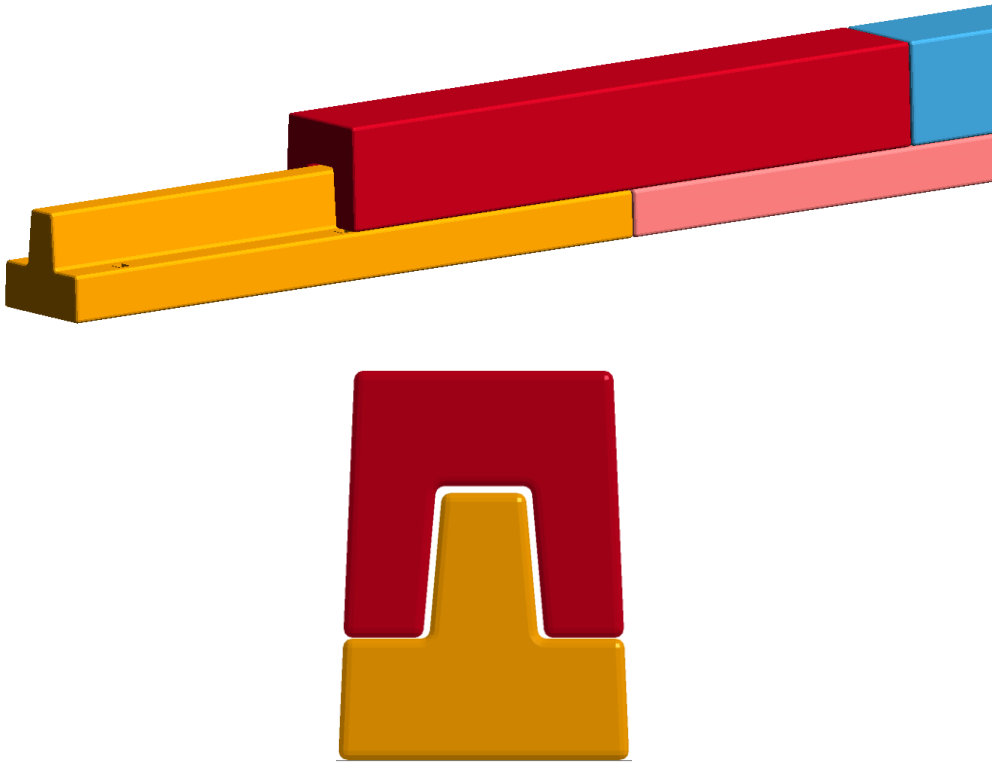

Figure 12. Concept 19: Near-Vertical PCB Comprised of Staggered, Interlocking Barrier Segments

To aid in the selection of a preferred concept for further development, the performance of the recommended concepts based on LS-DYNA modeling in the original research effort was compared with the performance of the F-shape PCB with a pin-and-loop connection used by several state DOTs [8]. A summary of the comparison between the various PCB systems is shown in Table 3. Note that Concept 19 had several potential cross-section variations that were deemed feasible – Concepts 19A, 19C, and 19D. As such, the viable variations of that concept are shown in the table as well. Note that all comparisons were based on 12.5-ft long barrier segments.

In general, all three recommended PCB concepts provided improved vehicle stability due to their near-vertical face. Additionally, the proposed concepts reduced barrier deflections through a combination of increased weight per foot and greater moment continuity at the segment joints. It was noted that increased moment continuity at the segment joints tended to increase the achievable curvature radius for the barrier system.

Table 3. F-Shape PCB and Preferred PCB Concepts Summary

Concept No.	Maximum Barrier Deflection (in.)	Linear Weight (lb/ft)	Radius Curve (ft)	Profile
F-shape PCB	80	399	~40	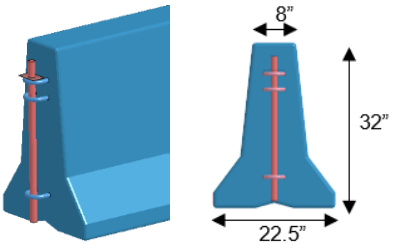
1	35	479	~100-150	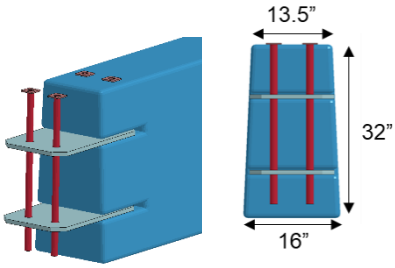
16	13 (Concept 16-C)	580	~800	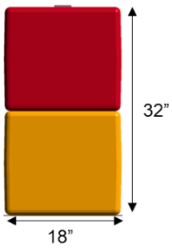
19-A	8.5	719	~1,120	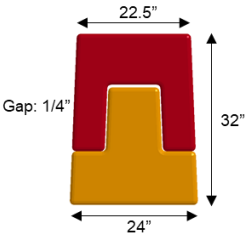
19-C	13.5	711	~490	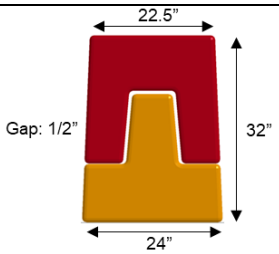
19-D	15	520	~720	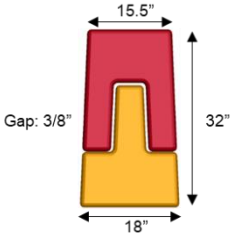

3.2 Design Concept Survey

The Midwest Pooled Fund Program member states were asked to review the three recommended concepts and rank them for further research and development. The concepts were ranked from one to three with one being the highest ranked concept and three being the lowest. Thirteen responses were received. The results of the state responses are shown in Table 4. The near-vertical PCB comprised of staggered, interlocking barrier segments was identified as the preferred concept. It had the best overall score and was ranked the most preferred concept by 8 of the 13 respondents. Comments from the respondents noted that the concept ranked highly due to the potential for extremely low barrier deflection under MASH TL-3 impact conditions and the omission of any external hardware required to connect the barrier segments. The near-vertical PCB with a pin and plate joint ranked second. Respondents generally liked this design but did not prefer the amount of external hardware required for the connection. Finally, the near-vertical PCB comprised of staggered, stackable rectangular segments was ranked the lowest of the three concepts with only one state ranking that concept as the most preferred and ten states ranking it lowest.

Table 4. Preferred PCB Concept Survey Results

Design Concept	Total Score (Lower = Higher Ranked)	No. of Highest Rankings	No. of Lowest Rankings
Near-Vertical PCB Comprised of Staggered, Interlocking Barrier Segments	19	8	1
Near-Vertical PCB with Pin and Plate Joint	24	4	2
Near-Vertical PCB Comprised of Staggered, Stackable Rectangular Segments	35	1	10

Based on the survey results, researchers focused on developing the near-vertical PCB comprised of staggered, interlocking barrier segments. If serious shortcomings or complications arose during concept refinement, the two remaining concepts could be revisited.

3.3 Initial Design Concept for Simulation

In order to begin design and analysis of the near-vertical PCB comprised of staggered, interlocking barrier segments, the research team developed an initial configuration for the basis of the design and outlined potential variations and options that would be considered as the design was analyzed and refined.

The first consideration was the basic overall dimensions and geometry of the barrier segments. Survey results had previously selected a 32-in. barrier height for the PCB segments. An initial barrier segment length of 12.5 ft was selected to be consistent with most existing PCBs and state DOT preferences. The barrier footprint was desired to be less than or equal to 24 in. The near-vertical profile of the barrier system dictated that variations in the segment width would create a compromise between structural capacity and segment weight. For a 32-in. tall PCB segment, 18-in. wide, 21-in. wide, and 24-in. wide variations of the staggered, interlocking barrier segments concept were estimated to weigh 520 lb/ft, 628 lb/ft, and 711 lb/ft, respectively. Review of the narrowest portions of the upper and lower segments of the barrier found that conventional barrier reinforcement would be difficult to fit in any barrier segment with a footprint of less than 21 in. Thus, a 21-in. wide barrier footprint was selected for the initial design as a compromise between barrier segment weight per foot and structural reinforcement demands. As noted previously, the barrier used a near-vertical draft of 0.5 in. per foot for fabrication purposes, which resulted in a barrier top width of $18^{5}/_{16}$ in.

Installation of the barrier segments for this concept would require offsetting the upper and lower barrier segments by ½ of the barrier segment length. To ensure proper alignment of the barrier segments during installation two options were considered. The first option was to provide a vertical alignment groove in the middle of the face of the upper barrier segment that could be aligned with the end of the lower barrier segment. A second option was to create a series of opposing divots and extensions in the opposing surfaces of the upper and lower barrier segments that forced self-alignment of the segments. The second option was considered too complex and could create with issues barrier reinforcement. As such, the vertical alignment groove was selected to facilitate proper barrier installation. An example of the vertical alignment groove is shown in Figure 13.

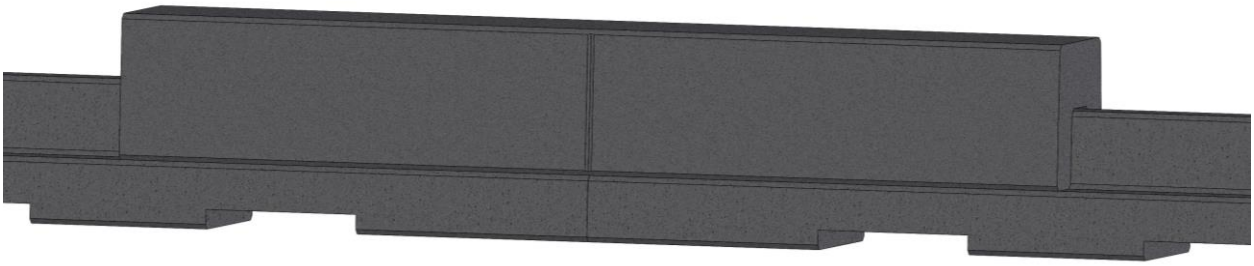

Figure 13. Vertical Alignment Groove

In the design criteria surveys sent to the sponsoring states, it was noted that a minimum curvature radius for the barrier segments of <300 ft would accommodate the majority of respondents, and many states desired curvatures of 200 ft or less. The achievable radius of curvature for the staggered, interlocking barrier concept was dependent on the barrier segment length and the internal tolerance gap between the upper and lower barrier segments, as shown in Figure 14. The effect of these parameters on the achievable curvature radius was investigated using 3D CAD to estimate the curvature radius for 21-in. wide barrier segments with tolerance gaps of ⅜ in. and ½ in. and segment lengths between 72 in. and 150 in. The results of that analysis are shown in Figure 15.

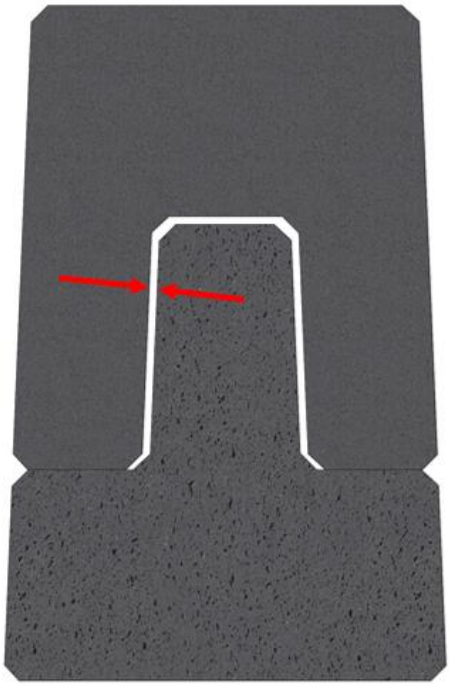

Figure 14. Internal Tolerance Gap

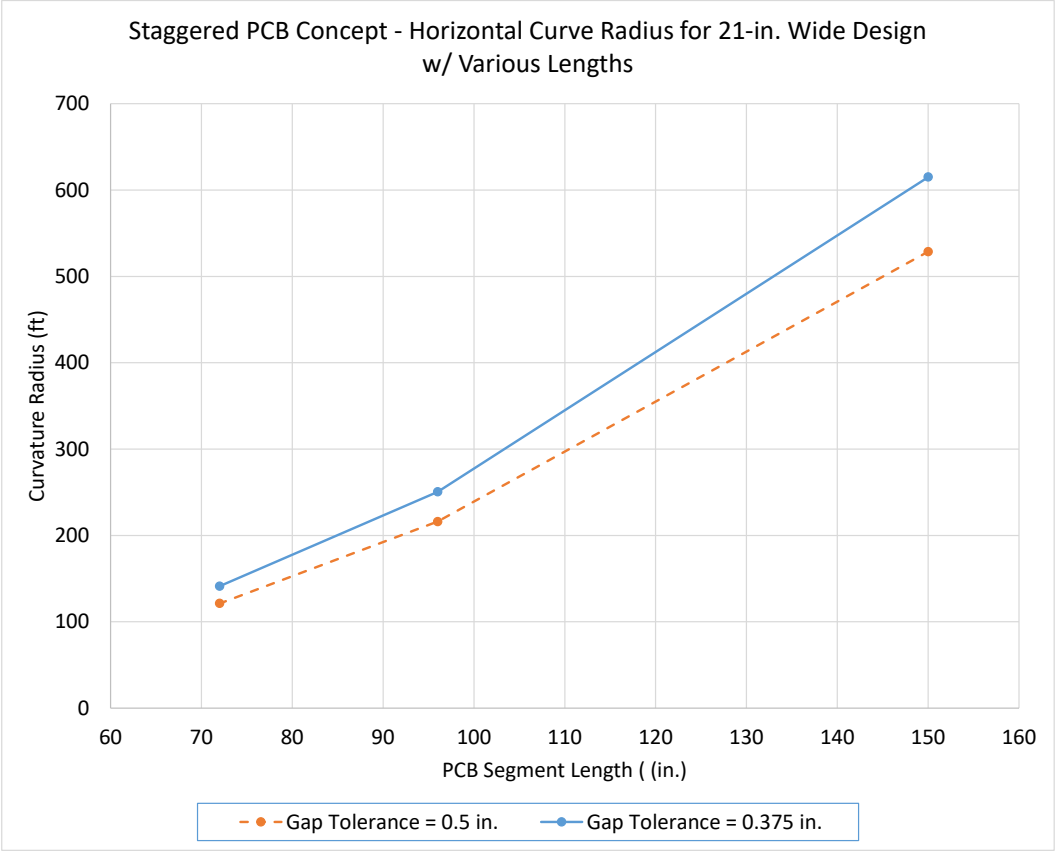

Figure 15. Estimated PCB Horizontal Curve Radius

The results found that a barrier segment length of 12.5 ft would not be able to achieve a 300 ft radius of curvature without widening the internal gap tolerance above ½ in. However, using shorter barrier segment lengths of 8 ft would allow a curvature radius of 216 ft. It was decided to proceed with a 12.5-ft segment length for the initial concept analysis with the intent to further investigate segment length during the analysis after the structural design needs were determined. It was also noted that barrier deflection and stiffness were directly correlated with segment length. Thus, if the final barrier design was developed and full-scale crash tested with a short segment length for curvature considerations, similar or improved performance would be expected for longer barrier segment lengths in terms of barrier loading and deflection. If states did not require the smaller curvature radius or desired a longer barrier segment to further reduce deflection, it was noted that longer segment lengths would not require full-scale crash testing as long as the structural capacity and reinforcement of the barrier was maintained for the increased length barrier segments. Additionally, it was noted that deflections could be estimated using computer simulation models validated against the full-scale crash tests of the shorter length barrier system.

As with any PCB system, the staggered, interlocking barrier segment concept would require some construction tolerances when assembled. The internal gap tolerance required for assembling the barrier segments was targeted to be between ⅜ in. and ½ in. The initial design configuration of the design would focus on the ½-in. gap, but the smaller gap size would be investigated during the analysis as needed. Similarly, it was noted that there could be potential gaps between the ends of the barrier segments during installation, as shown in Figure 16. The effect of these gaps on barrier performance would be investigated as the barrier design became more formalized. Simulation of the initial barrier configuration would focus on no end gaps between the barrier segments.

Figure 16. PCB End Gaps

The previous survey of sponsoring DOTs noted that 0.32 ft of drainage per foot of barrier length was desired. For the 12.5-ft segment length used in the initial design configuration, a pair of 24-in. long x 3-in. tall drainage slots were incorporated into the lower barrier segment to achieve the drainage requirements. Drainage slots in the lower portion of PCBs often limit the placement of longitudinal reinforcement in the lower portion of the barrier which can lead to increased damage in these areas of the PCB. To mitigate this issue, the lower longitudinal barriers in the barrier were bent to pass up and over the drainage slots, as shown in Figure 17.

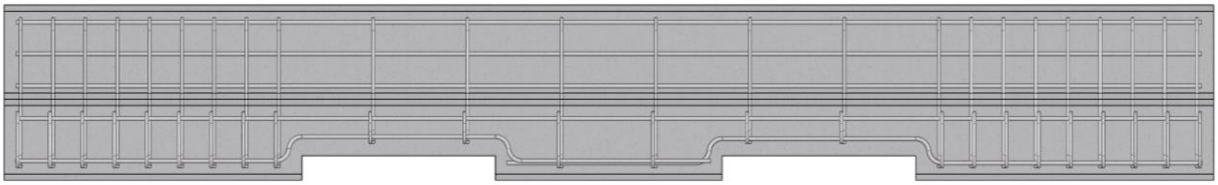

Figure 17. Drainage Slots and Reinforcement

With the basic layout of the preliminary staggered, interlocking barrier segment concept completed, the last component of the design needed to begin simulation analysis was the development of the initial structural reinforcement. It was anticipated that the barrier reinforcement would be revised based on the results of the simulation analysis. Reinforcement for the upper barrier segment consisted of no. 3 stirrups spaced a 4 in. near the ends of the barrier and 11.5 in. in the interior. No. 3 stirrups were selected for easier fit within the limited space available in the outer legs of the upper barrier segment. The longitudinal steel in the upper barrier segment consisted of no. 4 longitudinal bars. The lower barrier segment consisted of similar size and spacing for both the stirrups and longitudinal bars. The lower barrier segment also included bent longitudinal bars near the base of the segment to accommodate the drainage slots. The initial reinforcement configuration is shown schematically in Figure 18.

The initial barrier reinforcement for the concept was ASTM A615 Grade 60 rebar, which is commonly specified for a wide variety of reinforced concrete construction. During discussions with precast fabricators and steel manufacturers during the research effort, the potential to utilize Grade 80 reinforcing steel was noted as a potential option. Grade 80 reinforcing steel provided the potential for a 33 percent increase in bar strength, and steel manufacturer quotes denoted a price increase of only $0.03 per lb over Grade 60 steel. The use of high-grade reinforcing steel has become more prevalent in recent years due to the high-grade bars allowing the use of less overall steel, smaller structural sections, and lower placement costs. Due to the potential benefits of the use of Grade 80 steel for a minimal increase in cost, it was noted that Grade 80 reinforcing steel may be a desirable option for use in the staggered, interlocking barrier segment concept due to the potential structural capacity needs in the narrow sections of the barrier segments.

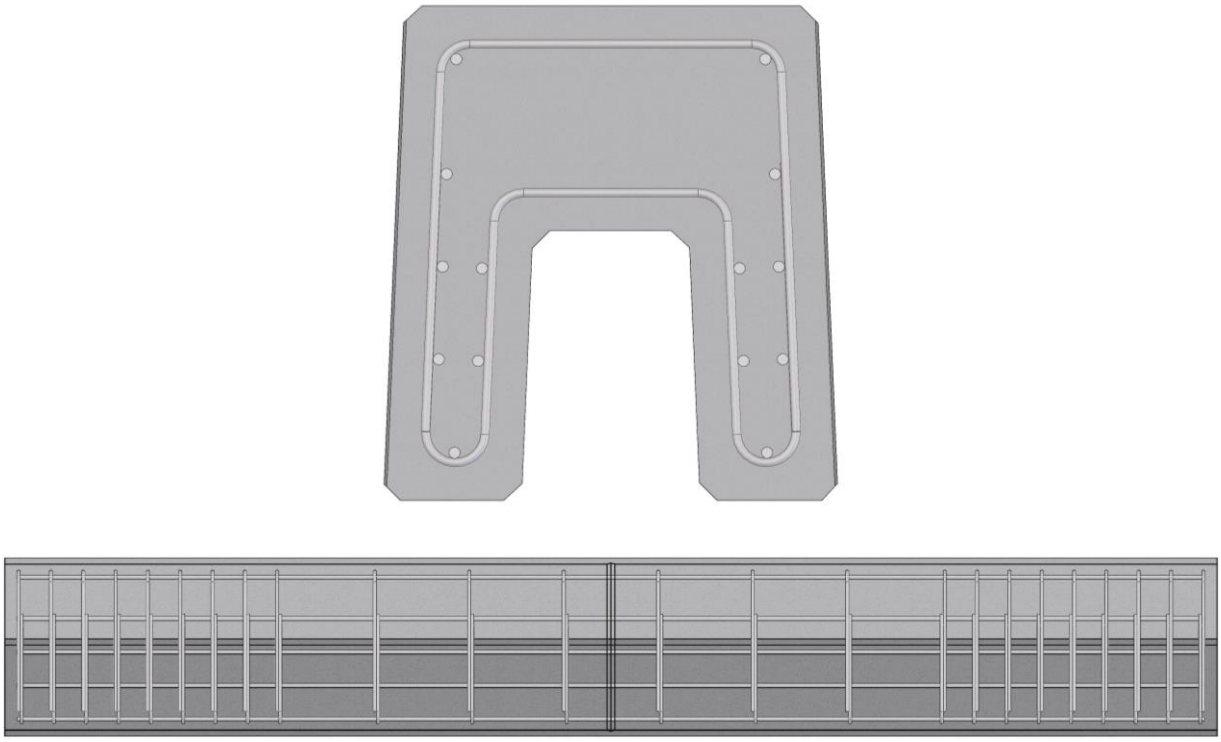

(a) Upper Barrier Segment

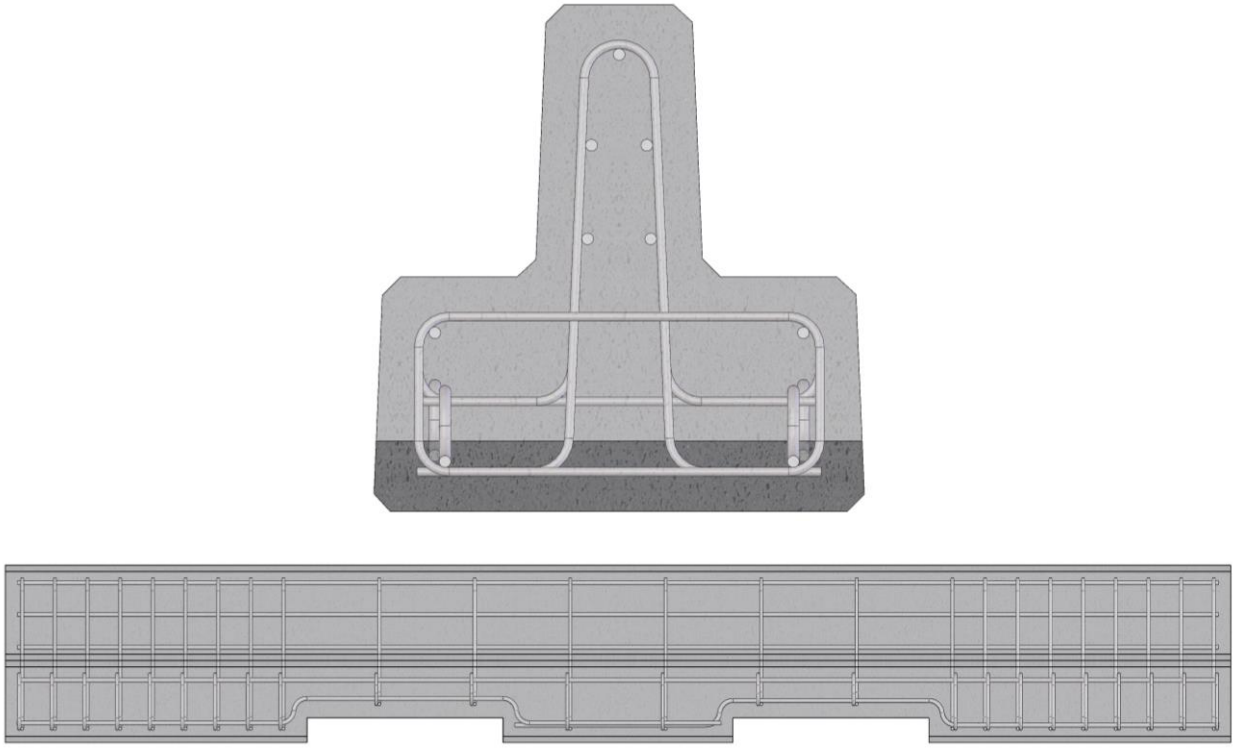

(b) Lower Barrier Segment

Figure 18. Preliminary Staggered, Interlocking Barrier Segment Concept Reinforcement

4 DESIGN AND SIMULATION OF PORTABLE BARRIER CONCEPT

The next phase of the development of a non-proprietary, high-performance portable barrier capable of meeting MASH TL-3 safety requirements consisted of applying LS-DYNA simulation analysis to the design of the staggered, interlocking barrier segment concept. LS-DYNA is a transient, non-linear finite element analysis code that is widely used for the modeling of crash events [9]. The focus of the simulation effort was to estimate the safety performance of the barrier system and refine the design as needed prior to developing final prototype details for full-scale crash testing. The simulation model details and analysis are summarized in the subsequent sections.

4.1 Simulation Model Details

4.1.1 Barrier Model

The simulation model of the staggered, interlocking barrier segment concept consisted of the concrete body of the barrier segments, reinforcing steel, and a ground to support the barrier segments.

Constant stress Type 1 solid elements were used to model the body of the barrier segments. In order to prevent hourglass energies from influencing the model results, hourglass type 6 with the hourglass coefficient set to qm=0.05 was applied to the concrete elements. The material model used for the concrete was the Karagozian & Case (K&C) concrete model in LS-DYNA with MAT_ADD_EROSION. This material model had been applied extensively to simulate reinforced concrete in previous research efforts and was validated against many impact cases involving reinforced concrete bridge rails and decks [10-11]. The K&C model was used to auto-generate parameters for an f'c = 5,000 psi concrete. Then a series of modifications were made to the auto-generated parameters based on the previous simulation calibrations conducted with the model. These modifications, as shown in Table 5, have consistently provided more accurate results in past modeling efforts of concrete bridge rail and deck overhang systems. Further, the addition of erosion to the K&C model resulted in reduced computation times at large deformations and more discernible damage patterns. The most notable deviation in the K&C model from the recommendations made in the LS-DYNA keyword manual is the specification of the localization width parameter, LOCWID, to a value less than the average characteristic length of the concrete elements. This modification has resulted in substantially more accurate predictions of post-peak softening behavior relative to the existing manual recommendation of three times the maximum aggregate diameter. In past experiences using the K&C concrete model, using a LOCWID parameter greater than the solid element size resulted in poor predictions of concrete behavior, particularly after cracking. In this application, LOCWID was set to a value of 0.75 in., which was less than the average concrete solid mesh size of 1.00 in.

Steel reinforcement used in the barrier was modeled using Type 1 Hughes-Liu beam elements with the proper cross-sectional properties for the given bar size. The rebar was restrained in the concrete mesh using the CONSTRAINED_BEAM_IN_SOLID command. The rebar steel was modeled with the MAT_PIECEWISE_LINEAR_ PLASTICITY material in LS-DYNA with the appropriate properties for ASTM A615 Grade 60 steel. ASTM A615 Grade 80 steel material properties were specified in some models later in the analysis.

Table 5. Summary of K&C Material Model Auto-Generated Parameter Modifications

K&C Concrete Model			
Parameter	**Auto-gen. Value**	**Modified Value**	**Effect of Change**
Element formulation	NA	1	Improved performance with reduced-integration solid elements
Tensile strength, f_t	$f(f'_c)$	Note 1	Affects severity of tensile and shear damage
Shear dilatancy, Ω	0.50	0.75	Better approximation of shear damage
Localization width, LOCWID	D_{agg} (note 3)	0.75-times mesh size	Improved post-peak softening performance
Max principal strain, MXEPS	NA	0.15	Consistently realistic depiction of cracking without eroding load-bearing elements
Max shear strain, EPSSH	NA	0.15	Consistently realistic depiction of cracking without eroding load-bearing elements
Hourglass control type, IHQ	5 (note 2)	6	Improved HG energy reduction without producing unrealistic strength
Hourglass coefficient, QM	0.02 (note 2)	0.05	Improved HG energy reduction without producing unrealistic strength

NA = not applicable
[1] Tensile strength is highly variable for a given f'_c.
[2] Values shown correspond to recommended hourglass parameters provided in the K&C Manual.
[3] D_{agg} = maximum aggregate diameter.

A critical component of the PCB model was the definition of the barrier-to-ground friction. PCB systems use a combination of inertial resistance and friction to redirect impacting vehicles. Previous research at Texas A&M Transportation Institute (TTI) and MwRSF measured the kinematic friction coefficient for a concrete PCB segment sliding on concrete and asphalt surfaces to be between 0.40 and 0.51 [12-14]. The lower friction value of 0.40 was selected for use in the analysis in order to better correlate with the road surface used in the full-scale testing and to maximize potential deflections. This friction value was applied in the LS-DYNA model between the barrier segments and a shell element ground. In addition to providing appropriate friction coefficients, the barrier model needed to develop the correct weight or normal forces on the ground. This was accomplished by allowing the barriers in the simulation model to reach quasi-static equilibrium on the ground prior to being impacted. Damping was used to help the barriers reach a steady normal force on the ground and was turned off prior to vehicle impact.

The completed barrier model is shown in Figure 19. A total of sixteen lower barrier segments and fifteen upper barrier segments were assembled to create a 200-ft long barrier system.

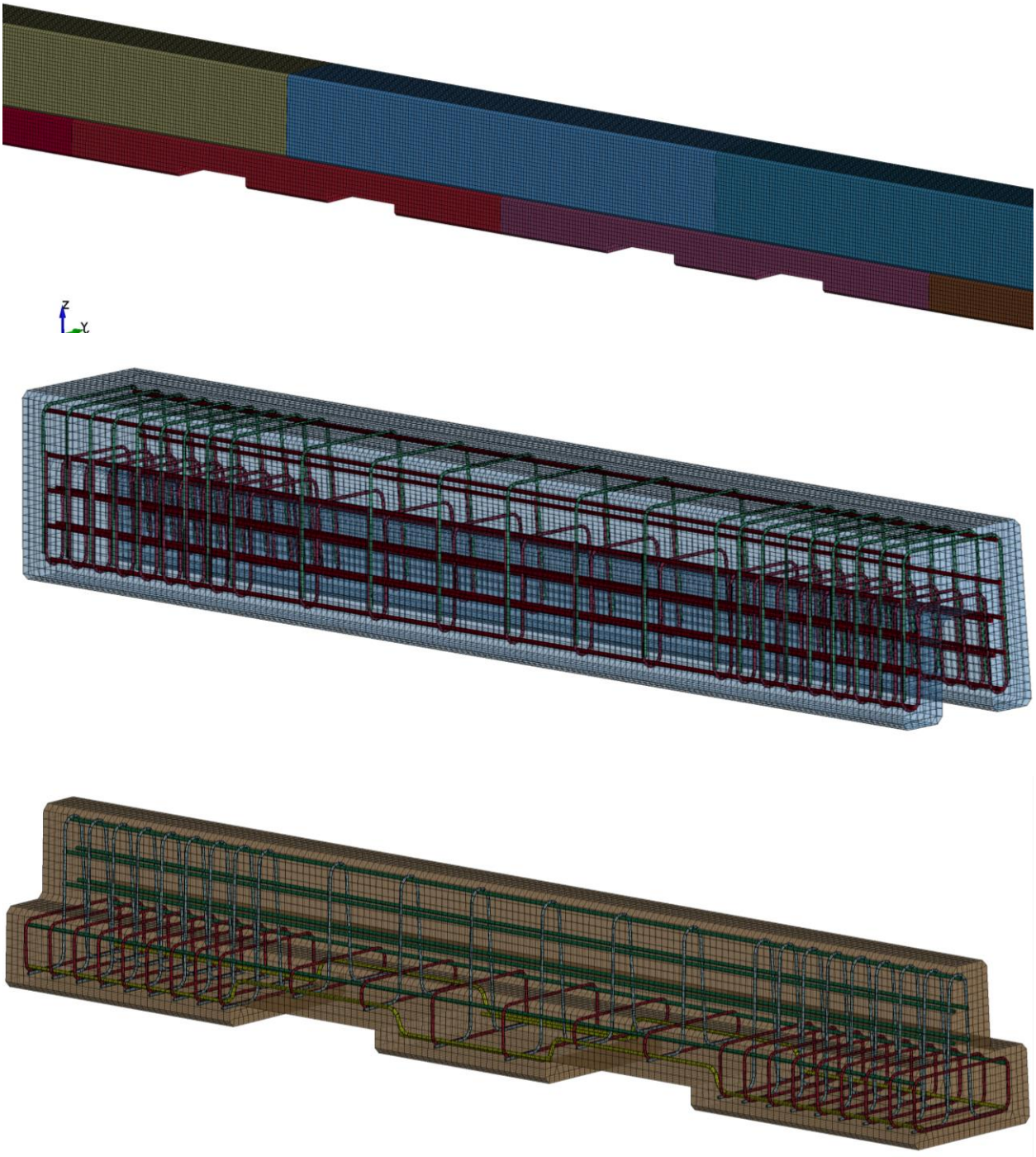

Figure 19. Near-Vertical Staggered, Interlocking PCB Model

4.1.2 Vehicle Model

The vehicle model used in the simulation analysis was a Dodge Ram 1500 quad cab model version 3d from the Center for Collision Safety and Analysis (CCSA), located at George Mason University (GMU) [15], as shown in Figure 20. The model was based on a pickup truck with Vehicle Identification Number (VIN) 2GCEC13C771511793, and was consistent with the MASH specifications for the 2270P test vehicle. The tires used on the vehicle were based on P265/70R17 wheels with steel rims. The model has been modified at MwRSF over time, including improvements to the steering system and suspension components as well as replacing the default wheel and tire models with modified or more detailed models. The pickup truck model impacted the PCB system 4.3 ft upstream from a joint between upper barrier segments at the midspan of the system, which was consistent with MASH recommendations for the critical impact point with PCBs. Impact conditions consistent with MASH TL-3 were applied. Thus, the vehicle model impacted the barrier system at a speed of 62 mph and an angle of 25 degrees.

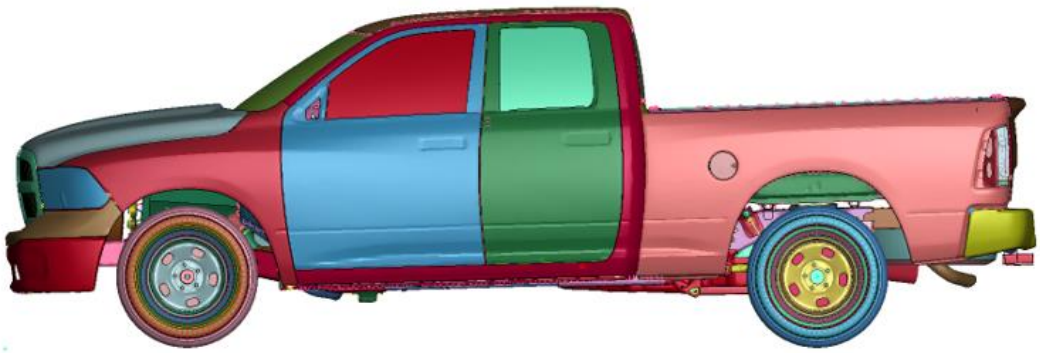

Figure 20. Ram 1500 Quad Cab Vehicle Model

No 1100C small car analysis was performed as part of the simulation analysis. The 1100C small car was not deemed critical for structural loading due to its lower overall weight. Additionally, previous full-scale crash testing of rigid, vertical bridge rails with 1100C vehicles had shown that there was little concern for excessive occupant risk values or vehicle instabilities [16-17].

4.2 Simulation Objectives

Simulation of the new PCB system with LS-DYNA was intended to address several needs in the development of the system. First, the simulation would attempt to predict if the staggered, interlocking barrier segment concept would provide acceptable safety performance in terms of stable and effective vehicle capture and redirection. The simulation would determine if the barrier concept performed as intended by providing moment continuity within the barrier system and capturing the impacting pickup truck with a stable trajectory and limited vehicle snag. Second, the simulation model was used to evaluate the structural capacity of the barrier and guide refinement of the barrier structure, including alteration of the geometry and/or reinforcement. Finally, the simulation models would be applied to investigate the variable segment lengths and internal tolerance gaps to fine tune barrier performance.

4.3 Simulation of Initial Staggered, Interlocking Barrier Segment Concept

The analysis of the staggered, interlocking barrier segment concept began with simulation of the preliminary barrier concept detailed in Section 3.3. Initial model results indicated good performance for the PCB system, as shown in Figures 21 and 22. The 2270P vehicle model was safely and stably redirected by the PCB segments. Dynamic barrier deflections were limited to a maximum of 17.5 in.

While the overall barrier performance was positive, there were some concerns identified with respect to the structure of the barrier segments. Review of the contours of concrete damage indicated that significant damage to the concrete was predicted to the outer legs of the upper barrier segments and the center pillar of the lower barrier segments near vehicle impact, as shown in Figures 23 and 24. This was not unexpected as these areas of the barrier segments had relatively narrow cross sections and would experience the highest loading during vehicle impact.

Previous modeling experience with the K&C concrete model had shown that the concrete damage contours can overestimate the level of concrete damage. As such, the plastic strain of the reinforcing steel in the critical barrier regions was also reviewed. Review of the reinforcing steel in the upper barrier segment, as shown in Figure 25, indicated significant plastic strains in the stirrup bars at the base of the upper barrier legs near the ends of the upper barrier segment. High plastic strains were also identified in the longitudinal steel along the outside of the upper barrier segment near the midspan of the barrier. Similar plastic bar strains were also noted in the lower barrier segment, as shown in Figure 26. The lower barrier segment reinforcement demonstrated plastic strains in the stirrups near the base of the center pillar near the midspan of the segment. Moderate plastic strains were also noted in the longitudinal bars near the drainage slots in the lower barrier segment. These widespread levels of plastic strain in the reinforcing steel of the upper and lower barrier segments would be consistent with damage and deformation of the concrete structure of the barrier in those locations which would require replacement of the barrier following a MASH TL-3 level impact. Additionally, the level of damage observed could allow localized deformation of the barrier segment, which would reduce the moment continuity of the barrier segments and allow for some increase in the overall barrier deflections.

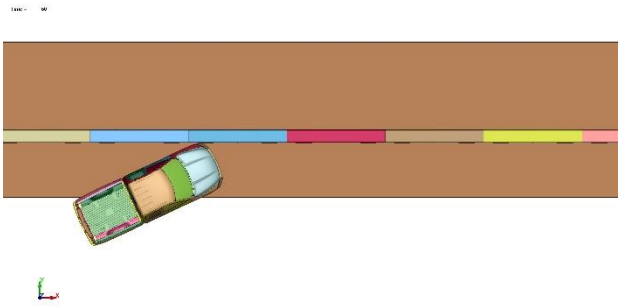

(a) 0.000 sec

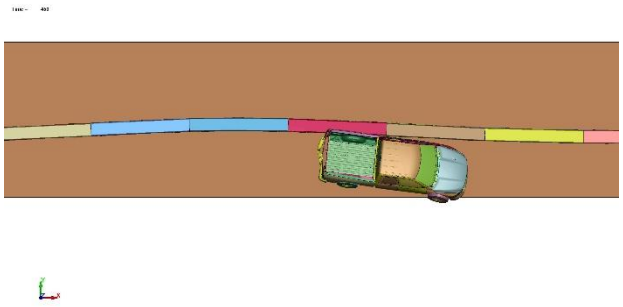

(e) 0.400 sec

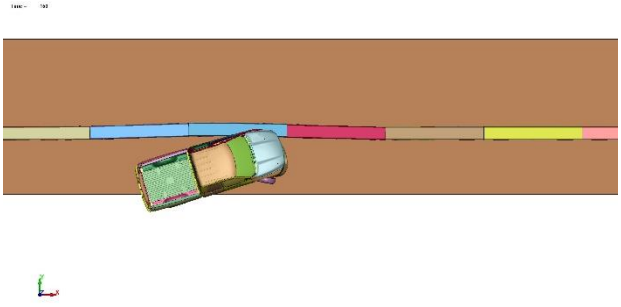

(b) 0.100 sec

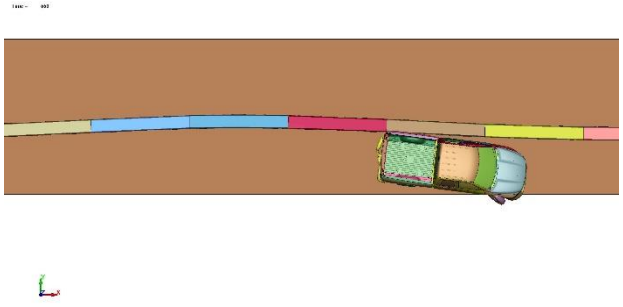

(f) 0.500 sec

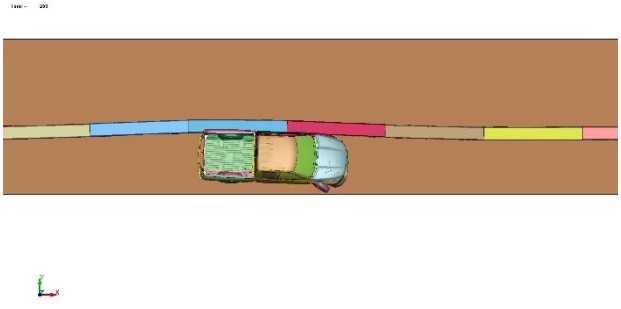

(c) 0.200 sec

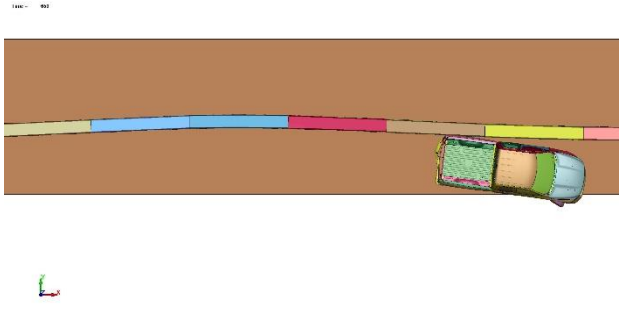

(g) 0.600 sec

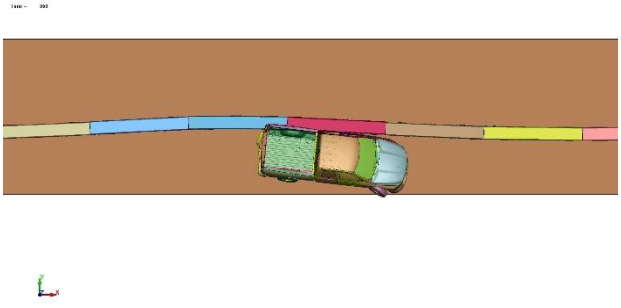

(d) 0.300 sec

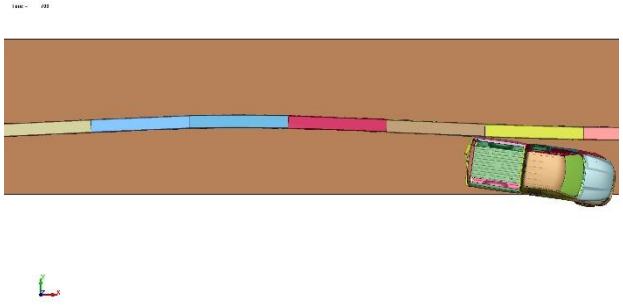

(h) 0.650 sec

Figure 21. Initial Staggered, Interlocking Barrier Segment Concept Model, Overhead Sequential Images

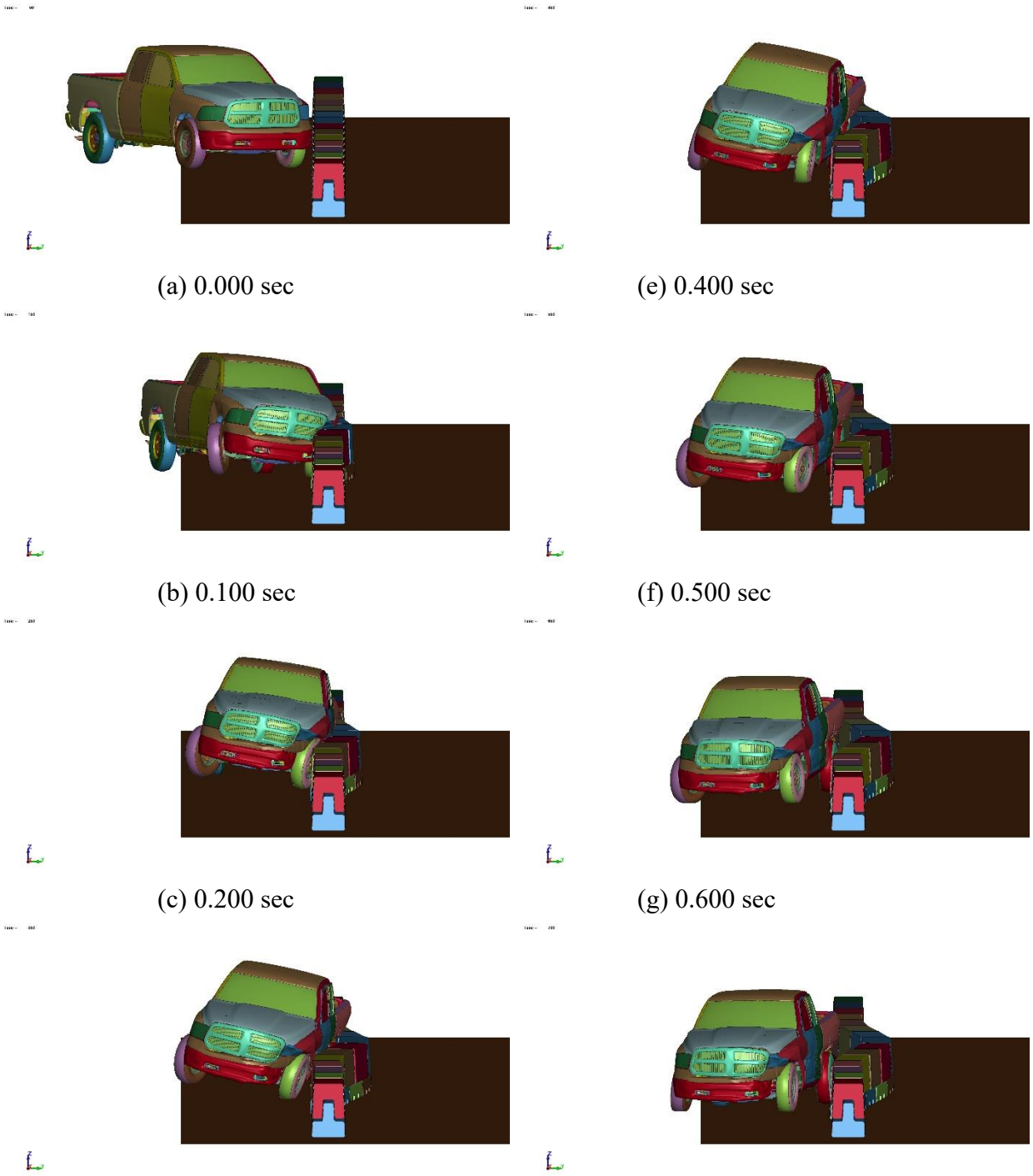

(a) 0.000 sec

(e) 0.400 sec

(b) 0.100 sec

(f) 0.500 sec

(c) 0.200 sec

(g) 0.600 sec

(d) 0.300 sec

(h) 0.650 sec

Figure 22. Initial Staggered, Interlocking Barrier Segment Concept Model, Downstream Sequential Images

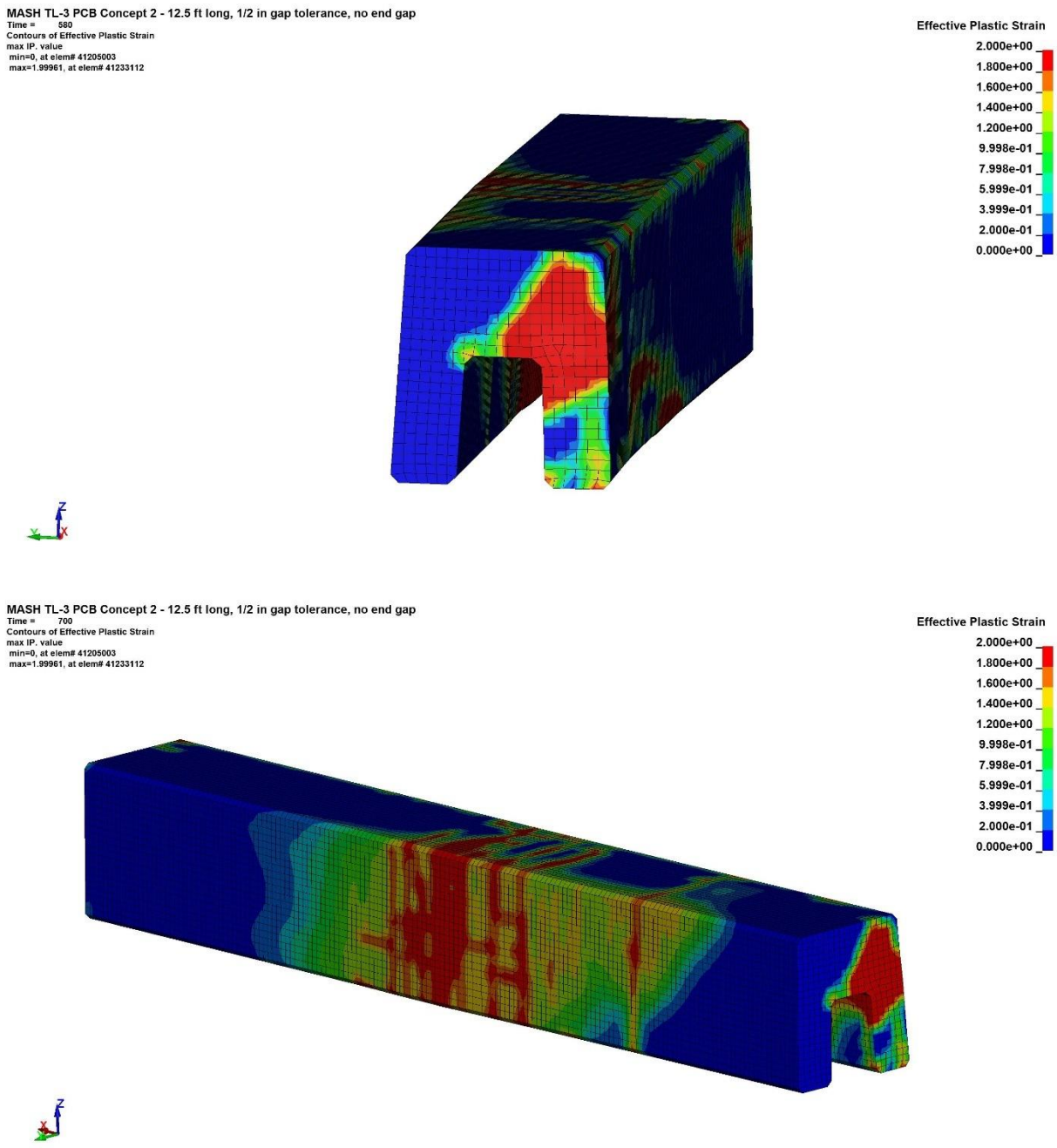

Figure 23. Initial Staggered, Interlocking Barrier Segment Concept Model, Upper Segment Concrete Damage

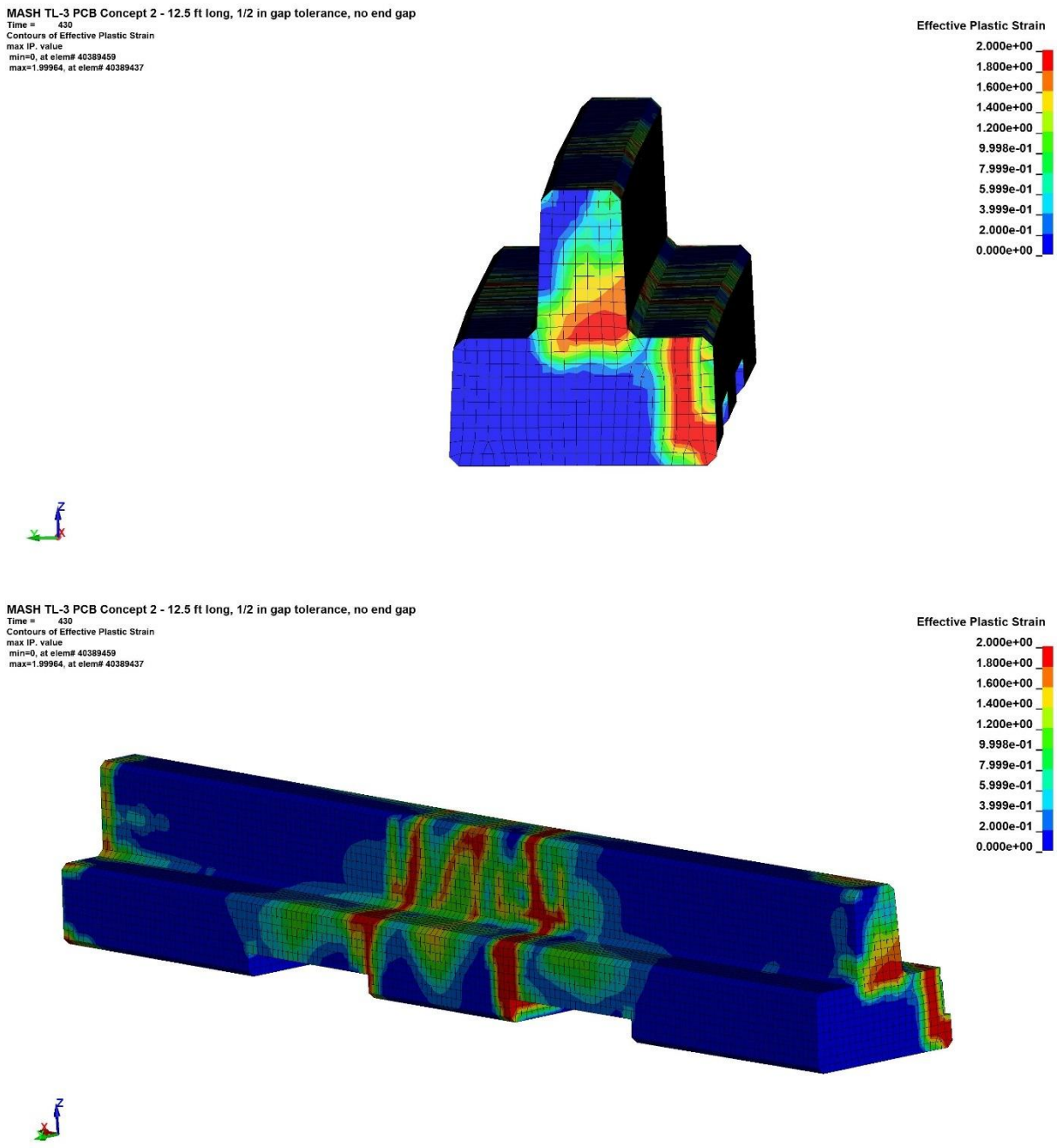

Figure 24. Initial Staggered, Interlocking Barrier Segment Concept Model, Lower Segment Concrete Damage

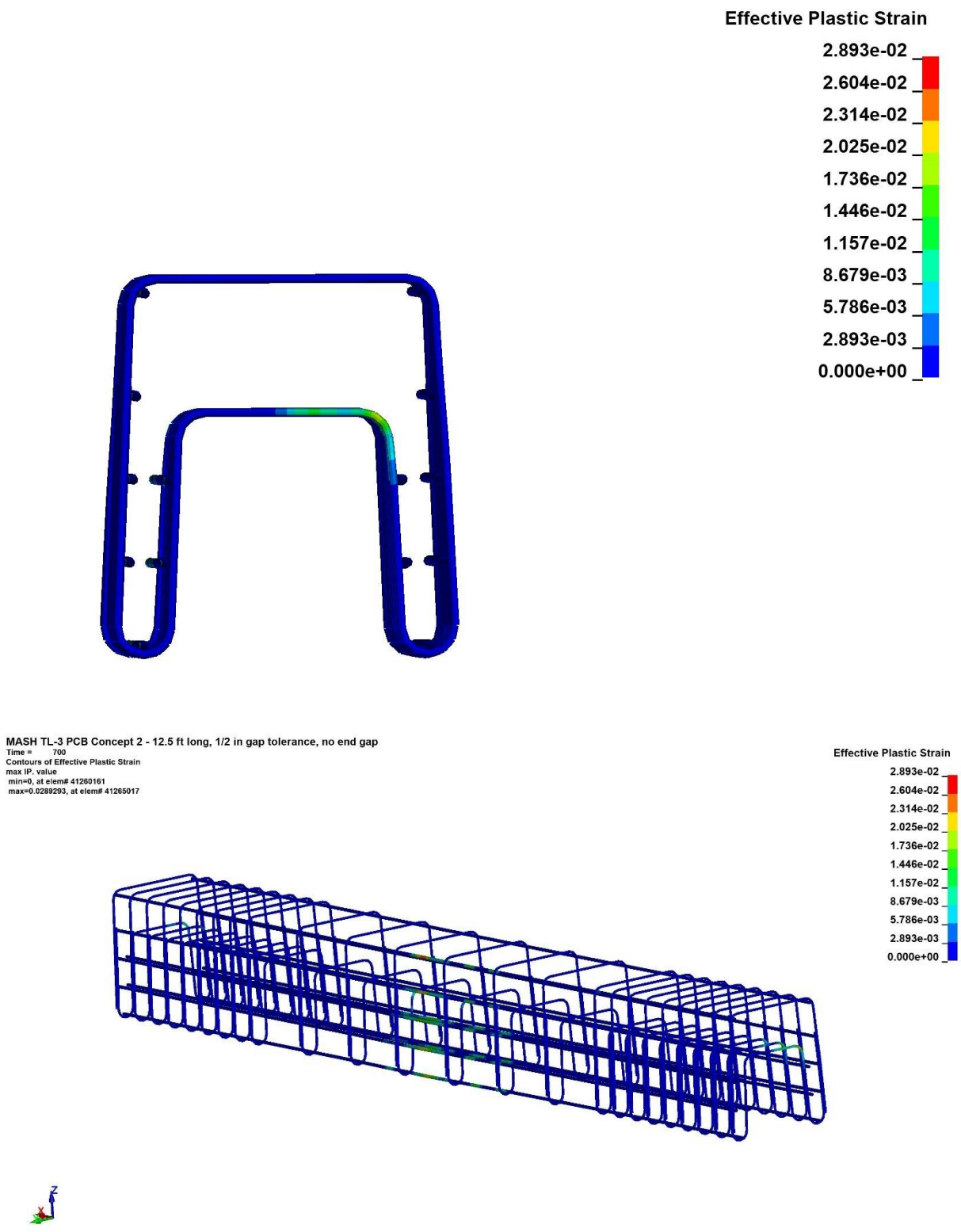

Figure 25. Initial Staggered, Interlocking Barrier Segment Concept Model, Upper Segment Rebar Plastic Strain

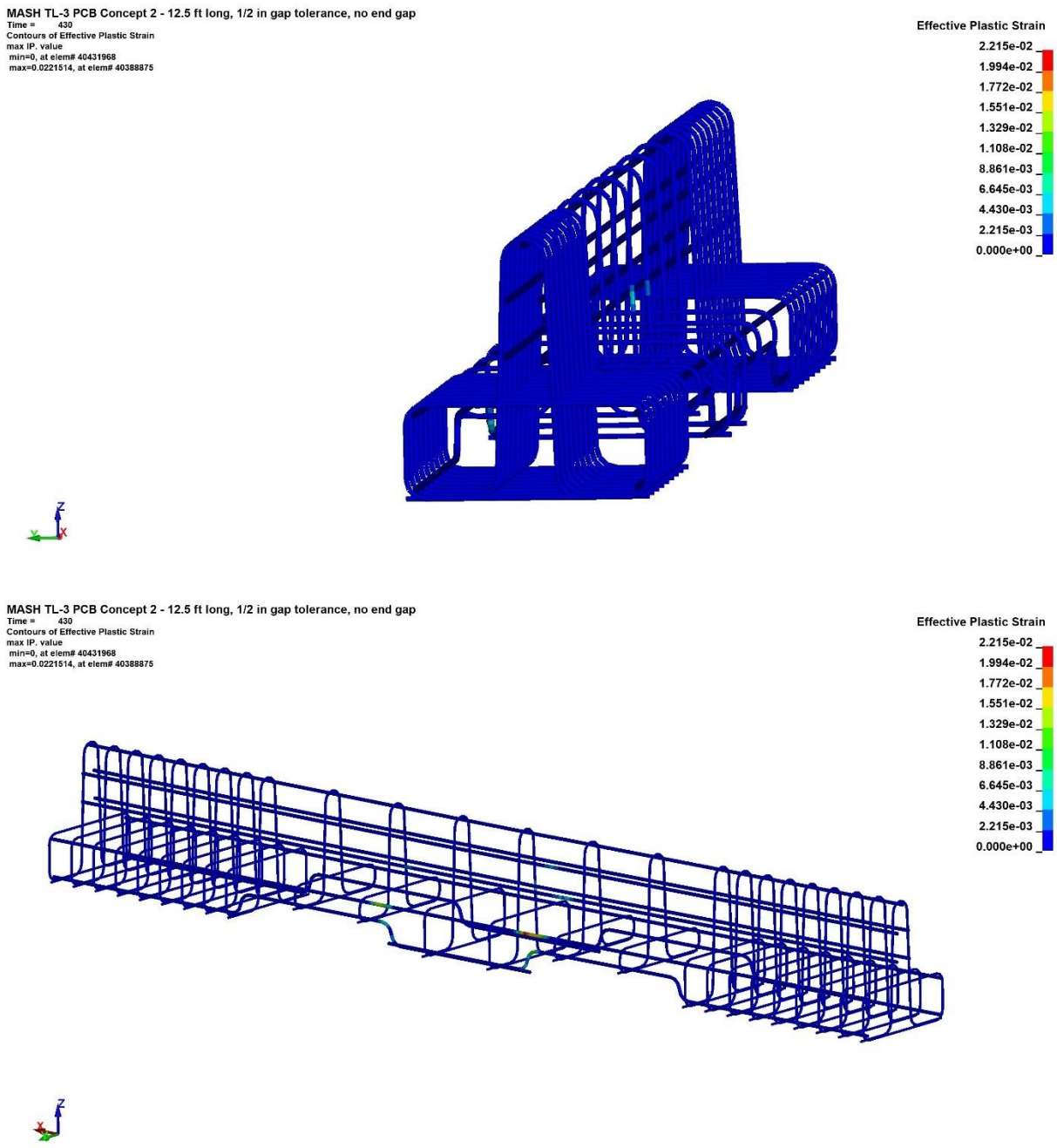

Figure 26. Initial Staggered, Interlocking Barrier Segment Concept Model, Lower Segment Rebar Plastic Strain

4.4 Simulation of Barrier Reinforcement Variations

The initial staggered, interlocking barrier segment concept displayed good performance in terms of the capture and redirection of the 2270P vehicle under MASH TL-3 impact conditions. However, the structural damage observed on the barrier segments suggested that improvements to the barrier structure could further improve performance and limit damage. In order to investigate increased barrier structural capacity, three variations of the initial design were simulated to determine their potential for improvement. The increased reinforcement options investigated started with minor reinforcement modifications and then increased the level of structural reinforcement more with each subsequent iteration. These variations included:

Option 1 – The first option for increased structural capacity was developed to limit damage to the upper barrier segment outer legs and the flexural damage observed on the lower barrier segment. Option 1 used the same basic reinforcement as the initial design for the top section except for the addition of no. 5, V-shaped bars near the ends of the segment that were added to reduce the opening of the upper segment under load, as shown in Figure 27. The base segment reinforcement for Option 1 was also the same as the initial design except for four additional longitudinal bars and additional stirrups over the drainage slots, as shown in Figure 28.

Option 2 – Reinforcement Option 2 made further modifications to Option 1 to increase the flexural capacity of the overall barrier section and limit the damage to the outer legs of the upper barrier and center pillar of the lower barrier. This reinforcement scheme for the top segment was the same as Option 1 except for the addition of six longitudinal bars and a $^{3}/_{16}$-in. thick steel end cap, as shown in Figure 29. The steel end cap was added to reduce damage and opening of the ends of the barrier segment under load. The base segment of reinforcement Option 2 was also the same as reinforcement Option 1 except for the addition of two longitudinal bars and a $^{3}/_{16}$-in. steel end cap, as shown in Figure 30.

Option 3 - Reinforcement Option 3 was identical to Option 2 for both the upper and lower barrier segments except all of the longitudinal steel was increased to no. 5 bars, and the steel grade for all bars was increased to Grade 80.

Each barrier reinforcement option was simulated in LS-DYNA using the same impact conditions as the initial barrier design configuration.

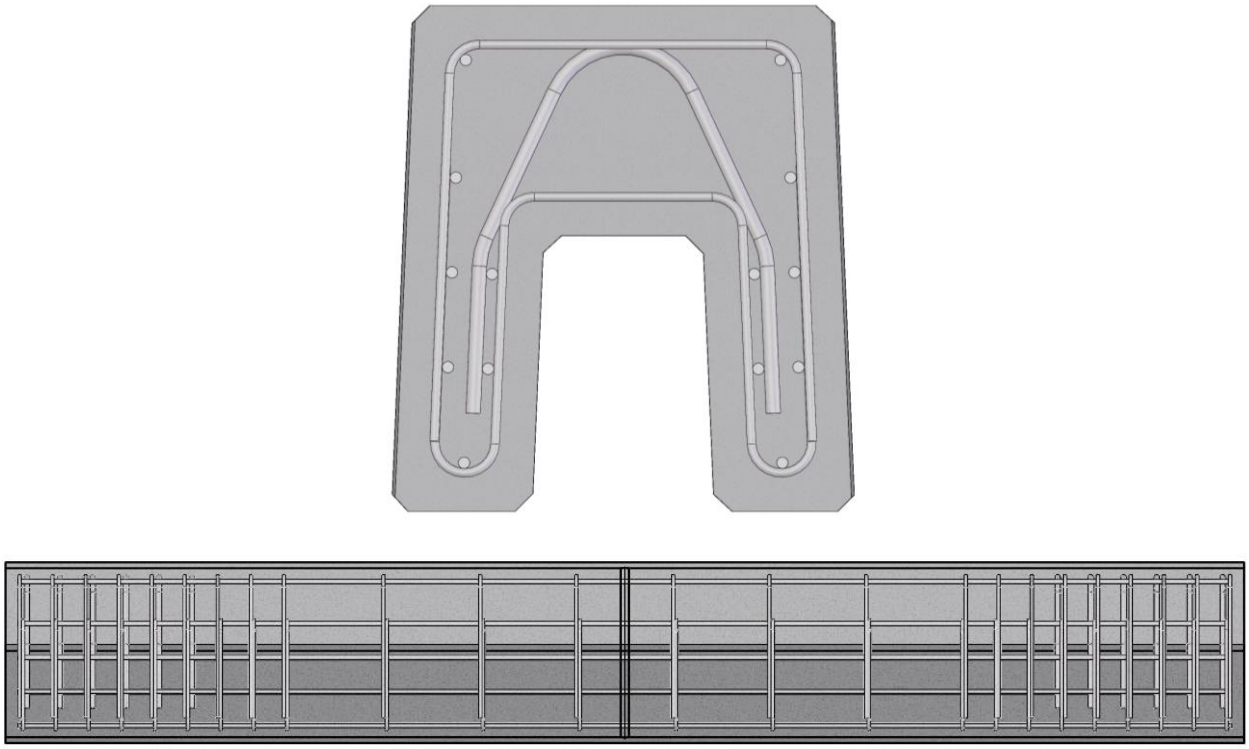

Figure 27. Option 1 PCB Reinforcement, Upper Segment

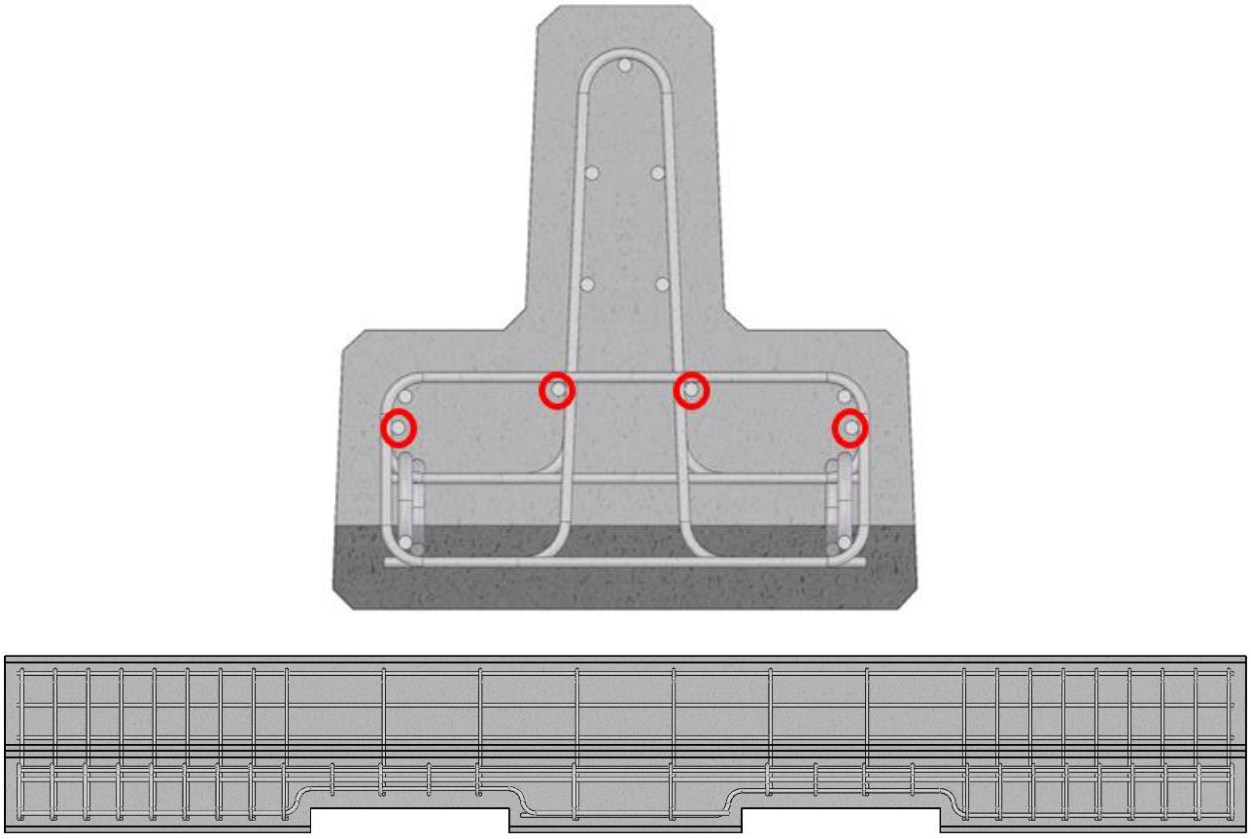

Figure 28. Option 1 PCB Reinforcement, Lower Segment

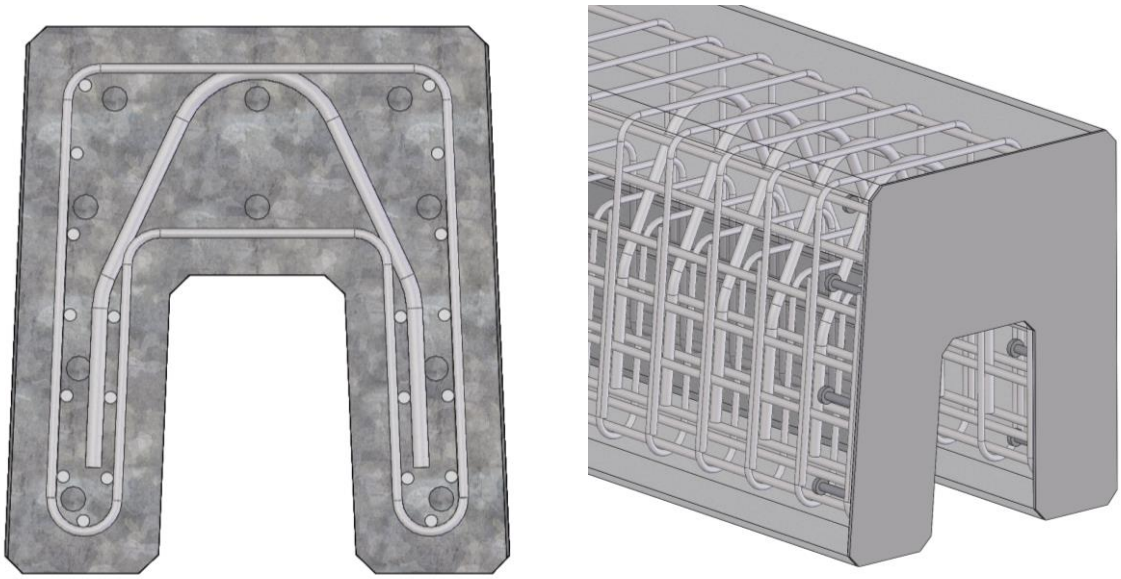

Figure 29. Option 2 PCB Reinforcement, Upper Segment

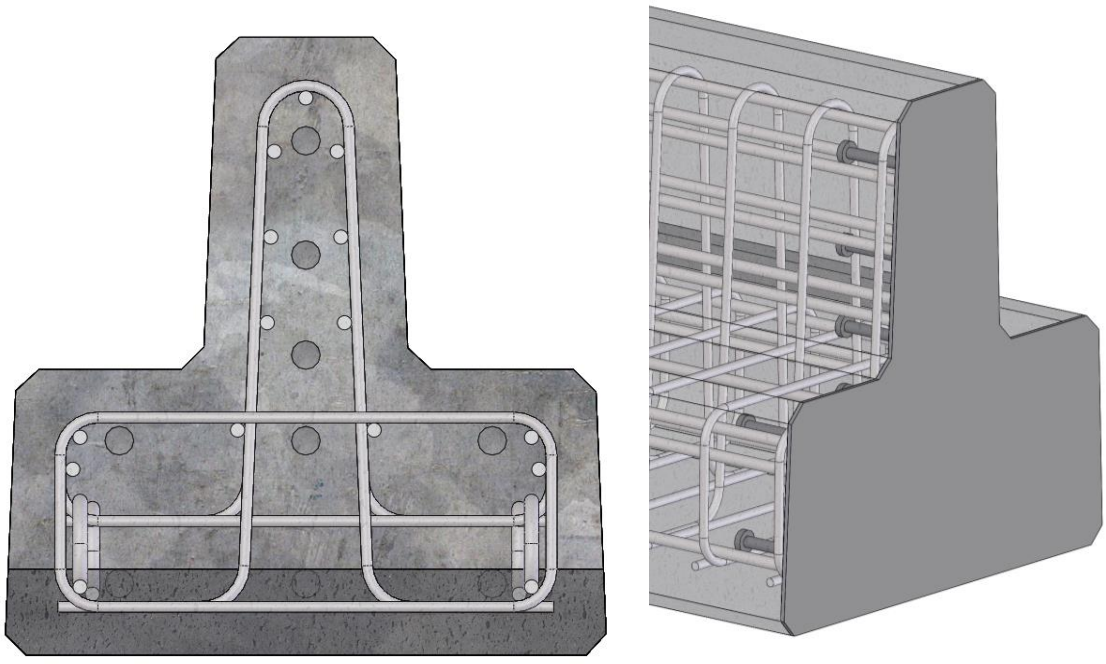

Figure 30. Option 2 PCB Reinforcement, Lower Segment

4.4.1 Simulation of Option 1 Reinforcement

Simulation of the Option 1 reinforcement configuration under MASH test designation no. 3-11 impact conditions resulted in the capture and stable redirection of the impacting pickup truck, as shown in Figures 31 and 32. The maximum dynamic deflection for the Option 1 reinforcement configuration was 17.6 in.

Concrete damage for the upper segment exhibited damage to the outer legs of near the end of the segment and flexural damage near the midspan similar to the initial reinforcement configuration, as shown in Figure 33. However, the magnitude of the damage was slightly less. Concrete damage on the lower barrier segment was also similar to the previous model, as shown in Figure 34.

Plastic rebar strains were also monitored in the simulation, as shown in Figures 35 and 36. Review of the plastic rebar strains found moderate plastic strains in the backside longitudinal bars and the backside of the stirrups on the upper segment of the barrier. The upper segment also showed moderate plastic strains in the outer leg of the inverted U near the end of the segment which allowed the top segment to open slightly. This increased barrier deflections slightly. Moderate plastic strain was also noted on the longitudinal bars near the backside of the lower barrier segment.

A second variation of the Option 1 reinforcement configuration was also simulated that added a hooked bar that spanned the top of the upper barrier segment just above the outer legs, as shown in Figure 37. This bar was intended to provide additional reinforcement similar to a strut and tie and further mitigate the damage and prying open of the outer leg.

Results from the simulation model with the additional hooked bar showed little to no reduction in concrete damage and plastic rebar strain, as shown in Figure 38, nor did it aid in preventing the prying open of the outer leg. As such the use of the hooked bar was not considered in any of the remaining reinforcement configurations.

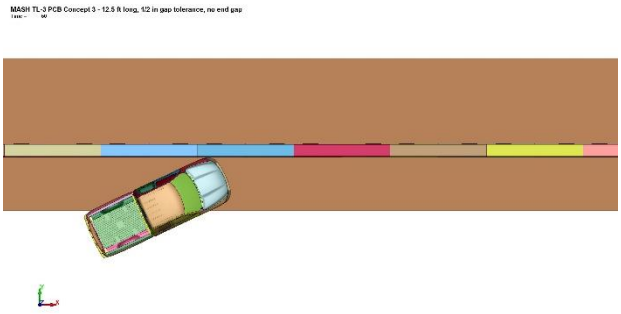

(a) 0.000 sec

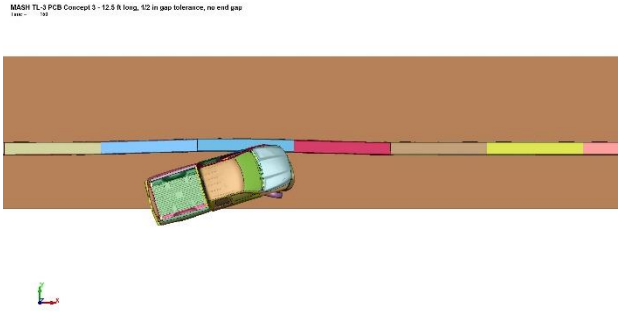

(b) 0.100 sec

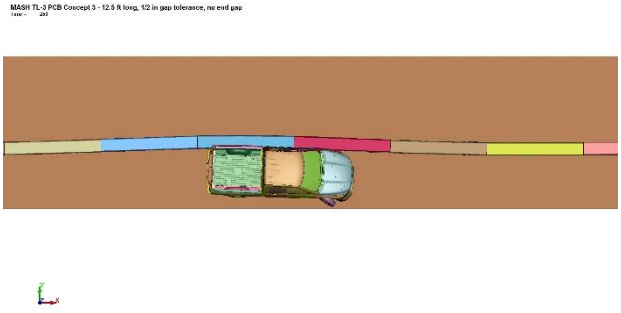

(c) 0.200 sec

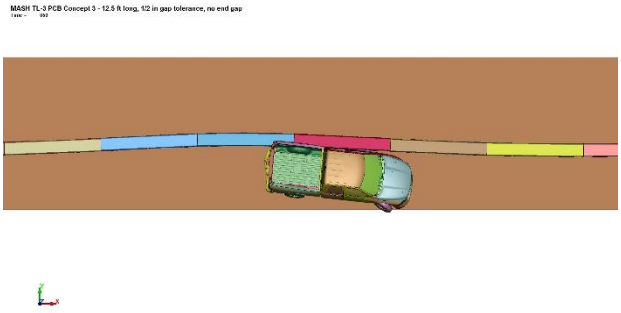

(d) 0.300 sec

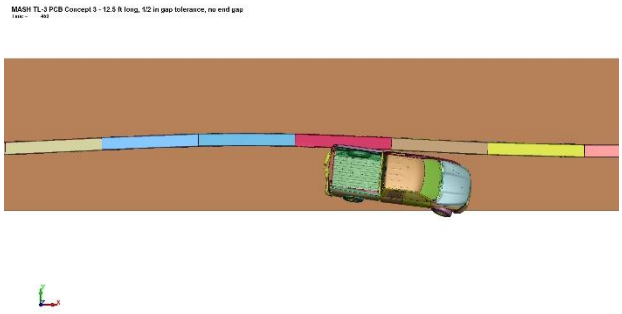

(e) 0.400 sec

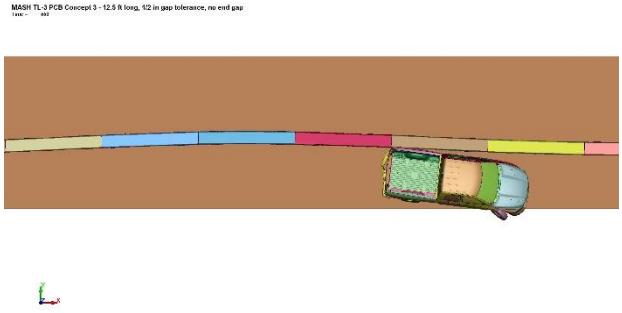

(f) 0.500 sec

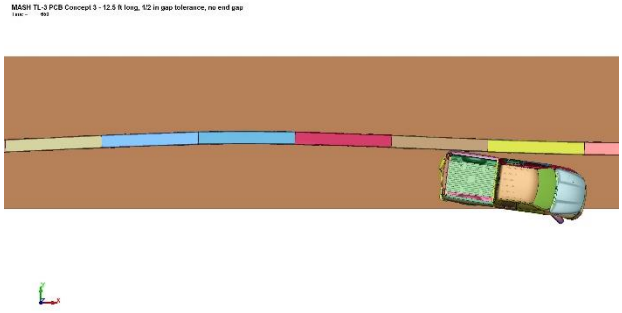

(g) 0.600 sec

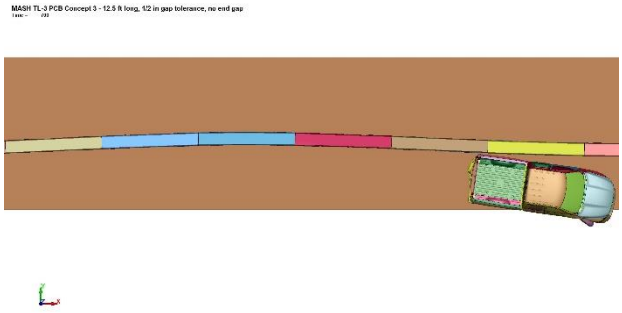

(h) 0.650 sec

Figure 31. Option 1 Reinforcement Configuration, Overhead Sequential Images

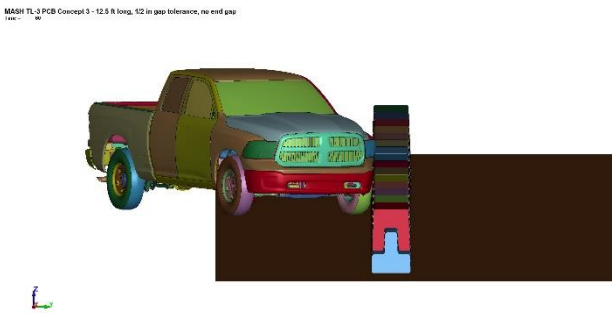

(a) 0.000 sec

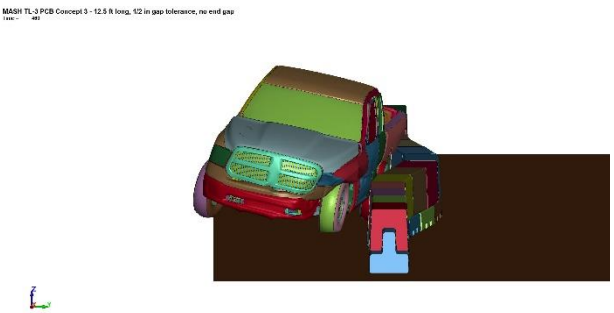

(e) 0.400 sec

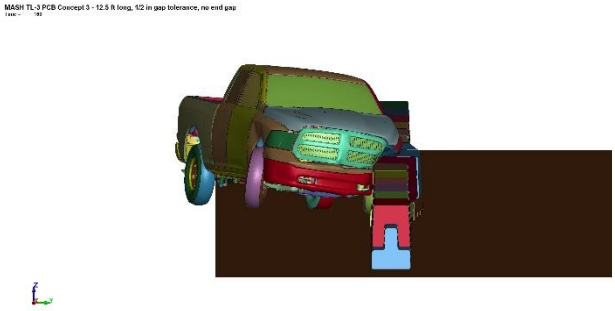

(b) 0.100 sec

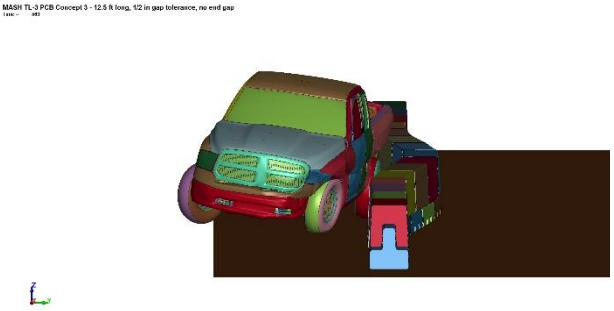

(f) 0.500 sec

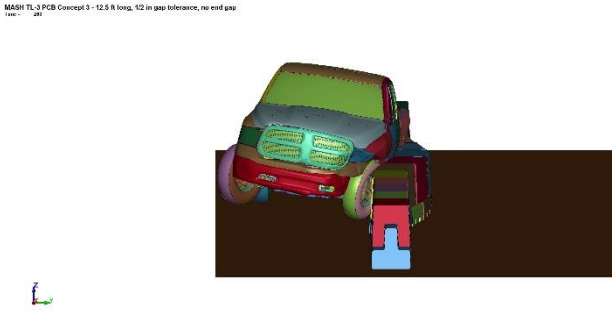

(c) 0.200 sec

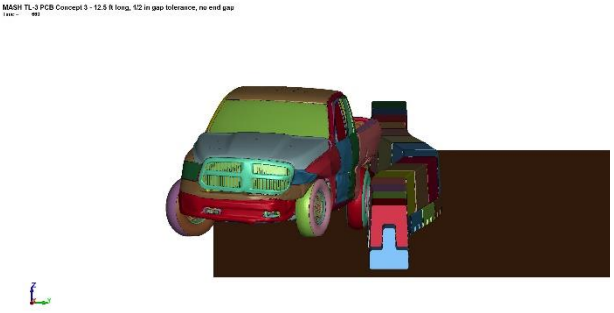

(g) 0.600 sec

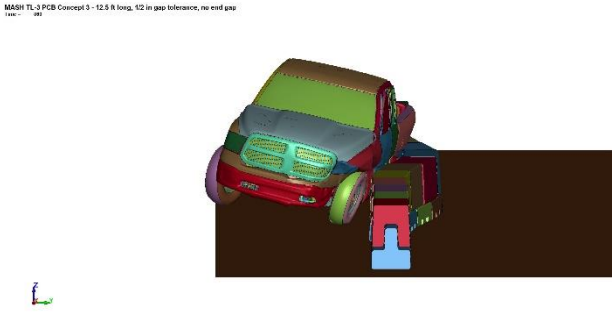

(d) 0.300 sec

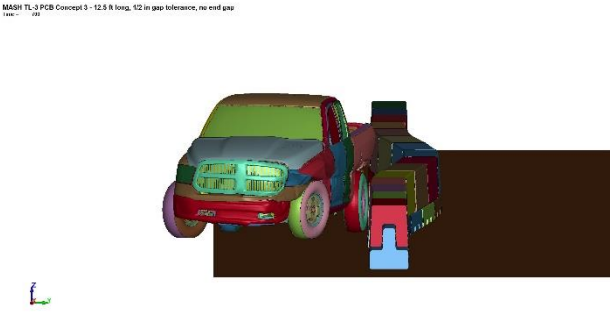

(h) 0.650 sec

Figure 32. Option 1 Reinforcement Configuration, Downstream Sequential Images

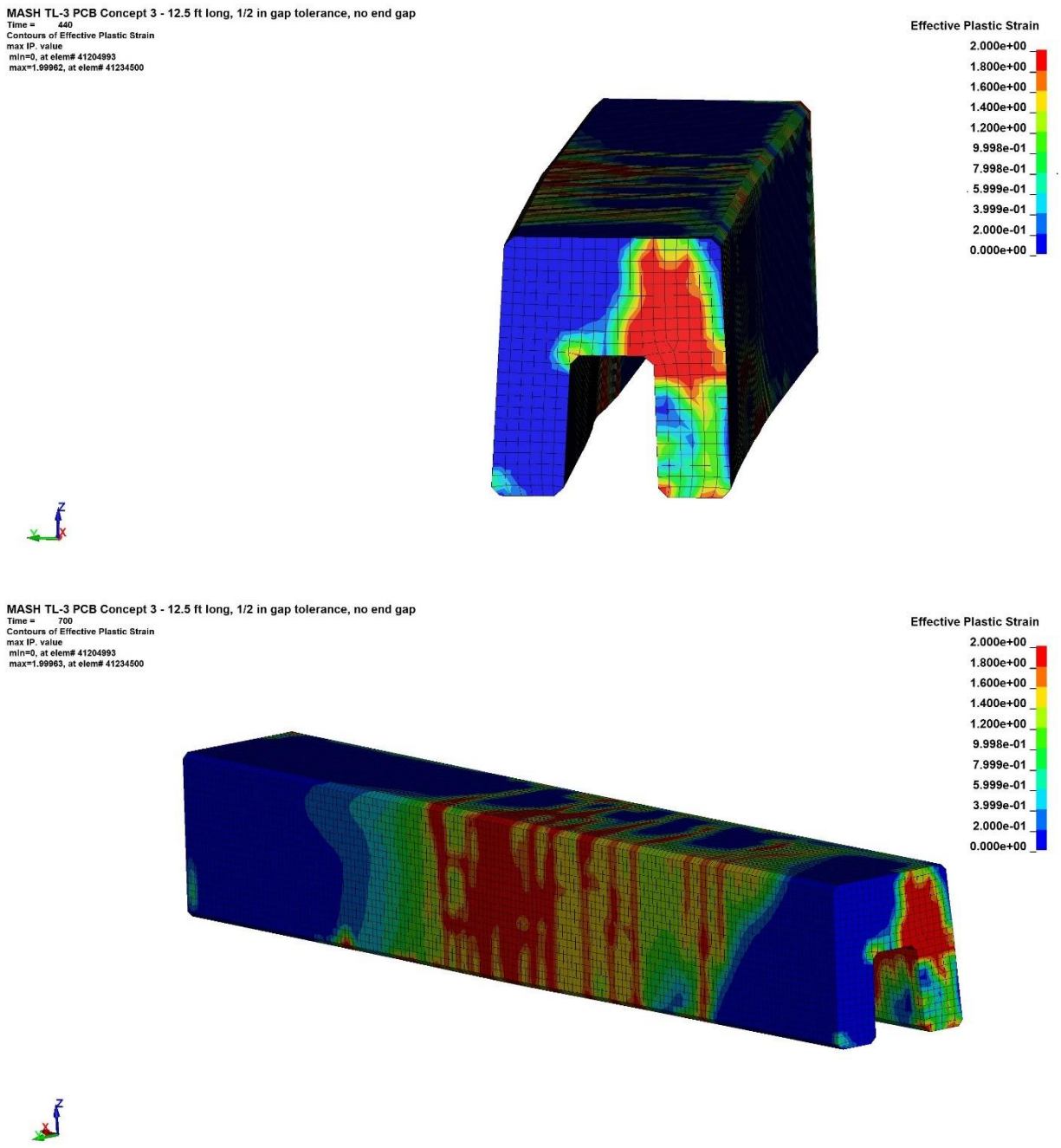

Figure 33. Option 1 Reinforcement Configuration, Upper Segment Concrete Damage

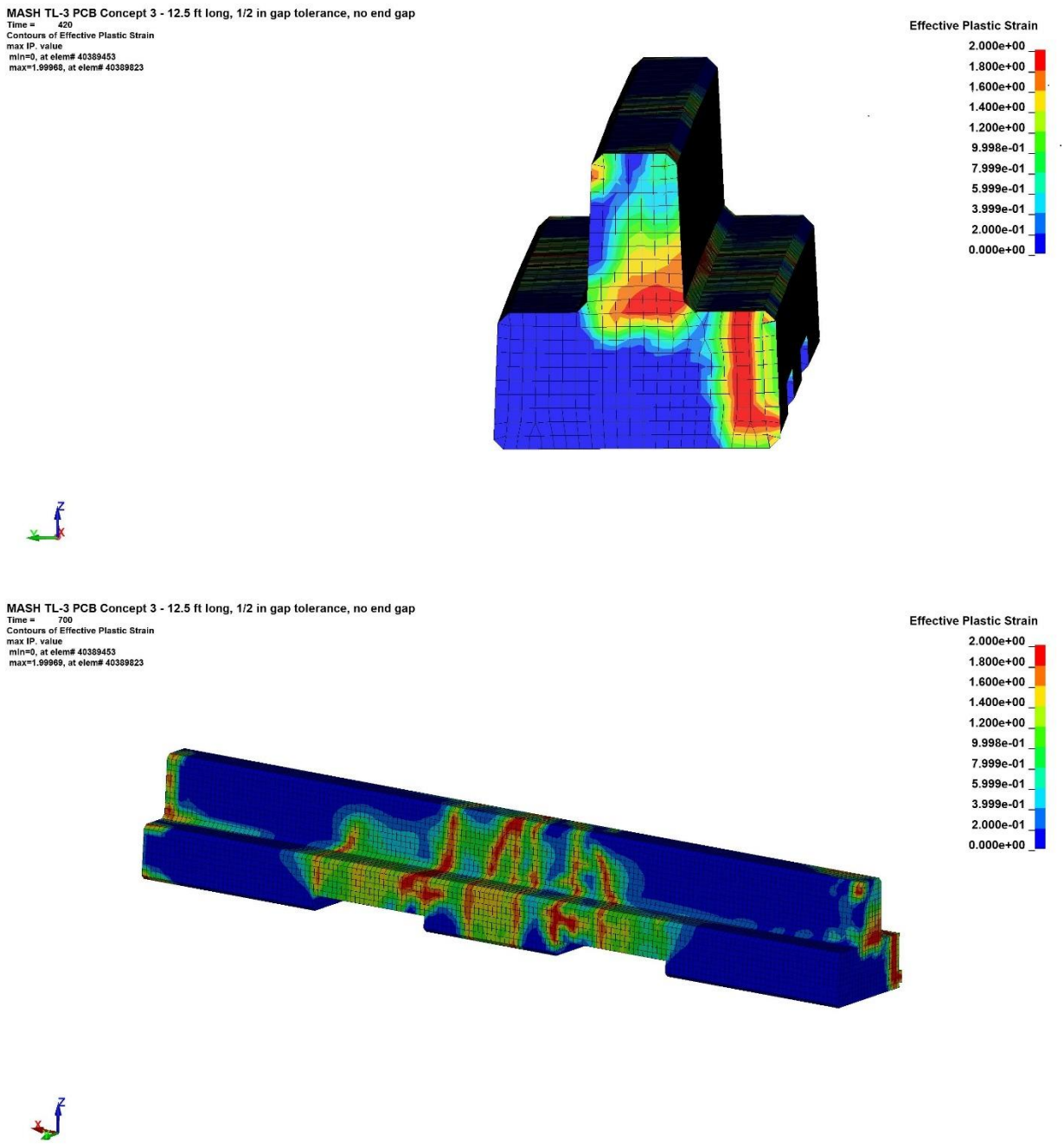

Figure 34. Option 1 Reinforcement Configuration, Lower Segment Concrete Damage

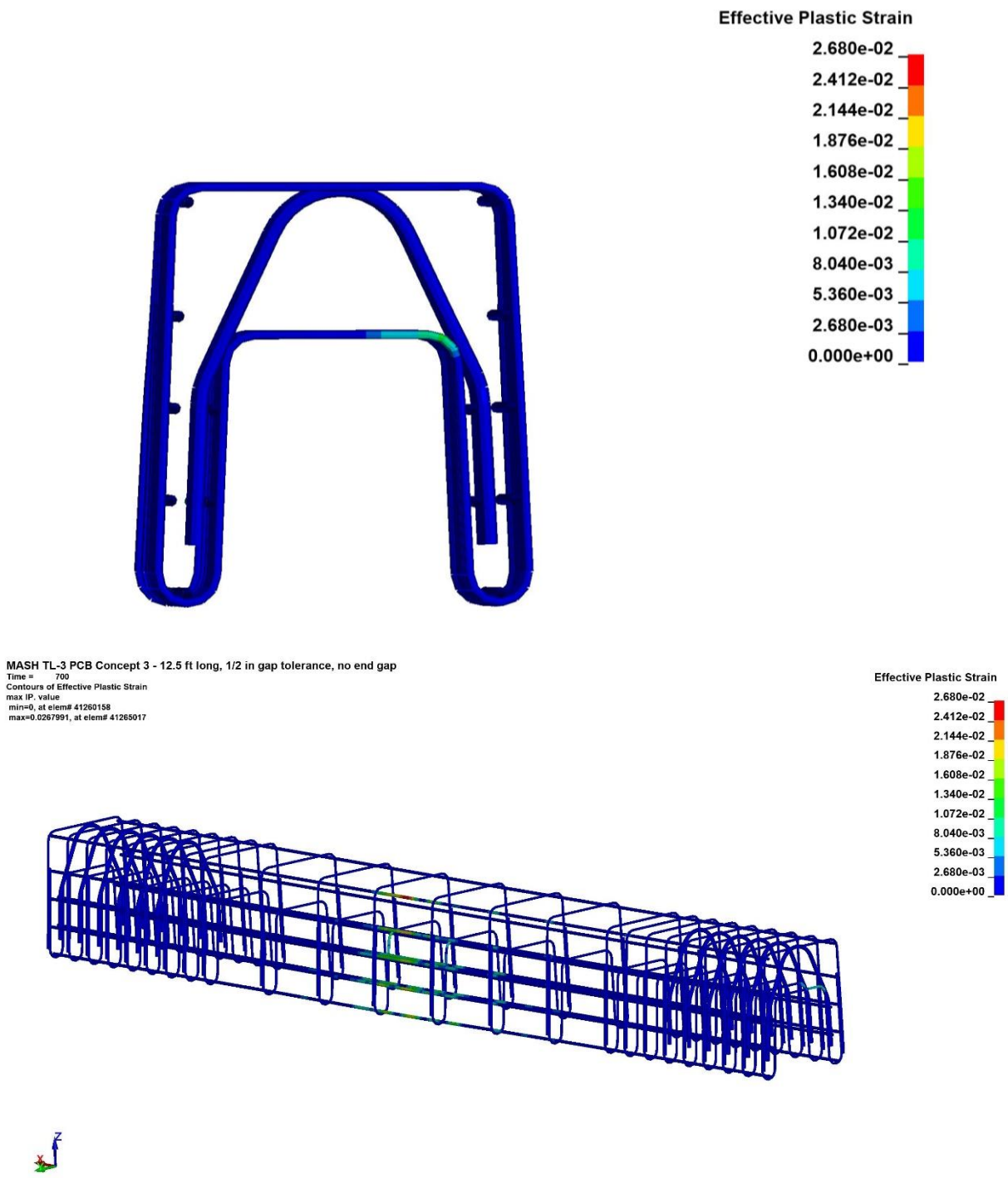

Figure 35. Option 1 Reinforcement Configuration, Upper Segment Rebar Plastic Strain

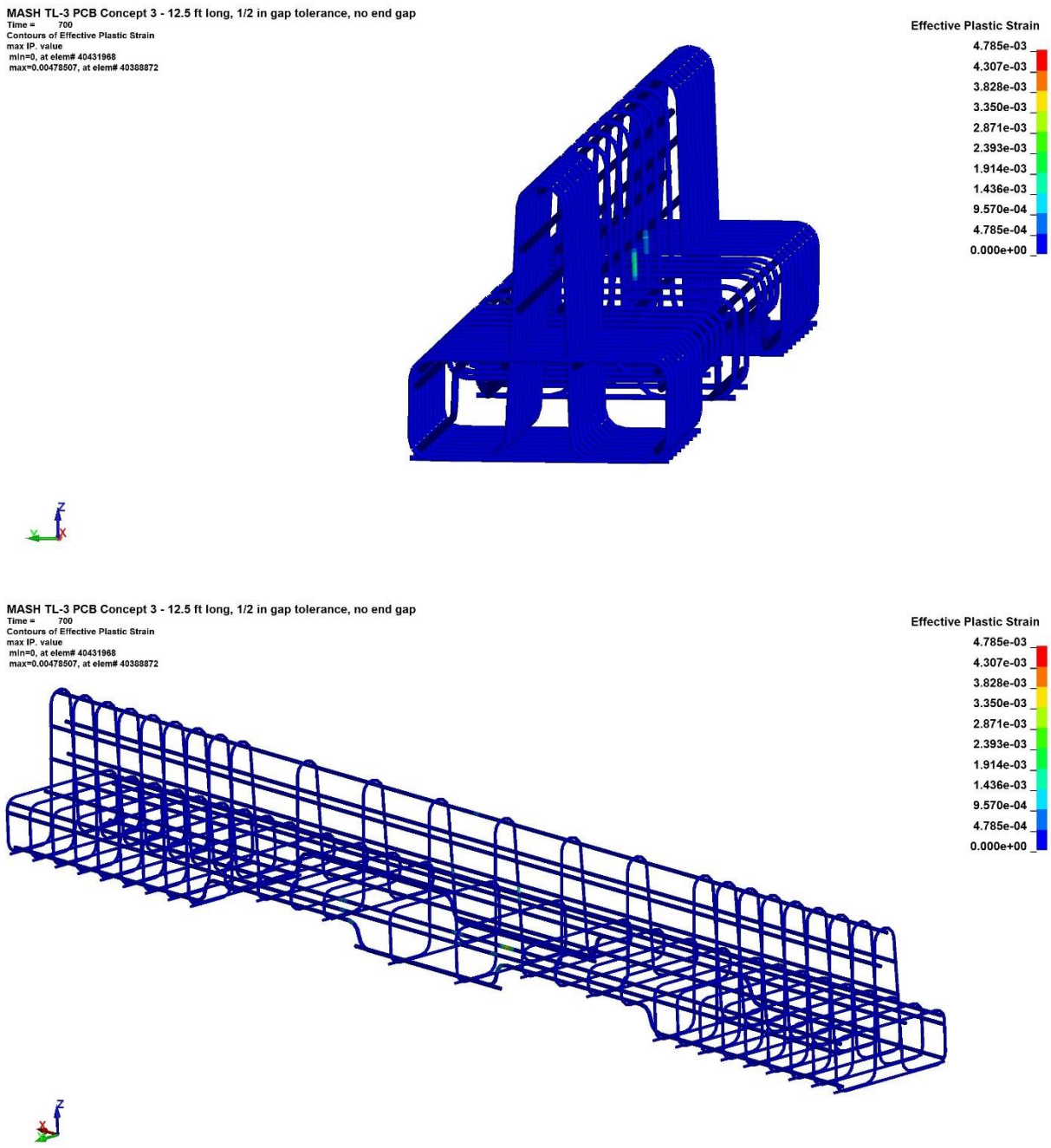

Figure 36. Option 1 Reinforcement Configuration, Lower Segment Rebar Plastic Strain

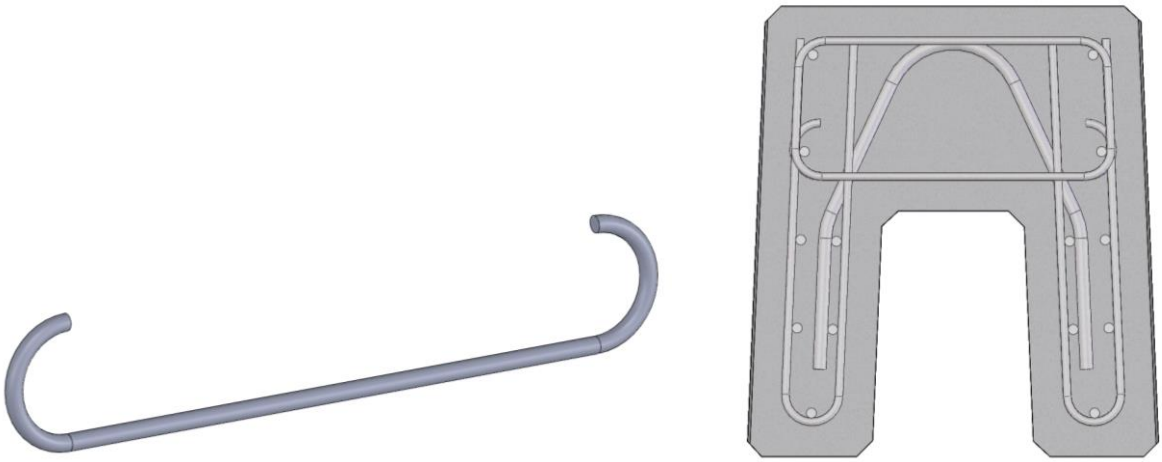

Figure 37. Option 1 Reinforcement Configuration with Hook Bar

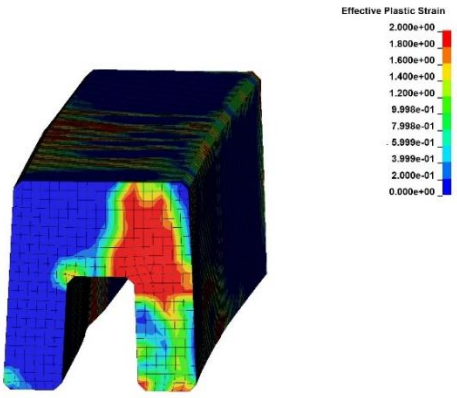

(a) Option 1 Reinforcement

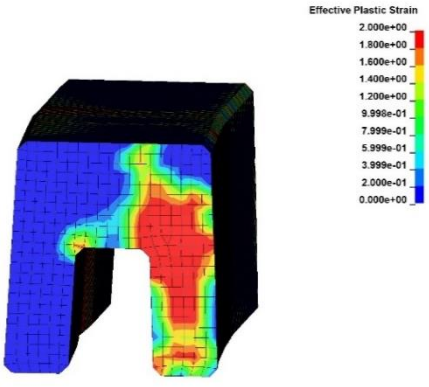

(b) Option 1 Reinforcement with Hook Bar

Figure 38. Option 1 Reinforcement Configuration with Hook Bar, Concrete Damage

4.4.2 Simulation of Option 2 Reinforcement

Simulation of the Option 2 reinforcement configuration under MASH test designation no. 3-11 impact conditions also resulted in a capture and stable redirection of the impacting pickup truck, as shown in Figures 39 and 40. The maximum dynamic deflection for the Option 2 reinforcement configuration was 14.1 in.

Concrete damage was improved due to the addition of the steel caps on the ends of the segments. The upper segment did not demonstrate deflection and opening of the outer legs near the end of the segment. Flexural damage near the midspan of the upper barrier segment was also reduced as compared to the Option 1 reinforcement configuration due to the increased longitudinal steel in the upper segment. Concrete damage on the lower barrier segment was also reduced with the steel end cap limiting deformation of the center pillar near the ends of the barrier, and the added longitudinal bars reduced flexural damage.

The improved structural capacity could be more easily quantified by examining the plastic rebar strains, as shown in Figures 41 and 42. Review of the plastic rebar strains found that the plastic strain in the stirrups near the ends of the outer legs of the upper barrier segment were largely eliminated. Moderate plastic strains were still observed in the longitudinal bars due to flexural loading of the upper segment, but the magnitude of the strains was significantly reduced when compared to Option 1. Plastic rebar strains in the lower barrier segment were also reduced in terms of their location and magnitude.

Simulation of the Option 2 reinforcement configuration under MASH test designation no. 3-11 impact conditions demonstrated improved structural performance as compared to the previous variations. Deformation of the thin sections of the upper and lower barrier segments was mitigated, and overall plastic rebar strains were reduced. Plastic strain was still noted in the outer longitudinal bars of both the upper and lower segments due to flexural loading of the barrier. The improvement in structural capacity lowered local deformations of the segments which led to a decrease in the dynamic deflection of the system as a whole as compared to the two previous reinforcement configurations.

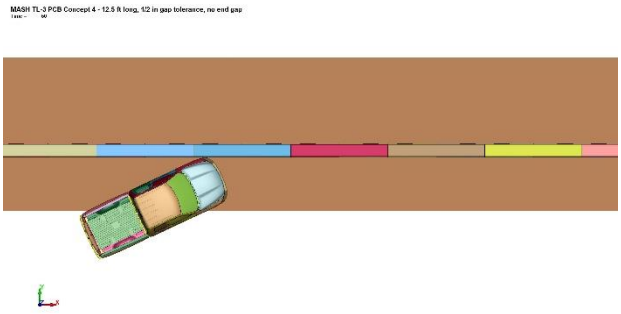

(a) 0.000 sec

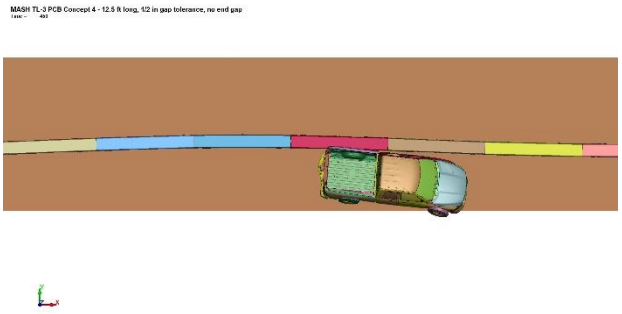

(e) 0.400 sec

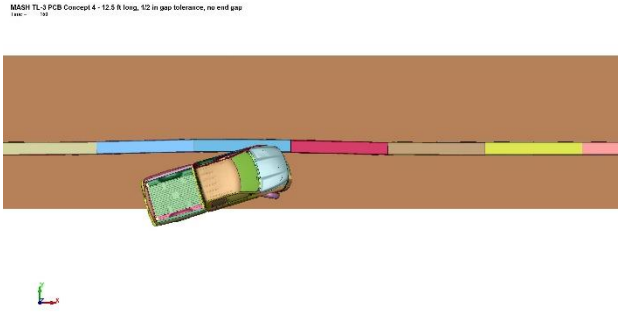

(b) 0.100 sec

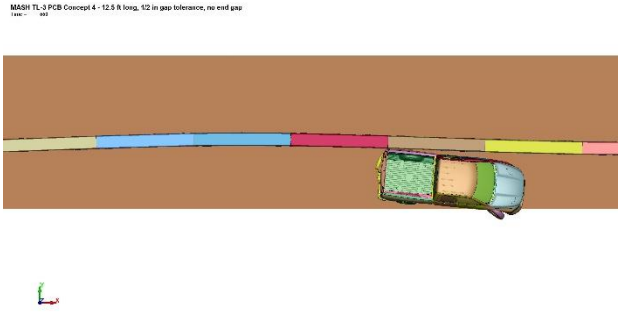

(f) 0.500 sec

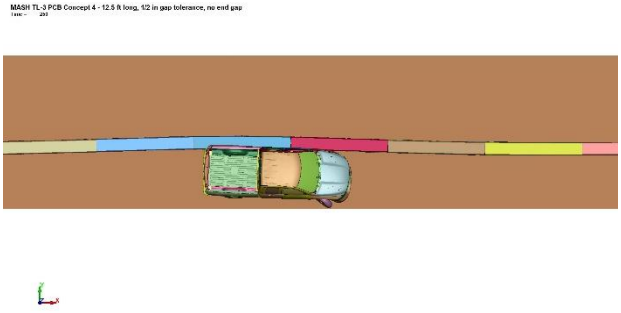

(c) 0.200 sec

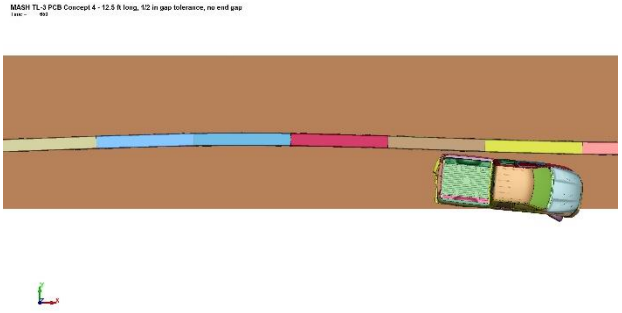

(g) 0.600 sec

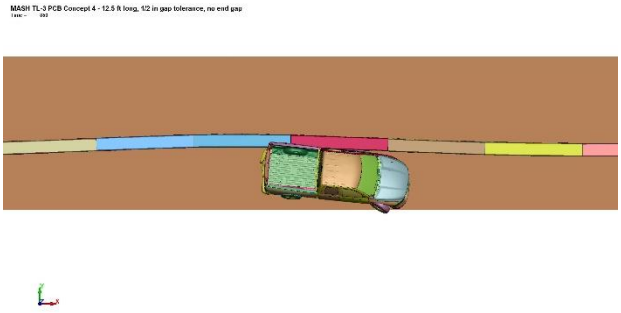

(d) 0.300 sec

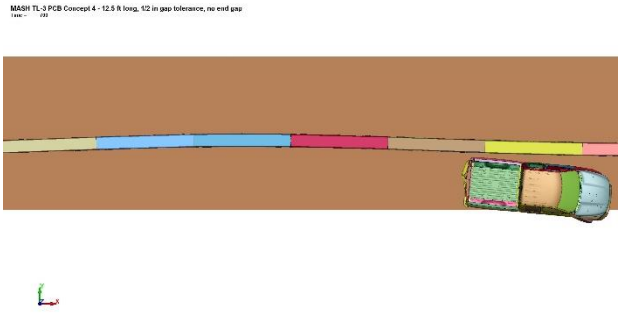

(h) 0.650 sec

Figure 39. Option 2 Reinforcement Configuration, Overhead Sequential Images

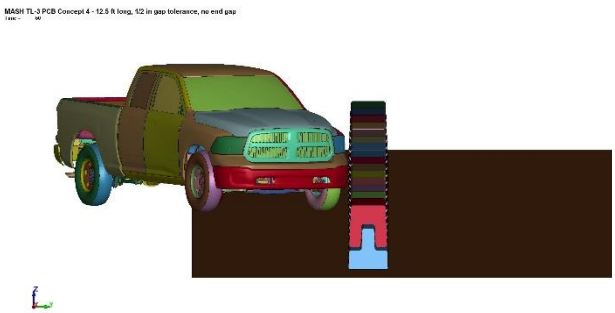

(a) 0.000 sec

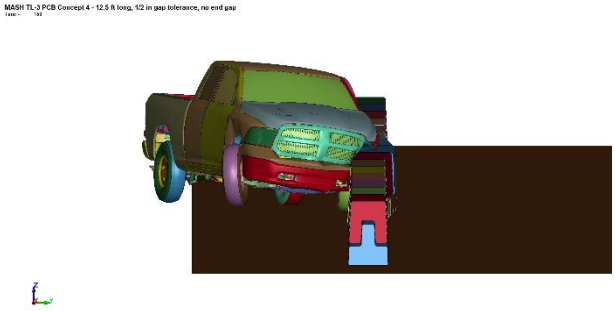

(b) 0.100 sec

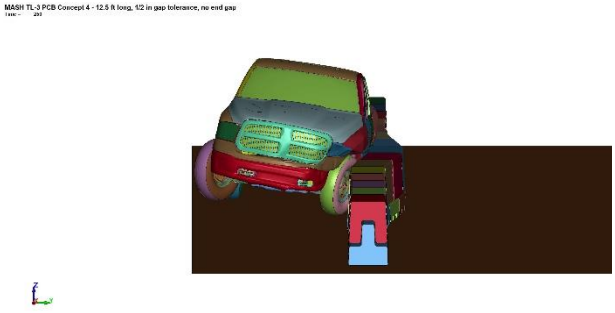

(c) 0.200 sec

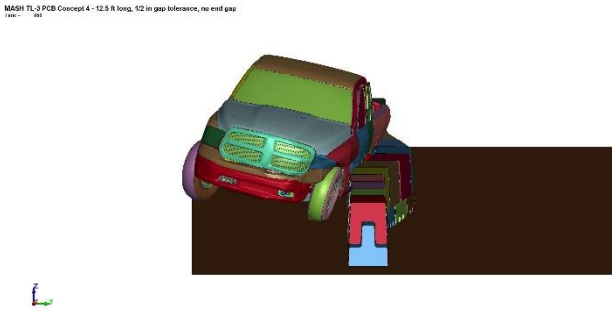

(d) 0.300 sec

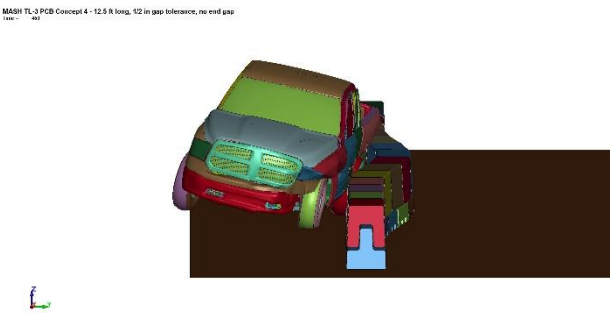

(e) 0.400 sec

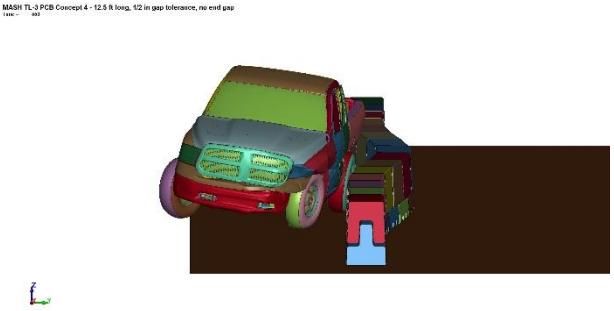

(f) 0.500 sec

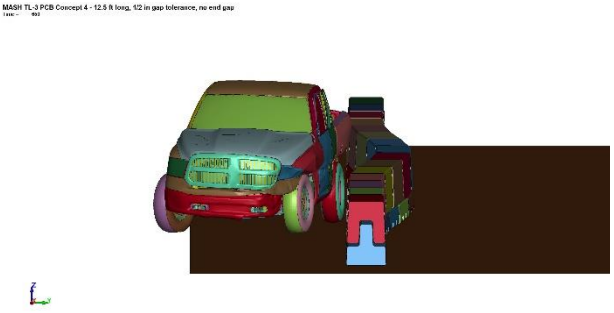

(g) 0.600 sec

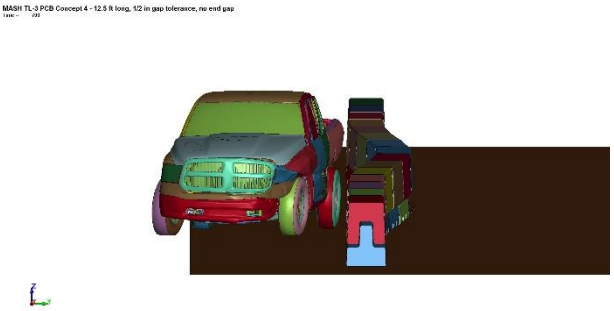

(h) 0.650 sec

Figure 40. Option 2 Reinforcement Configuration, Downstream Sequential Images

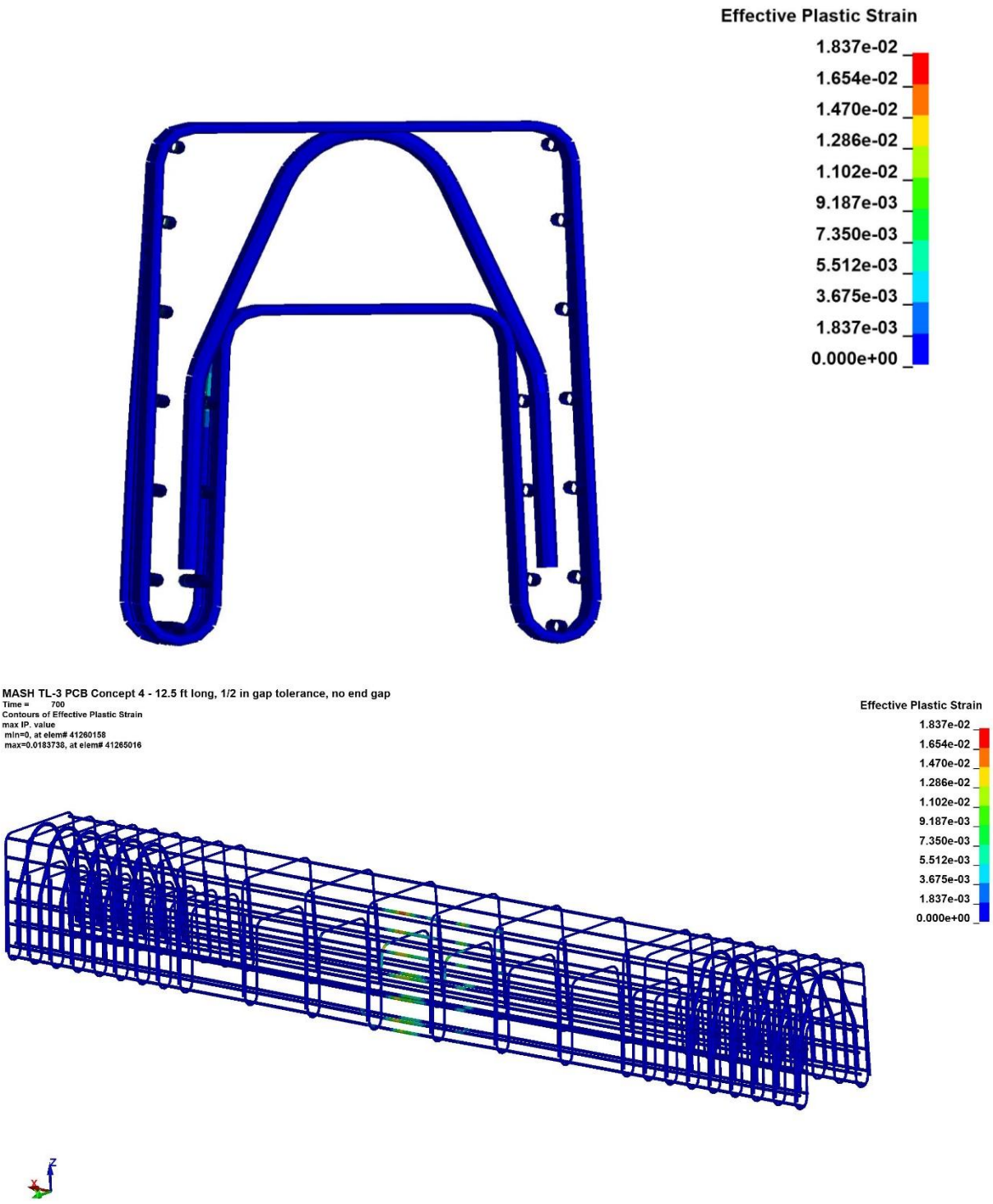

Figure 41. Option 2 Reinforcement Configuration, Upper Segment Rebar Plastic Strain

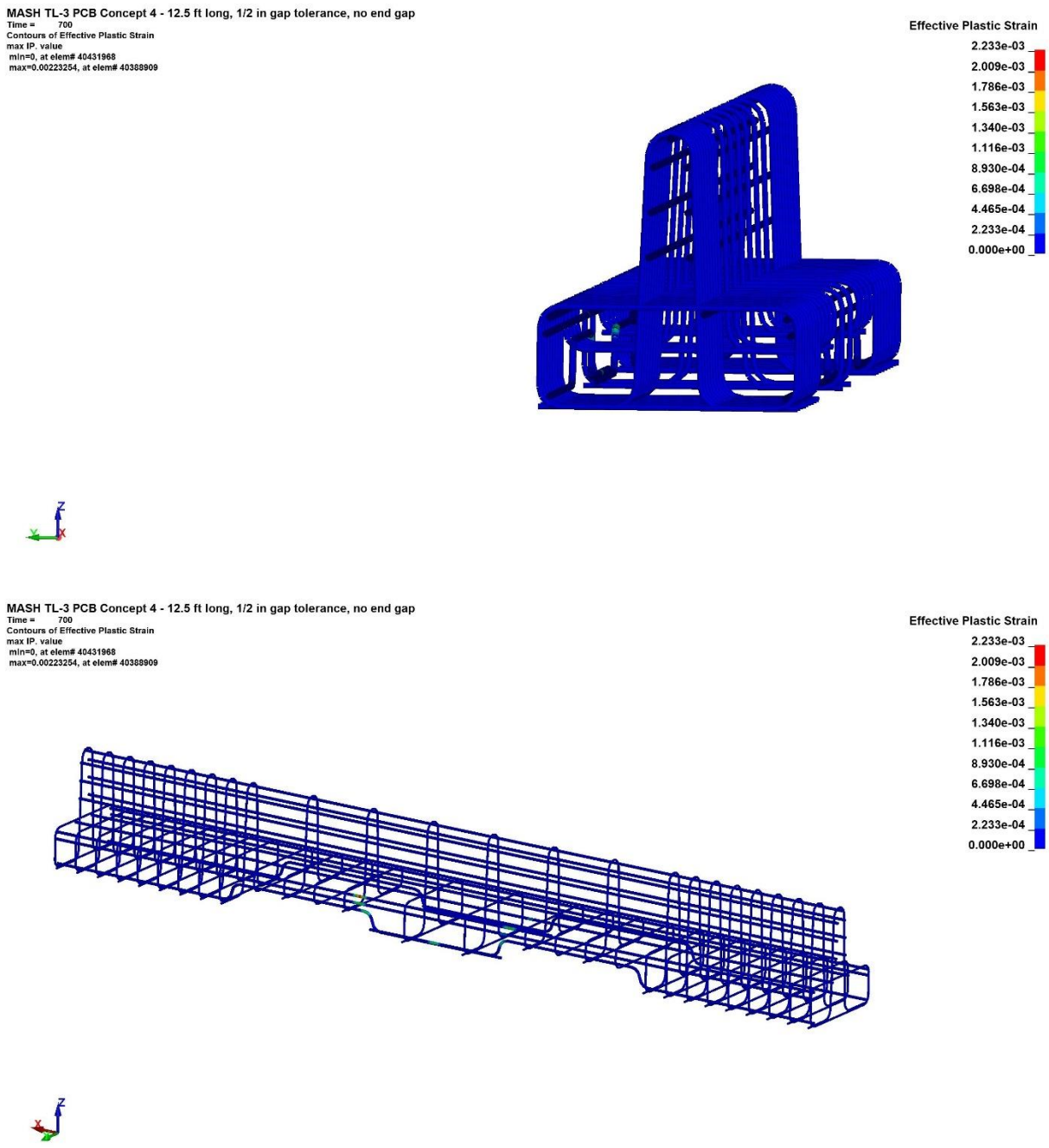

Figure 42. Option 2 Reinforcement Configuration, Lower Segment Rebar Plastic Strain

4.4.3 Simulation of Option 3 Reinforcement

Simulation of the Option 3 reinforcement configuration under MASH test designation no. 3-11 impact conditions resulted in a capture and stable redirection of the impacting pickup truck and the lowest overall deflection and barrier damage due to the use of Grade 80 steel and no. 5 longitudinal bars, as shown in Figures 43 and 44. The maximum dynamic deflection for the Option 2 reinforcement configuration was 13.8 in.

The use of larger longitudinal bars and higher-grade steel further reduced concrete damage and deformation. The narrow sections of both the upper and lower barrier segments did not exhibit deformations and flexural damage of both segments was further reduced.

The plastic rebar strains observed in the simulation of the Option 3 barrier reinforcement were also improved, as shown in Figures 45 and 46. Review of the plastic rebar strains found that plastic strains in the stirrups near the ends of the outer legs of the upper barrier segment and center pillar of the lower barrier segment were largely eliminated. Only minor plastic strains were observed due to flexural loading of the upper segment, and no plastic rebar strains were observed in the lower barrier segment.

Simulation of the Option 3 reinforcement configuration under MASH test designation no. 3-11 impact conditions demonstrated improved structural capacity as compared to the previous variations and largely mitigated the potential for structural damage to the barrier segments during impact. The reinforcement configuration also provided for the lowest dynamic deflection of the barrier system.

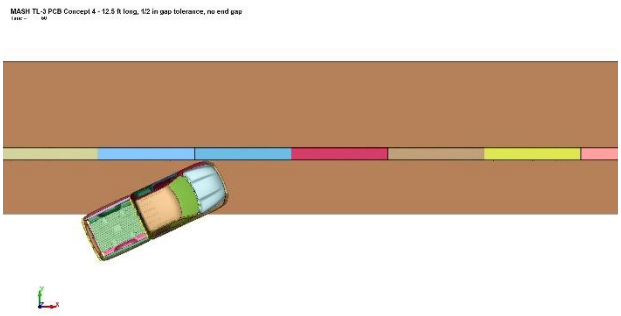

(a) 0.000 sec

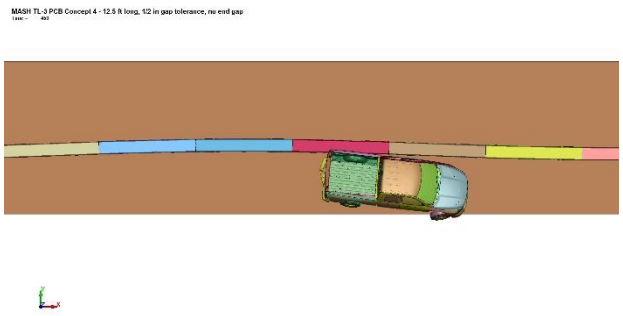

(e) 0.400 sec

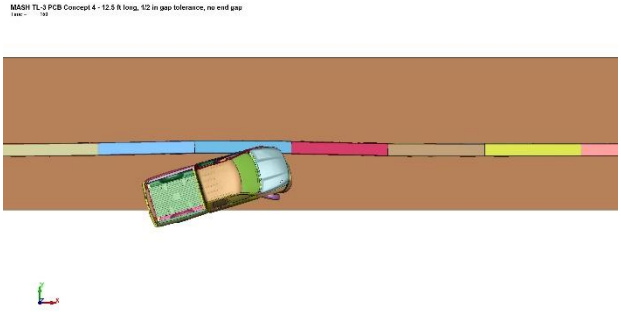

(b) 0.100 sec

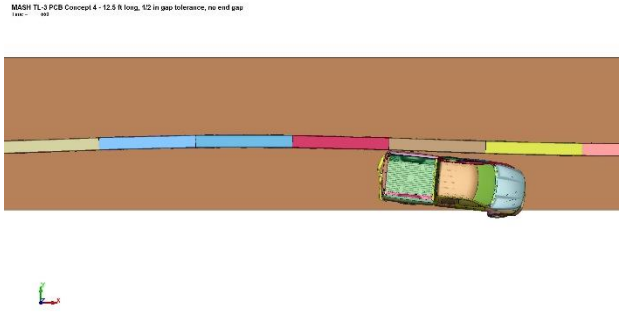

(f) 0.500 sec

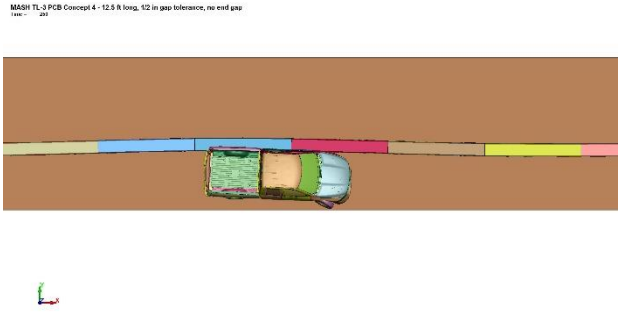

(c) 0.200 sec

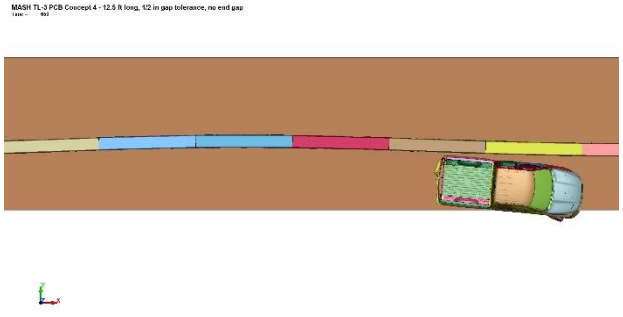

(g) 0.600 sec

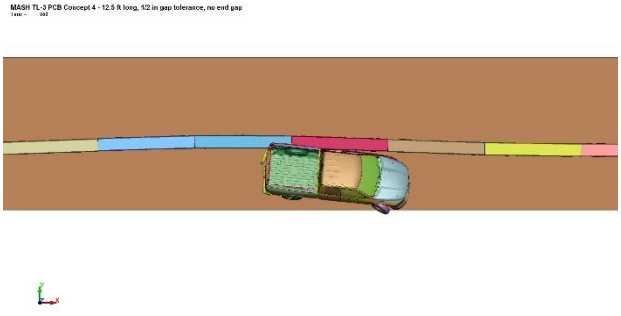

(d) 0.300 sec

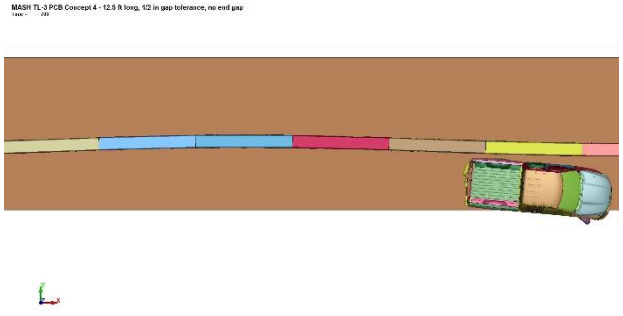

(h) 0.650 sec

Figure 43. Option 3 Reinforcement Configuration, Overhead Sequential Images

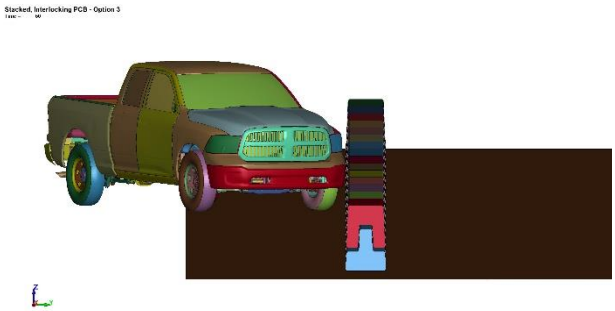

(a) 0.000 sec

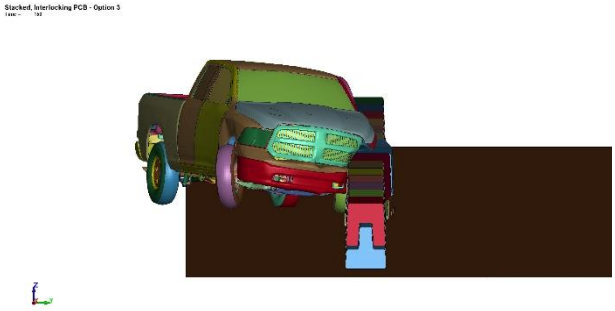

(b) 0.100 sec

(c) 0.200 sec

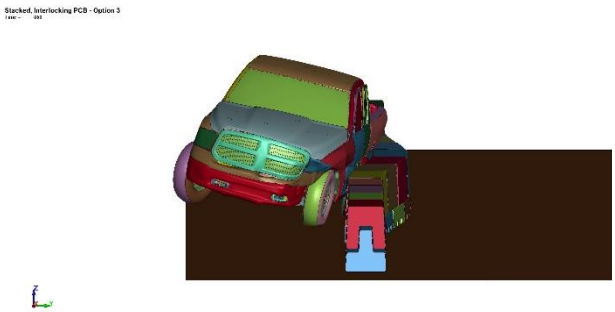

(d) 0.300 sec

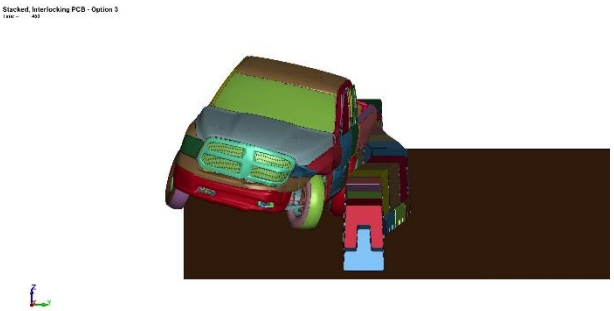

(e) 0.400 sec

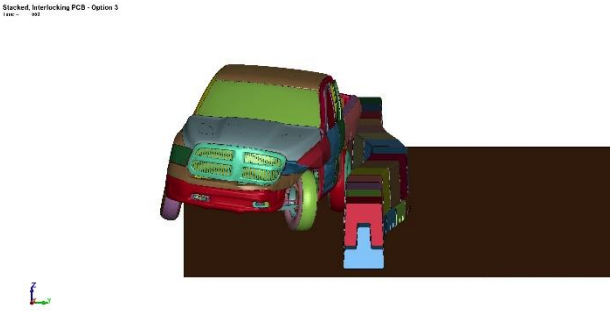

(f) 0.500 sec

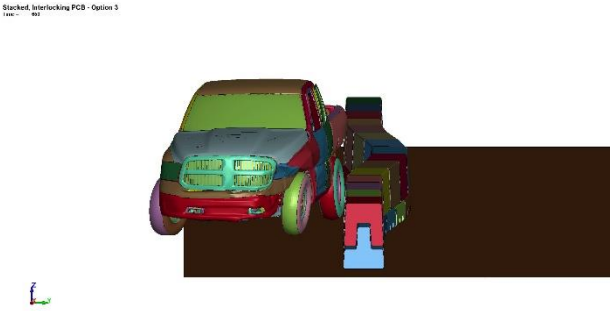

(g) 0.600 sec

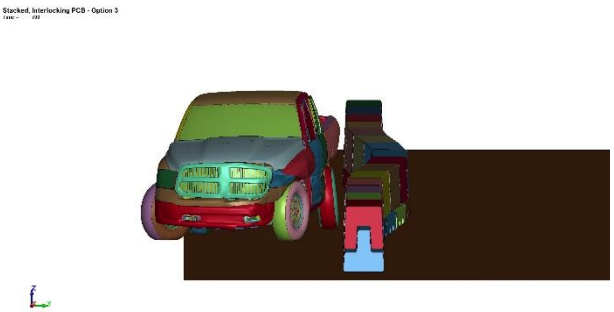

(h) 0.650 sec

Figure 44. Option 3 Reinforcement Configuration, Downstream Sequential Images

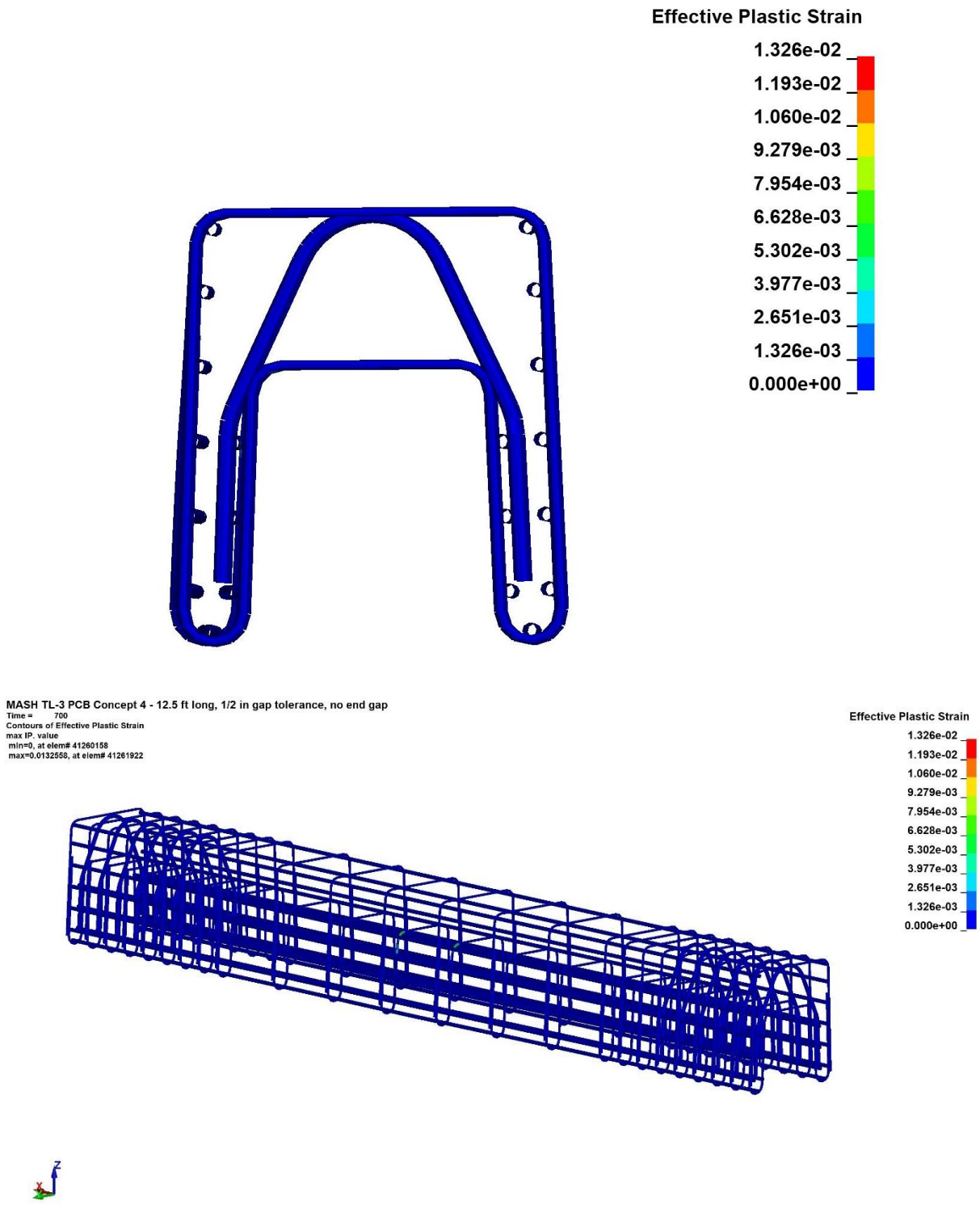

Figure 45. Option 3 Reinforcement Configuration, Upper Segment Rebar Plastic Strain

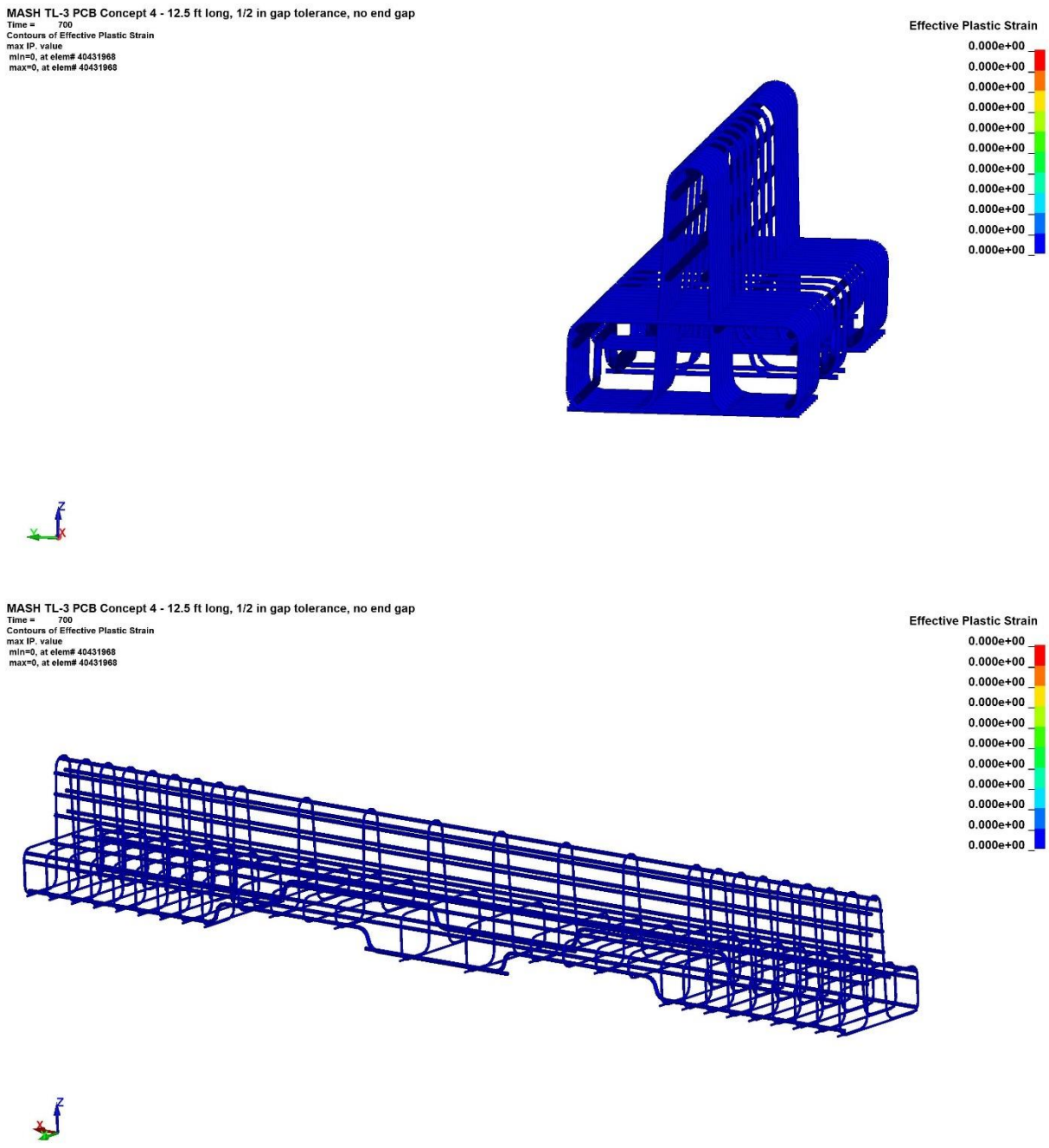

Figure 46. Option 3 Reinforcement Configuration, Lower Segment Rebar Plastic Strain

4.5 Simulation of Barrier Segment Length and Curvature

The achievable horizontal curvature radius was another parameter that was investigated through LS-DYNA simulation. As noted previously, the curvature radius that could be achieved by the staggered, interlocking barrier segment concept was dependent on the segment length and the internal tolerance gap between the upper and lower barrier segments. While the horizontal curvature radius could be estimated based on the barrier geometry in CAD, the effect of modifications to allow tighter curvature radii on the overall barrier performance during impact had not been investigated. Specifically, it was desired to determine what level of increase in barrier dynamic deflection may be induced if the curvature radius was reduced.

A simulation model of the staggered, interlocking barrier segment concept with the Option 2 reinforcement configuration was performed with the segment length reduced to 8 ft. The barrier simulations to date had already used a larger internal tolerance gap of ½ in., so reduction of that tolerance would only serve to increase the curvature radius and reduce barrier dynamic deflections. The simulation of the staggered, interlocking barrier segment concept with 8-ft long segments demonstrated similar vehicle capture and redirection performance as the previously simulated barrier with 12.5-ft long segments, as shown in Figures 47 and 48. Barrier structural damage was nearly identical between the 8-ft long and 12.5-ft barrier segment lengths. The primary difference induced by the shorter segment length was an increase in the dynamic deflection of the barrier system due to the increased number of joints in the system allowing increased flexibility. The dynamic deflection of the 8-ft long segment similar increased to 20.9 in. as compared to 14.1 in. for the 12.5-ft long segment simulation.

The researchers believed that shorter segment lengths were a more critical barrier configuration due to the increased barrier deflection observed. If shorter segment lengths were successfully full-scale crash tested to MASH TL-3, it was also believed that longer barrier lengths could safely be used as long as the structural properties of the longer segments were consistent with the as-tested barrier. Validated simulations of the as-tested barrier system could then be modified to incorporate longer segment lengths and estimate dynamic deflections for the longer segments lengths if desired.

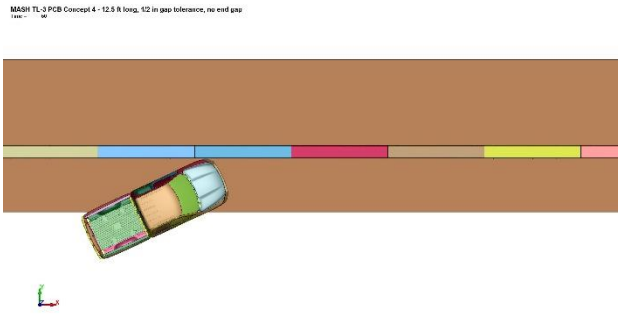

(a) 0.000 sec

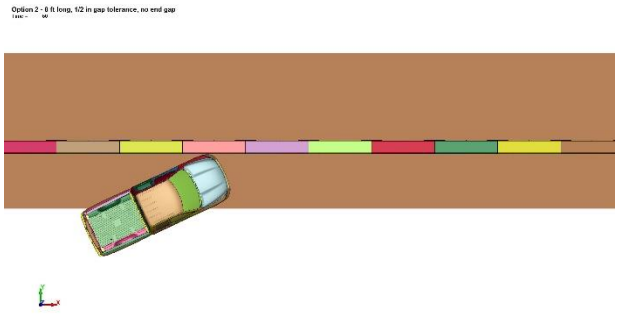

(1) 0.000 sec

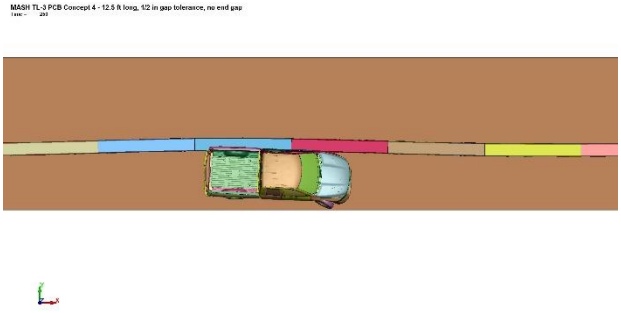

(b) 0.200 sec

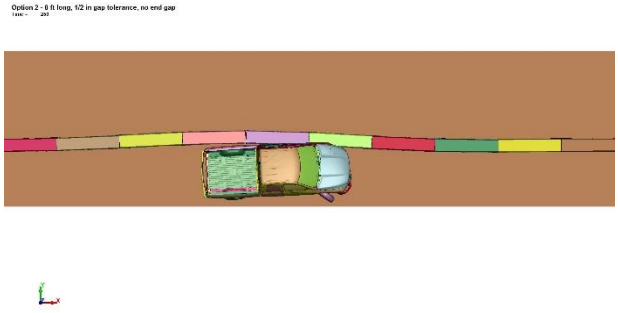

(b) 0.200 sec

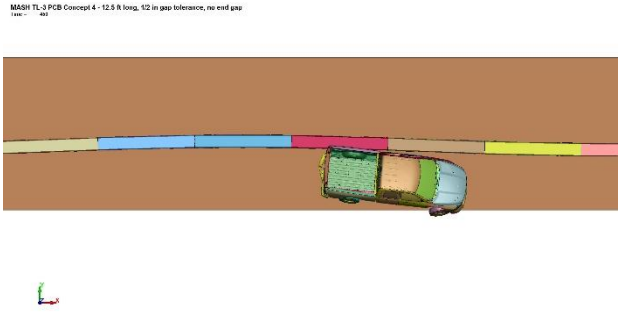

(c) 0.400 sec

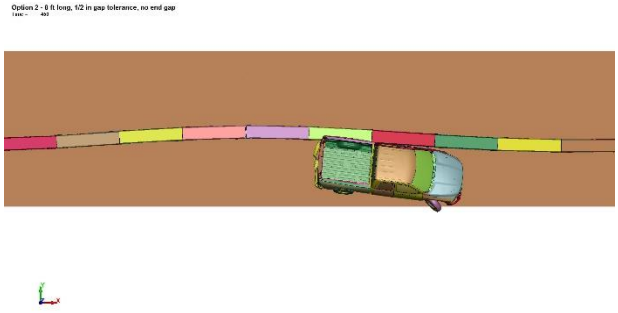

(c) 0.400 sec

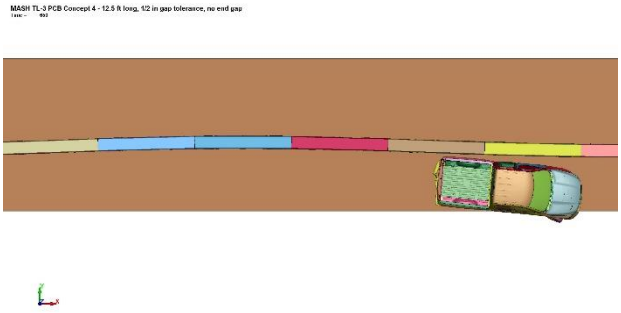

(d) 0.600 sec

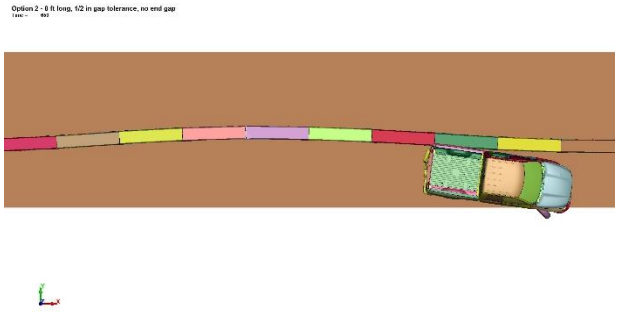

(d) 0.600 sec

12.5-ft Long Segment

8-ft Long Segment

Figure 47. Option 2 Reinforcement Configuration with Variable Segment Lengths, Overhead Sequential Images

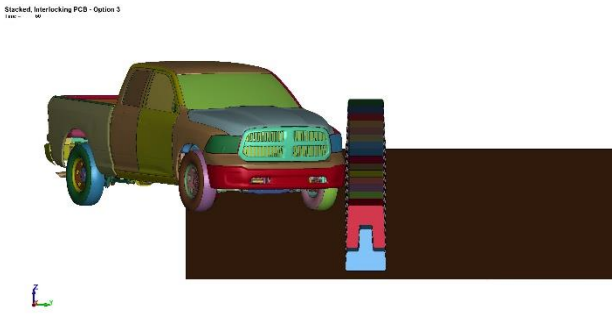

(a) 0.000 sec

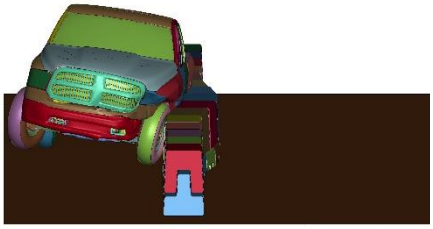

(b) 0.200 sec

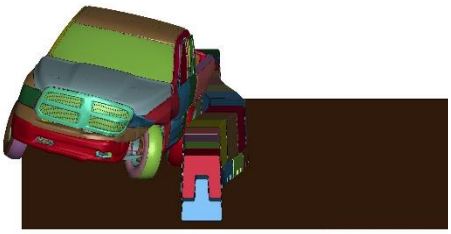

(c) 0.400 sec

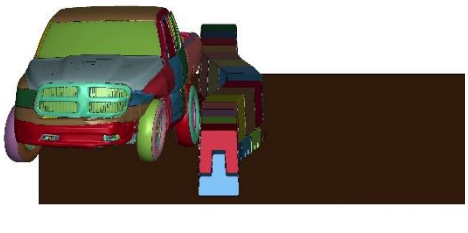

(d) 0.600 sec

12.5-ft Long Segment

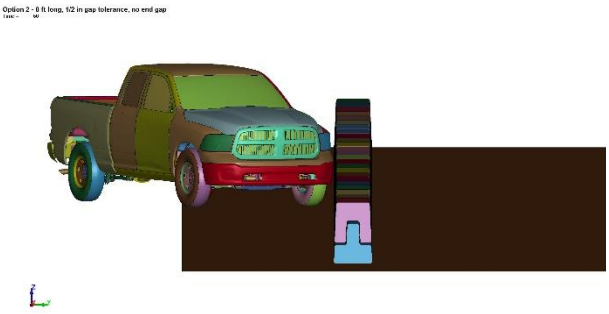

(a) 0.000 sec

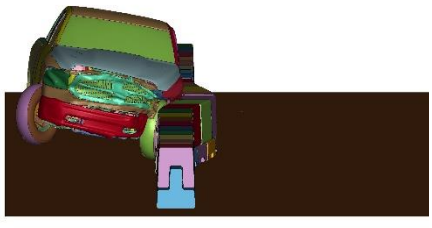

(b) 0.200 sec

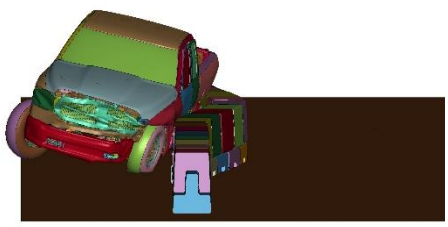

(c) 0.400 sec

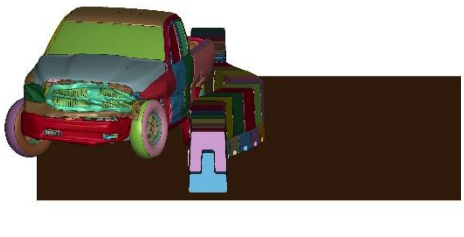

(d) 0.650 sec

8-ft Long Segment

Figure 48. Option 2 Reinforcement Configuration with Variable Segment Lengths, Downstream Sequential Images

4.6 Determination of Prototype PCB Reinforcement and Segment Length

Following the simulation analysis of barrier reinforcement and segment length, the results were reviewed with the sponsors to determine the best option for the configuration of a prototype PCB design for full-scale crash testing.

4.6.1 Selection of Barrier Reinforcement

The staggered, interlocking segment PCB design required increased reinforcement as compared to conventional PCB segments due to the reduced barrier deflection increasing the overall barrier loading and the geometry of the upper and lower segments creating high load demands on relatively thin reinforced concrete sections. Analysis of four potential PCB reinforcement configurations showed that all of the proposed reinforcement configurations appeared capable of meeting MASH TL-3 impact loading by safely capturing and redirecting the impacting vehicle. Increased barrier reinforcement tended to reduce the level of barrier damage observed and reduce the dynamic deflection of the barrier system.

While increased steel reinforcement reduced damage and barrier deflection, any increase in steel reinforcement has an associated cost. To better illustrate the tradeoff between barrier damage, deflection, and cost, Table 6 summarizes barrier damage, dynamic deflection, and estimated material costs for the four reinforcement concepts. Additionally, two current MASH TL-3 compliant PCBs, the Midwest F-shape PCB and the Oregon F-shape PCB, were included for comparison purposes. Costs for each PCB system were based on material costs only with assumed concrete costs of $200/cubic yard and steel costs of $2.50/lb. Barrier damage and dynamic deflection were based on observed damage in MASH TL-3 simulation or crash testing.

The staggered, interlocking segment PCB provided a 78.1 percent to 82.2 percent reduction in barrier deflection as compared to the existing F-shape PCBs, but the increased steel reinforcement for the design increased the cost by at least 66.6 percent over existing F-shape PCB designs. Providing sufficient reinforcement to minimize damage to the PCB segments can be achieved, but doing so will potentially increase the cost 193.5 percent over conventional F-shape PCBs, which represented nearly three times increase in cost. The increased costs were partially induced by the design criteria of the barrier system which required a simple barrier section with limited joint hardware and joint complexity combined with a drastic reduction in dynamic deflection. Because the proposed PCB designs reduced deflection significantly, cost comparisons may be more appropriately compared to anchored PCB designs with similar deflections. In that case, the estimated material costs for the new PCB system variations may be less of a concern. Finally, the costs calculated were only based on material costs and not the service life of the barrier segments. Increased reinforcement and associated increases in barrier durability may result in cost savings through increased service life and fewer segment replacements following impacts.

In the end, the comparison suggested that the staggered, interlocking segment PCB will greatly reduce deflections with an associated cost increase. Additionally, completely preventing damage to the new PCB system during impact appeared to be cost prohibitive. Current F-shape PCBs show a high degree of barrier damage during MASH TL-3 impacts, as shown in Figure 49. As such, there was likely a compromise between barrier performance and damage that was desired by end users.

Table 6. PCB Reinforcement Configuration Comparison

PCB Configuration	Dynamic Deflection (in.)	MASH TL-3 Damage Level	Total Mass (lb/ft)	Total Cost ($/ft)	% Cost Increase	% Deflection Reduction
MwRSF F-shape PCB	80	Through cracking of the barrier section in multiple locations	407.3	$62.21	0.0	0.0
Oregon F-shape PCB	63.4	Through cracking of the barrier section in multiple locations	475.9	$61.72	-0.8	-20.8
Staggered, Interlocked PCB Reinforcement - Initial Reinforcement	17.5	**Upper segment** – Major plastic strain in longitudinal bars and stirrups. Opening of outer leg at end of segment. **Lower Segment** – Moderate plastic strain of longitudinal bars	619.6	$103.62	66.6	-78.1
Staggered, Interlocked PCB Reinforcement - Option 1 Reinforcement	17.6	**Upper segment** – Moderate plastic strain in longitudinal bars and stirrups. Opening of outer leg at end of segment. **Lower Segment** – Moderate plastic strain of longitudinal bars	623.9	$119.43	92.0	-78.0
Staggered, Interlocked PCB Reinforcement - Option 2 Reinforcement	14.1	**Upper segment** – Moderate/minor plastic strain in longitudinal bars and stirrups. **Lower Segment** – Moderate/minor plastic strain of longitudinal bars	632.0	$149.28	140.0	-82.4
Staggered, Interlocked PCB Reinforcement - Option 3 Reinforcement	13.8	**Upper segment** – Minor plastic strain in longitudinal bars. **Lower Segment** - None	640.6	$182.59	193.5	-82.8

(a) Midwest F-shape PCB

(b) Oregon F-Shape PCB

Figure 49. F-shape PCB Damage in MASH TL-3 Impacts

In order to determine the preferred reinforcement configuration for the prototype design, the sponsoring state DOTs were asked several questions.

1. Please provide which PCB reinforcement configuration your state prefers based on the four simulated options.

2. Would your state be willing to utilize Grade 80 rebar in the new PCB design given it provides a 33% strength increase at a cost increase of only $0.03/lb? This is roughly a 1% cost increase over Grade 60 rebar.

3. Based on the simulation analysis, the use of the steel end cap was the most effective means for preventing significant damage to the ends of the PCB segments. Does your state desire use of the steel end caps regardless of the reinforcement configuration chosen, or would you prefer to avoid the cost of the end cap?

The feedback from the sponsors with respect to these questions aided in selection of a prototype barrier configuration. States preferred the initial simulated reinforcement configuration

and the Option 1 reinforcement configuration equally. Further discussion found that Option 1 was more preferred due to the inclusion of the V-shaped bar for mitigating damage and opening of the outer leg of the upper barrier segment. The Option 2 and Option 3 reinforcement configurations were not as preferred due to concerns with additional cost. Similarly, there was not widespread support for the use of the steel end caps due to cost concerns. Several states did prefer the steel end caps as it was believed that they would improve durability, but cost concerns tended to overwhelm the desire for the steel end caps. Almost all of the sponsoring states supported the use of the Grade 80 rebar due to the 33% increase in bar strength at a minimal cost. It was hoped the use of Grade 80 steel would improve the overall barrier structural capacity and durability. Based on this feedback, the Option 1 barrier reinforcement configuration with Grade 80 steel was selected for use in the final PCB prototype.

4.6.2 Selection of Barrier Length and Curvature

The final PCB design parameter required for the prototype PCB design was selection of the desired barrier length. Barrier length correlated directly with the curvature radius achievable by the proposed PCB design. However, accommodation of smaller curve radii will inherently increase the barrier deflections due to the flexibility required to achieve them. Thus, achieving very small curvature radii would potentially be difficult based on the design requirement for reduced barrier deflection. Previous surveys of the Midwest Pooled Fund members indicated that a curvature radius of 200-300 ft would accommodate the majority of end users.

In order to limit relative lateral barrier segment displacement at the barrier joints and the associated risks for vehicle snag, the researchers are proposing to limit the internal gap tolerance between ⅜ in. and ½ in. This gap tolerance range was preferred as it will allow for more forgiveness in the barrier installation and assembly. MwRSF performed an analysis of the achievable curve radii based on gap tolerance and segment length for the new PCB design. For the ½-in. gap tolerance, a 12.5-ft long PCB segment will be able to achieve a curve radius of 528 ft. Reducing the segment length to 8 ft allows for a 216-ft curvature radius. Similarly, for the ⅜-in. gap tolerance, a 12.5-ft long PCB segment will be able to achieve a curve radius of 615 ft. Reducing the segment length to 8 ft allows for a 250-ft curvature radius.

MwRSF simulated the staggered, interlocking, segment PCB design with reinforcement Option 2 with both 12.5-ft long and 8-ft long segments. Dynamic deflection of the 8-ft long segments increased to 20.9 in. as compared to 14.1 in. for the 12.5-ft long segments. In order to determine the barrier length for the prototype barrier design, the sponsoring states were asked to provide input on if they desired to focus on a 12.5-ft long barrier segment to limit deflections and provide larger curve radii, or if it was preferable to utilize an 8-ft long barrier segment with slightly higher deflections and a smaller curve radius between 200 ft to 300 ft. It was be noted that MASH TL-3 crash testing of the system with the smaller segment length would allow use of longer segments if desired by certain states.

Results from the state sponsor feedback provide equal support for both segment length options. As such, it was agreed to evaluate the barrier prototype with the shorter, 8-ft segment length as that would allow the use of longer segment lengths if desired by the end user. It was also decided to use the ⅜-in. internal tolerance gap to create less variation in the segment alignments during installation and limit potential vehicle snag due to lateral shifting of the barrier segments at joints.

4.7 Simulation of Prototype PCB

Prior to developing final prototype barrier details and fabricating barrier segments for full-scale crash testing, it was desired to simulate the final prototype barrier configuration to estimate its performance. A LS-DYNA model was created of the staggered, interlocking PCB with 8-ft long barrier segments, a ⅜-in. internal tolerance gap, and the Option 1 reinforcement configuration with Grade 80 rebar throughout, as shown in Figure 50.

The prototype PCB simulation found that the barrier system captured and stably redirected the impacted 2270P vehicle, as shown in Figures 51 and 52. the Maximum dynamic deflection of the barrier system was found to be 23.3 in. This was as slight increase over the 20.9 in, deflection measured in the simulation of the Option 2 reinforcement with 8-ft long segments. This slight increase in deflection was attributed to a slight increase in the deformation of the outer leg of the upper barrier segment due to the omission of the steel end cap in that region in the prototype simulation.

Damage to the concrete structure of the barrier was similar to the damage observed in the previous simulation of Option 1 reinforcement with the 12.5-ft long barrier segment, as shown in Figures 53 and 54. Concrete damage on the upper barrier segment consisted of flexural damage to the outer leg of the segment near the joint and flexural damage across the midspan of the back side of the segment. The lower barrier segment displayed concrete damage around the end of the narrow center pillar and flexural damage near the midspan of the entire segment.

A better estimate of prospective barrier damage was provided by review of the plastic strain observed in the reinforcing steel, as shown in Figures 55 and 56. The upper segment reinforcing steel showed minor plastic strains of a few stirrups near the base of the outer leg of the segment. No plastic stains were observed in the longitudinal bars in the upper segment. For the lower barrier segment, minor plastic strains were observed in the vertical legs of the stirrups in the center pillar of the segment, and no plastic strains were observed in the longitudinal bars. The plastic strains observed in the model suggested that the reinforcement of the prototype PCB segments was sufficient to handle the overall flexural loads of the segments based on the lack of plastic strain observed in the longitudinal bars. Some localized damage may be expected in the center pillar of the lower segment and the outer legs of the upper segment, but that damage would be expected to be minimal based on the low-level plastic bar strains.

The simulation of the prototype PCB design demonstrated that the design had a high potential to meet MASH TL-3 with limited damage. As such, this design was selected for fabrication and full-scale crash testing.

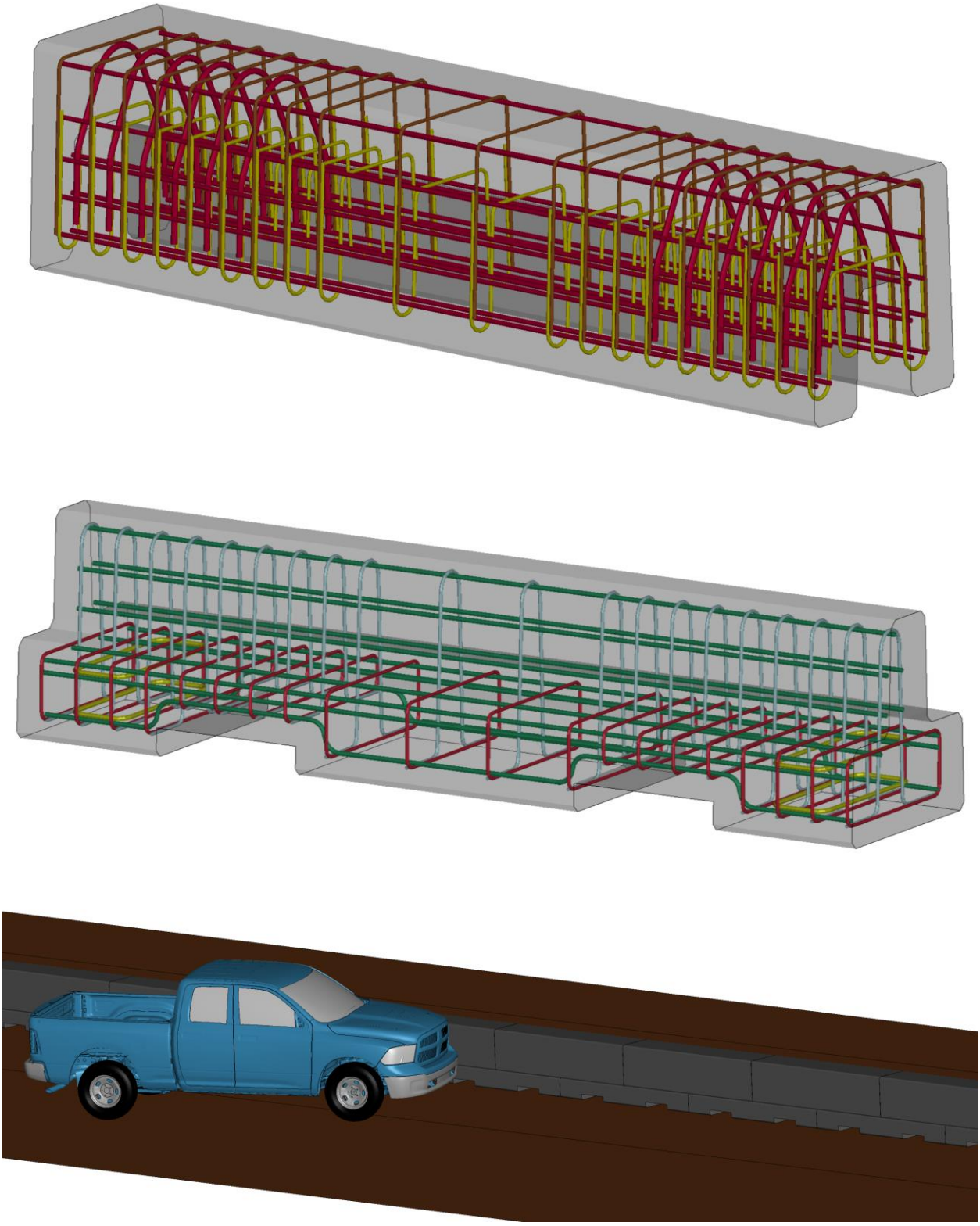

Figure 50. LS-DYNA Model of Staggered, Interlocking PCB Prototype

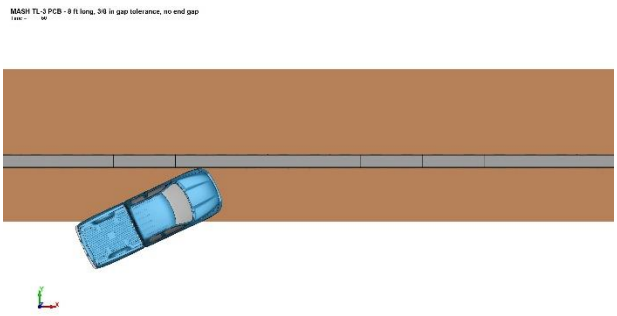

(a) 0.000 sec

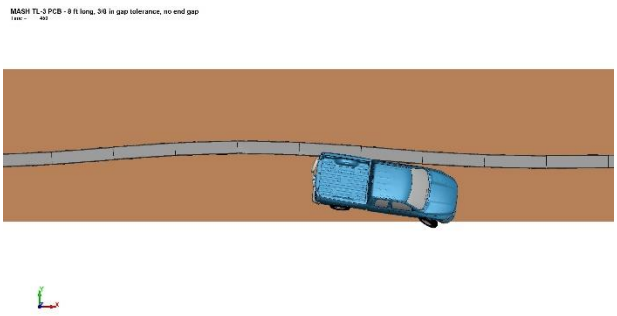

(e) 0.400 sec

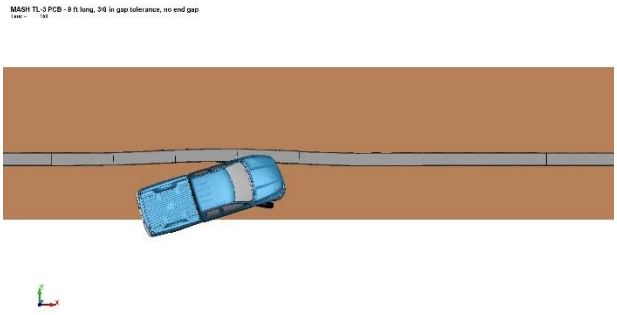

(b) 0.100 sec

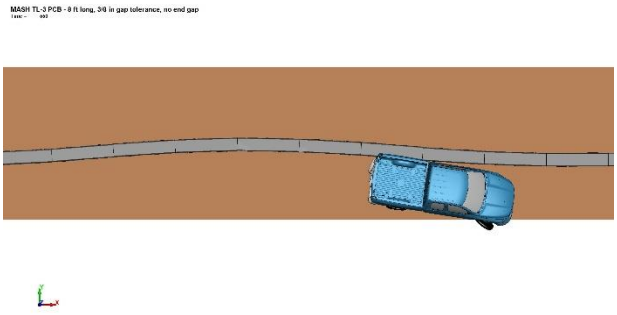

(f) 0.500 sec

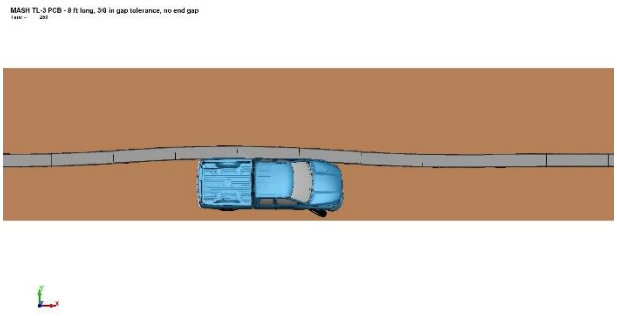

(c) 0.200 sec

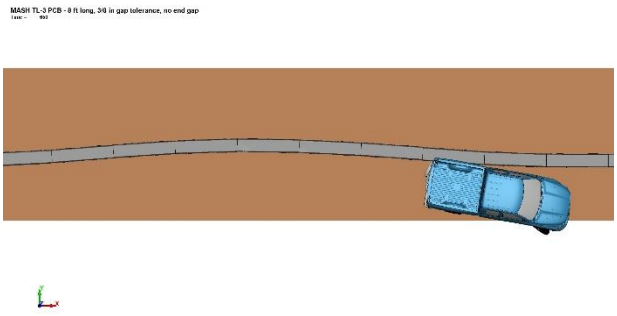

(g) 0.600 sec

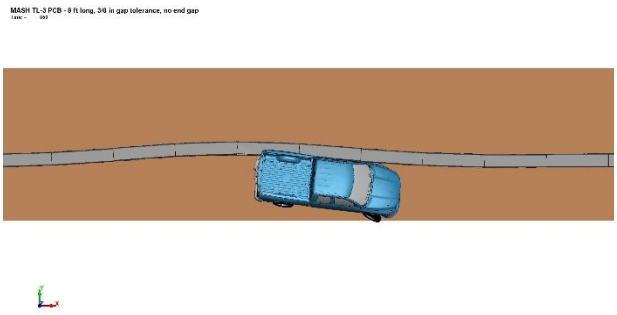

(d) 0.300 sec

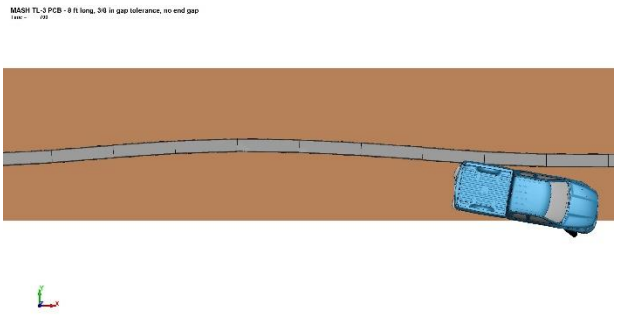

(h) 0.650 sec

Figure 51. Prototype PCB Design, Overhead Sequential Images

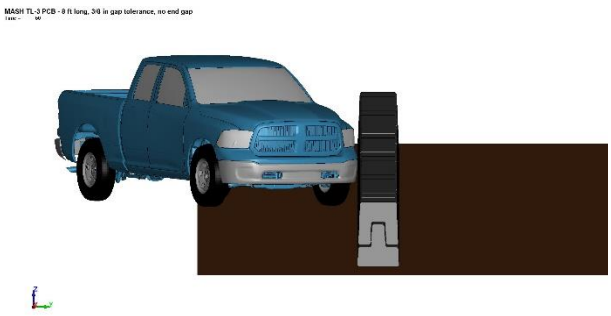

(a) 0.000 sec

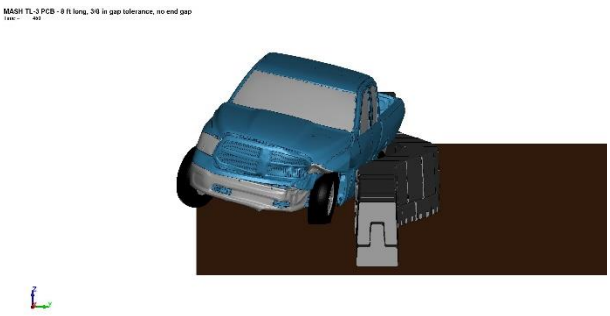

(e) 0.400 sec

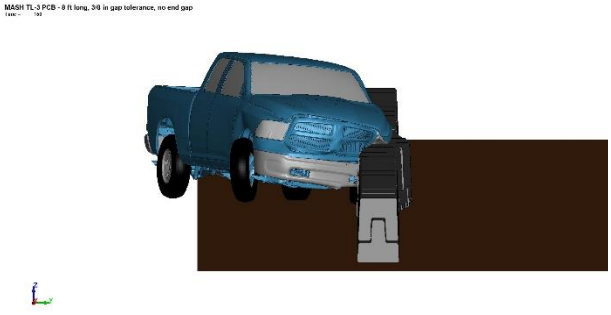

(b) 0.100 sec

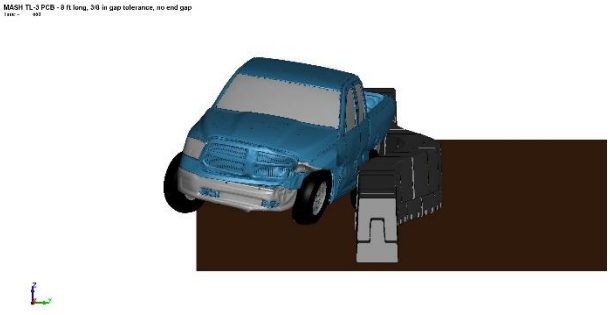

(f) 0.500 sec

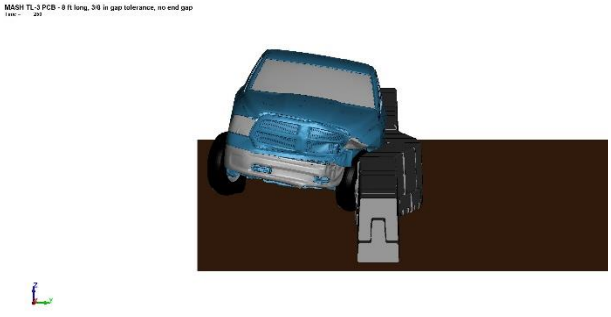

(c) 0.200 sec

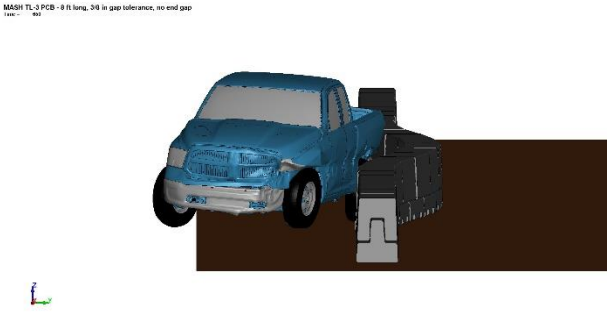

(g) 0.600 sec

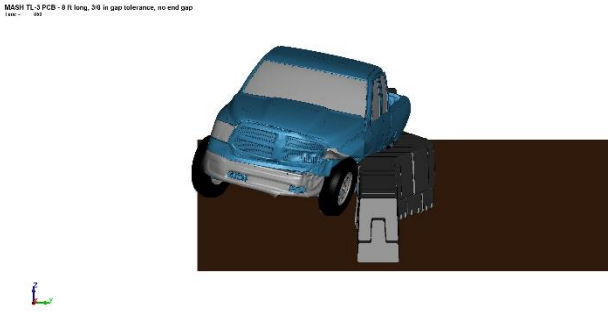

(d) 0.300 sec

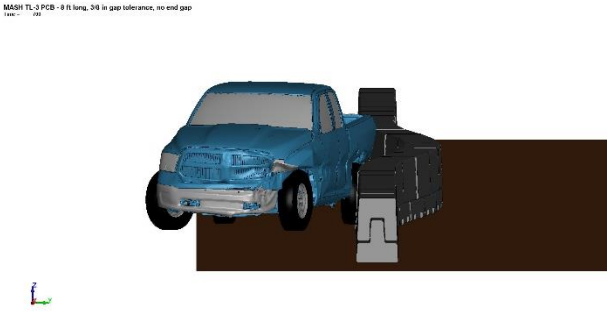

(h) 0.650 sec

Figure 52. Prototype PCB Design, Downstream Sequential Images

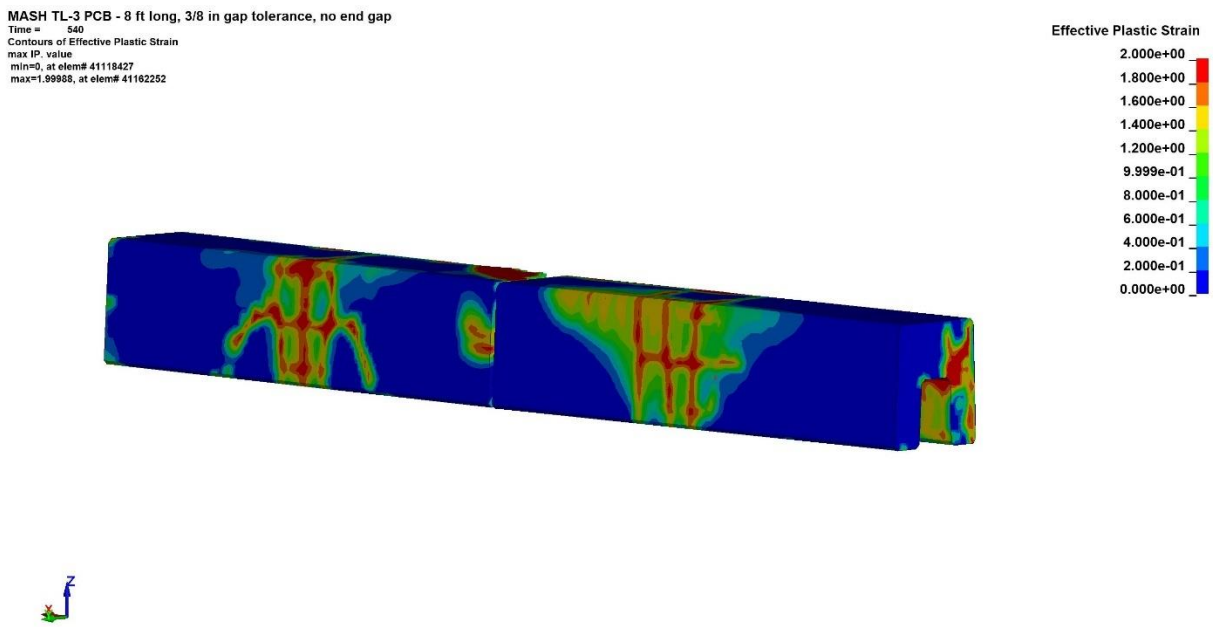

Figure 53. Prototype PCB Design, Upper Segment Concrete Damage

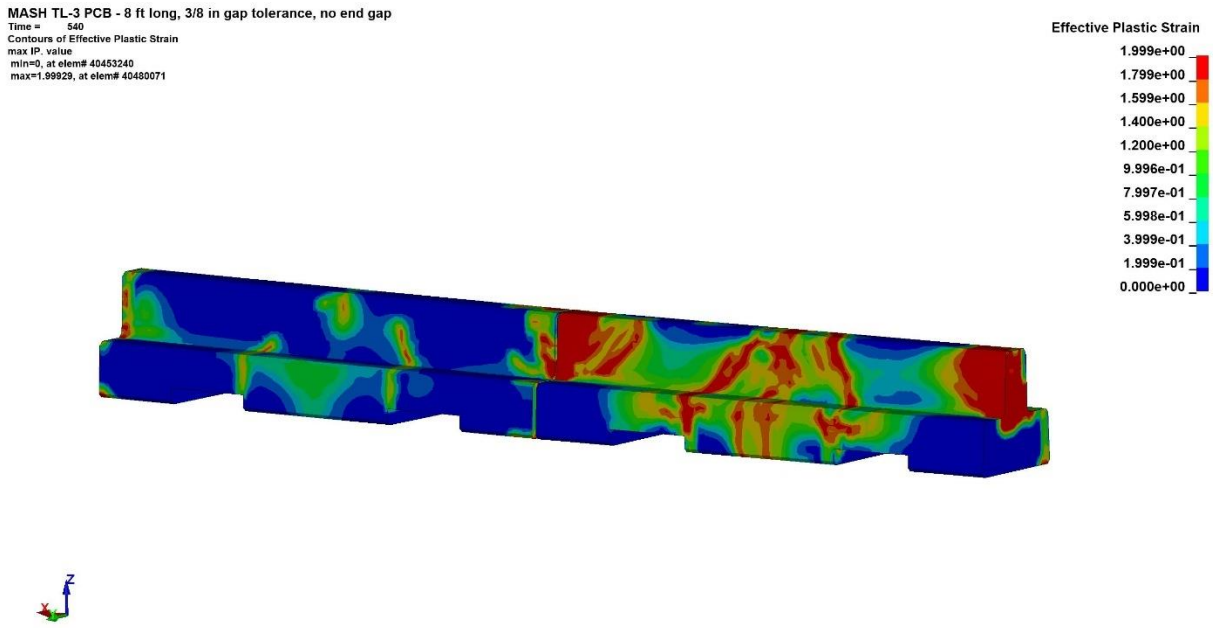

Figure 54. Prototype PCB Design, Lower Segment Concrete Damage

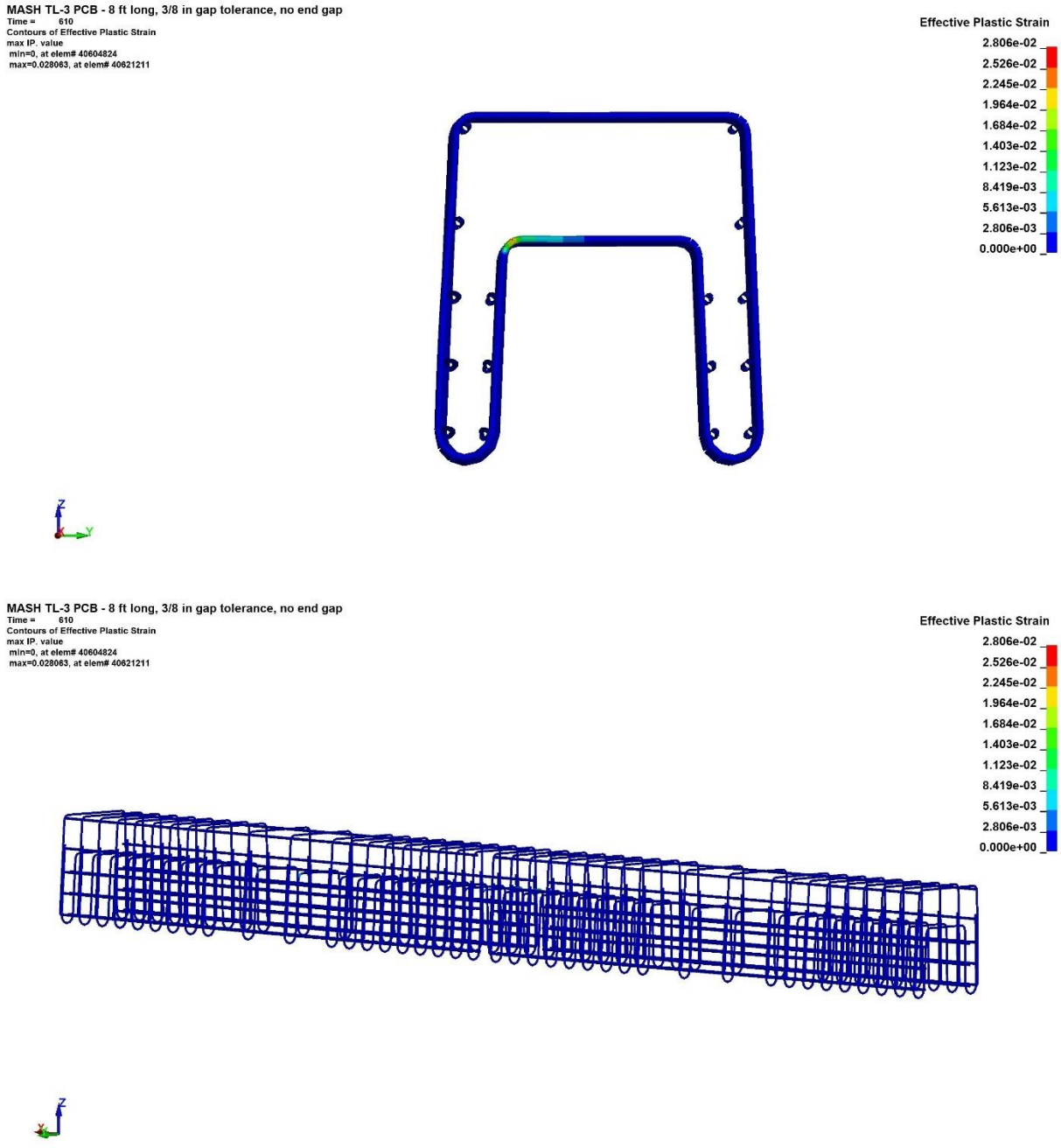

Figure 55. Prototype PCB Design, Upper Segment Rebar Plastic Strain

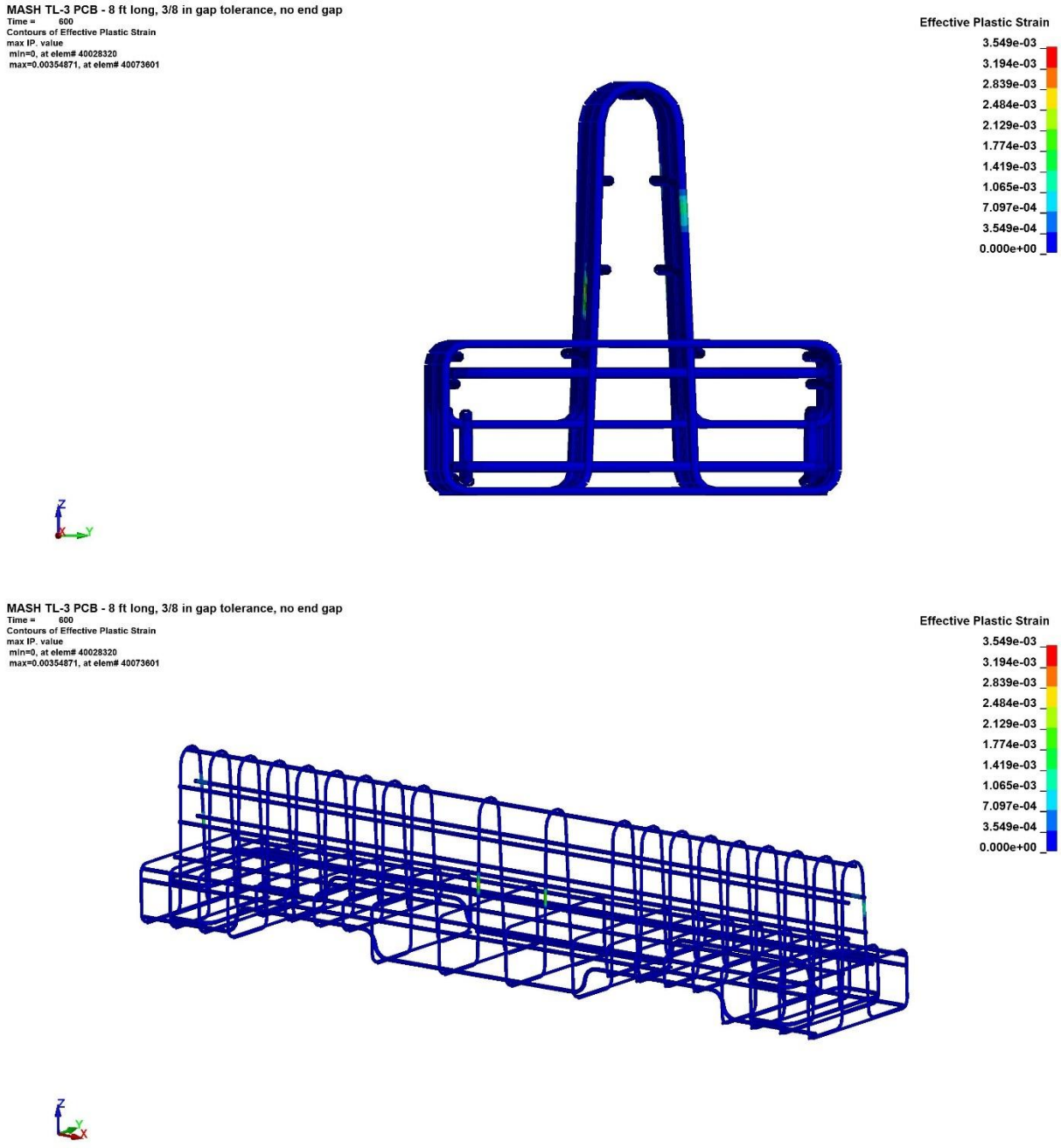

Figure 56. Prototype PCB Design, Lower Segment Rebar Plastic Strain

4.8 Simulation of PCB End Gaps

A final simulation analysis was performed to investigate the effect of gaps between the end of the barrier segments during installation. Up to this point, all of the PCB simulations were performed with all of the barrier segments butted end to end with little to no gap between the ends, which was the intended installation configuration. In real-world installations, small gaps may occur between the ends of the segments. While the intent would be to minimize those gaps, a simulation model of the barrier with end gaps was created to determine what effect barrier end gaps may have on performance.

A simulation model of the staggered, interlocking PCB prototype was created that placed 1-in. wide gaps between adjacent upper barrier segments and adjacent lower barrier segments, as shown in Figure 57. A 1-in. wide gap was selected because it was a reasonable gap size, and gap sizes larger than 1 in. would likely be undesirable as the staggering of the upper and lower barrier segments would rapidly become misaligned in a barrier installation.

Figure 57. LS-DYNA Model of Staggered, Interlocking PCB Prototype with 1-in. Wide End Gaps

Simulation of the barrier system with 1-in. wide gaps throughout showed little difference from the performance of the barrier with no gaps. Capture and redirection of the 2270P vehicle was very similar, and the inclusion of the gaps did not cause any increase in vehicle snag at the joints between segments. Dynamic deflection did increase slightly to 23.9 in.

5 PROTOTYPE DESIGN CONSIDERATIONS

Following simulation analysis and determination of a staggered, interlocking PCB design prototype for full-scale crash testing, the proposed design was further reviewed by the research team and shared with fabricators to provide feedback on the design and suggest changes and/or modifications that may make the barrier easier to fabricate, implement, and install.

5.1 Lifting Options

Lifting options for the barrier segments had yet to be incorporated into the design. Because the barrier segments were to be installed vertically, dedicated lifting mechanisms were desired. Many options for lifting the barrier segments were considered, including V-anchors, dog bone inserts, wire rope lifting loops, and erection anchors. Examples of those lifting elements are shown in Figure 58. Many of these options had sufficient capacity to lift and place the barrier segments. It was noted that any lifting mechanism used had to be counter sunk or recessed into the top of the barrier such that it did create a vehicle snag hazard, nor would it interfere with placement of the upper barrier segment on the lower barrier segment. Another option that was considered was the use of squeeze lifts which are friction lifts that grab the face of the barrier segment directly to lift it, as shown in Figure 59. Fabricators did not indicate any issues with providing any of the lifting options reviewed.

It was determined that the dog bone inserts provided the best lifting option for the barrier system. These inserts were easy to implement in both the upper and lower barrier segments and were easy and secure for crews to use during installation. Two dog bone inserts were placed in each of the upper and lower barrier segments as a lifting device. Other lifting options would still be available for use in with the barrier system as long as they had sufficient capacity to support the weight of the segments and did not extend externally outside of the barrier geometry.

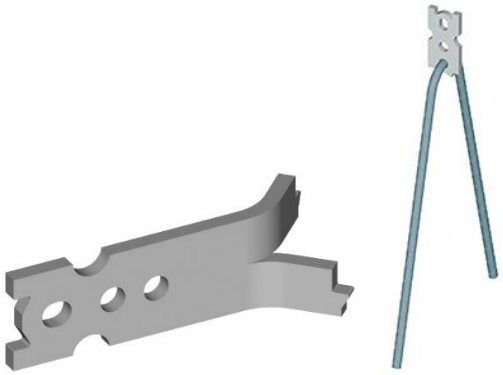

(a) Erection Anchor

(b) V-Anchor

(c) Wire Rope Insert

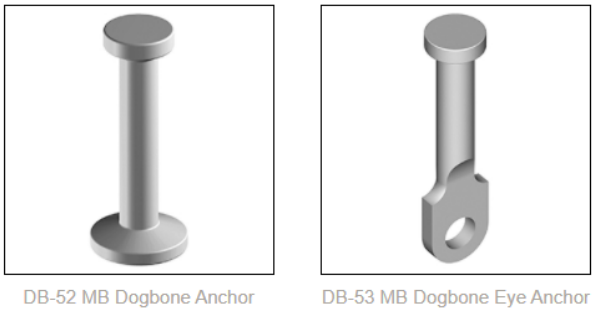

(d) Dog Bone Insert

Figure 58. PCB Lifting Options

Figure 59. PCB Squeeze Lift

5.2 Anchor Pockets

While the design effort detailed herein was focused on the development of a portable barrier system with reduced dynamic deflections, there are situations where PCBs must be installed in critical, space-limited applications where barrier deflection must be even more severely restricted such as PCB installations next to drop-offs or bridge deck edges. Design of anchorage for the staggered, interlocking PCB system was outside the scope of the current effort, but it was desired to include accommodations for future anchors if and when they were designed and tested.

Anchorage for PCB systems is typically accomplished by passing some form of anchor through the barrier and into the supporting pavement to restrain barrier motion. Previous anchorage systems have been developed for the Midwest F-shape PCB systems for both concrete and asphalt road surfaces [18-20]. As such, similar anchor pockets were incorporated into the lower segment of the staggered, interlocking PCB to accommodate similar types of anchorage in the future, as shown in Figure 60. Two anchor pockets were placed on each side of the lower barrier segment near the ends of the barrier. The pockets were similar in size and geometry to those utilized in the previous F-shape PCB anchorages to allow for the use of similar threaded rod or steel pin anchors, and two no. 4 rebar loops were placed around the anchor pockets to aid in retention of the anchors under impact loading.

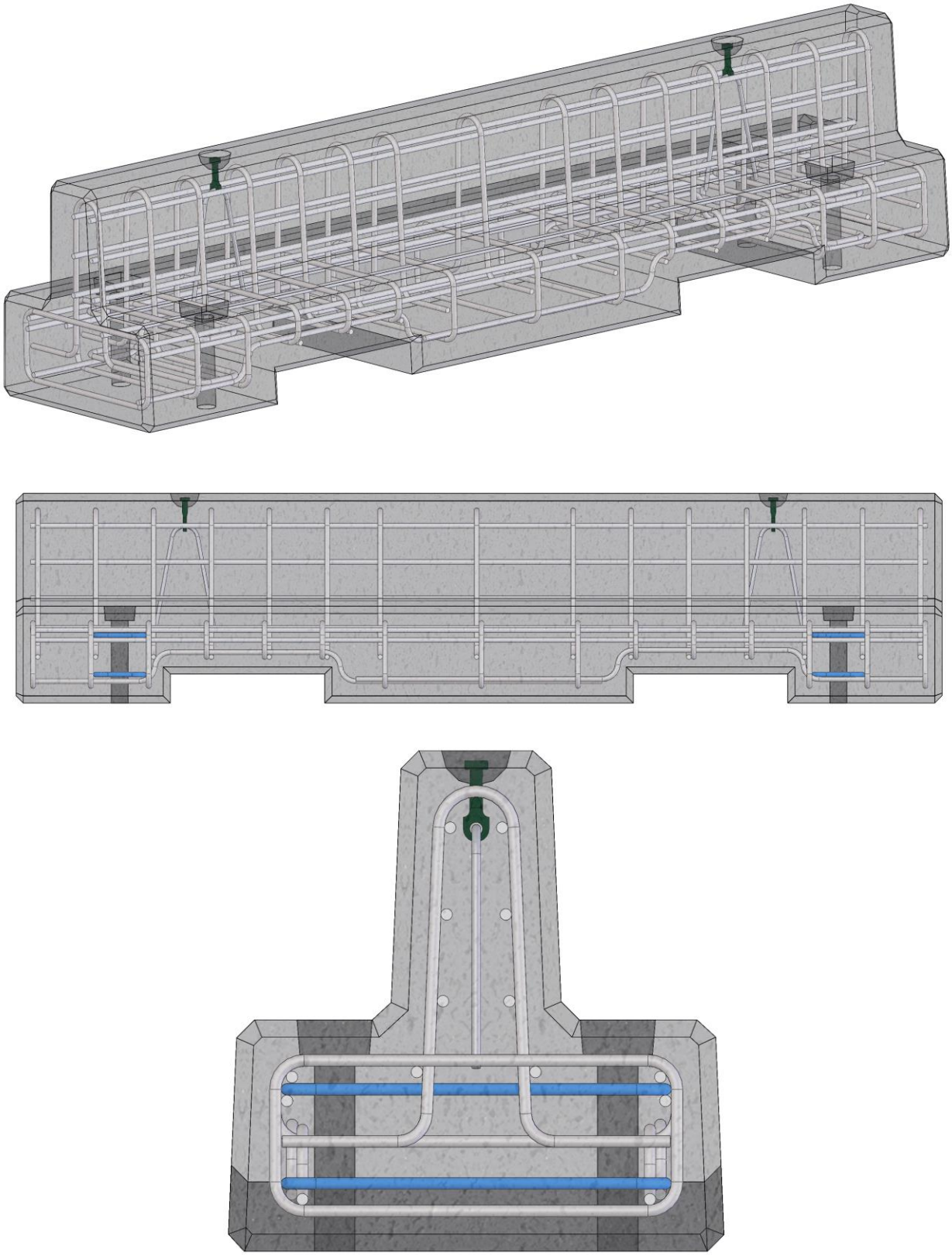

Figure 60. PCB Anchor Pockets

5.3 End Barrier Segments

Due to the staggering of the upper and lower barrier segments, the new PCB system does not have a continuous profile at the ends of the system. The lower barrier segment extends half the barrier length beyond the barrier upper barrier segments on each end of the system. To address this, end sections of the barrier were created to create a continuous barrier profile throughout the entire system length.

The barrier end segments consisted of a half-length upper barrier segment, as shown in Figure 61. The end segment was identical in cross section and reinforcement to the standard upper barrier segment used in the system. In order to prevent the end segment from "walking" off the end of last lower barrier segment due to roadway vibrations or nuisance hits near the end of the system, vertical cavities were placed near the ends of the outer legs of the end segment to receive steel dowel pins. The dowel pins fit inside the anchor pockets in the lower barrier segment and the cavities in the end segment to prevent significant longitudinal motion of the end segment.

Alternative end sections were considered and could potentially be implemented at a later date if preferred by end users. Alternative end sections considered included the use of a half-length lower barrier segment or a special lower barrier segment that utilized a full barrier cross-section for one half of the segment length. Additionally, alternative end sections may be developed and implemented for transitioning and attachment of the PCB system to rigid barriers and crash cushions.

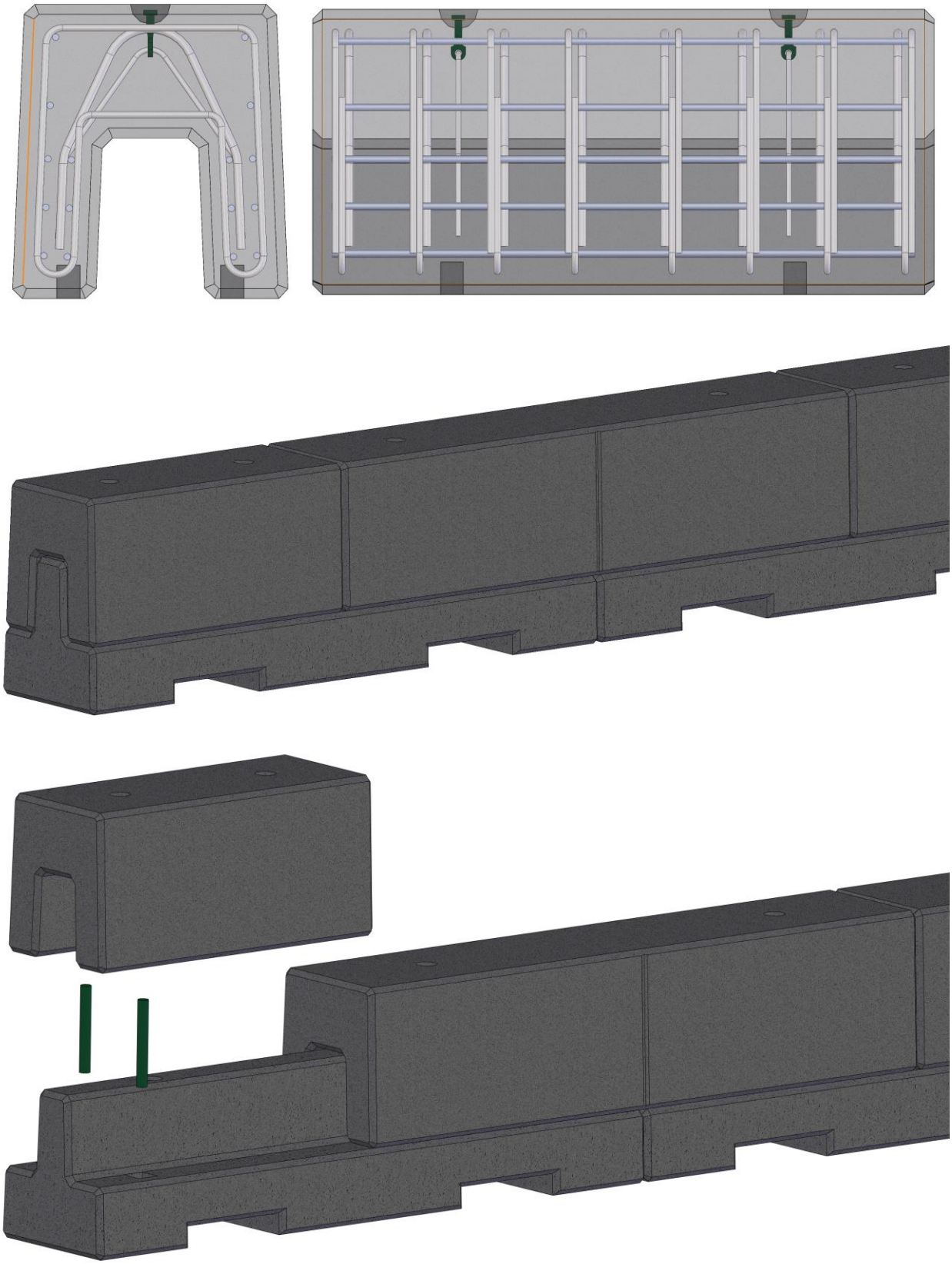

Figure 61. PCB End Segment

5.4 Fabrication Modifications

Fabricators were consulted to determine potential concerns with making the staggered, interlocking PCB segments and identify potential modifications to ease or simplify the fabrication process. The fabricators were shown preliminary details consisting of 8-ft long barrier segments utilizing the Option 1 barrier reinforcement with Grade 80 bars selected during the simulation analysis. Feedback from several manufacturers did not present any general concerns with forming the basic barrier geometry or the reinforcement of the barrier sections. Discussions with the fabricators did identify several minor modifications or considerations that were incorporated into the PCB prototype design

1. The fabricators had no issues with the use of Grade 80 reinforcing steel. Several fabricators noted that Grade 80 reinforcing steel is becoming much more common in precast concrete structures, and they were familiar with the material. An issue did occur with the availability of the Grade 80 no. 3 rebar that was specified for the stirrups in the barrier. Grade 80 rebar was not readily available in a no. 3 bar size. In order to alleviate this issue, the Option 1 reinforcement configuration was modified by increasing the barrier stirrups to no. 4 bars and increasing the spacing of the stirrup bars due to the use of a larger bar diameter. In order to accommodate the bend radius for a no. 4 bar in the narrow sections of the upper and lower barrier segments, the overall width of the barrier was increased ½ in. to 21½ in. Minor variations were also made to the locations of some of the longitudinal steel to accommodate the larger diameter stirrups.

2. Discussions with the fabricators led to improvements in the design of the stirrups used in the barrier. The original stirrup configuration used in the PCB segments consisted of two-piece stirrups to keep the stirrup bend geometry simple while allowing the stirrups to extend into both the main body of the segments as well as the narrow sections, as shown in Figure 62. Fabricators noted that rebar bending equipment has advanced significantly, and the capability to bend more complex stirrups was available. As such, single piece stirrup options were proposed for the two-piece options originally specified, as shown in Figure 63. Both options were included in the barrier details as options for end users.

3. It was noted that welded wire reinforcement options could be made available for the staggered, interlocking PCB. It was decided to detail and test the new PCB system with conventional steel reinforcement. However, if the design was successfully crash tested, it was noted that a welded wire reinforcement equivalent could be developed.

4. Chamfers were added to all of the edges of the PCB segments to reduce damage to the edges during transportation and installation of the barrier segments and to improve overall durability of the segments.

(a) Two-Piece Upper Stirrup

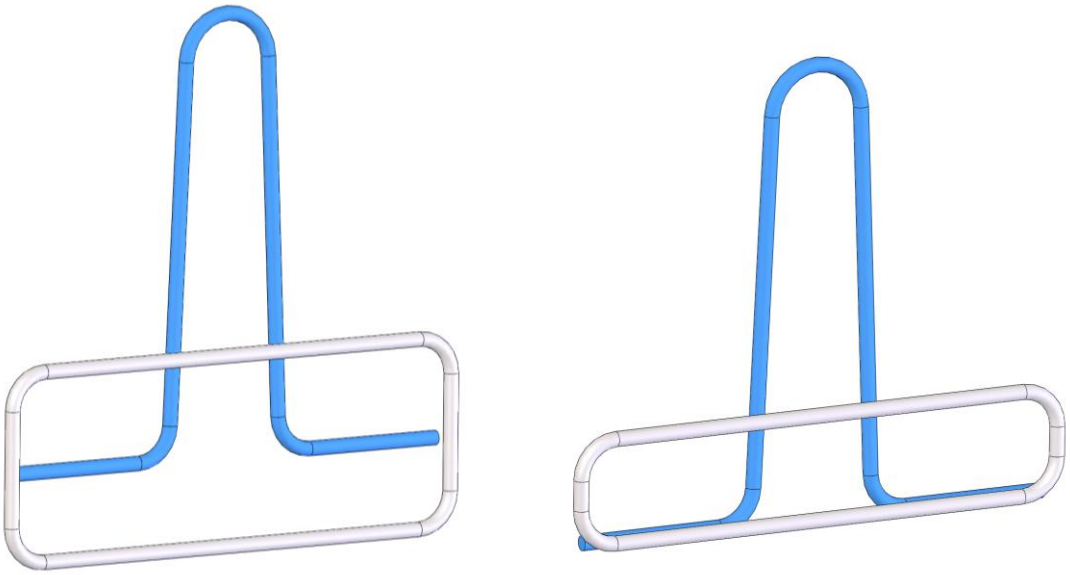

(b) Two-Piece Lower stirrups

Figure 62. Original Two-Piece Stirrup Configurations

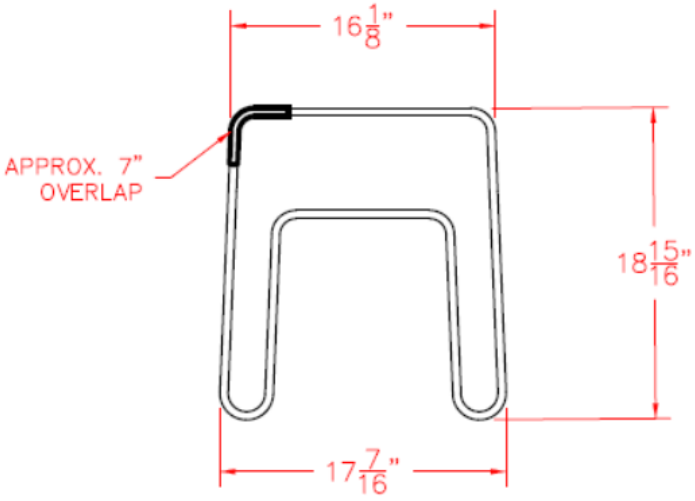

(a) Upper Stirrup

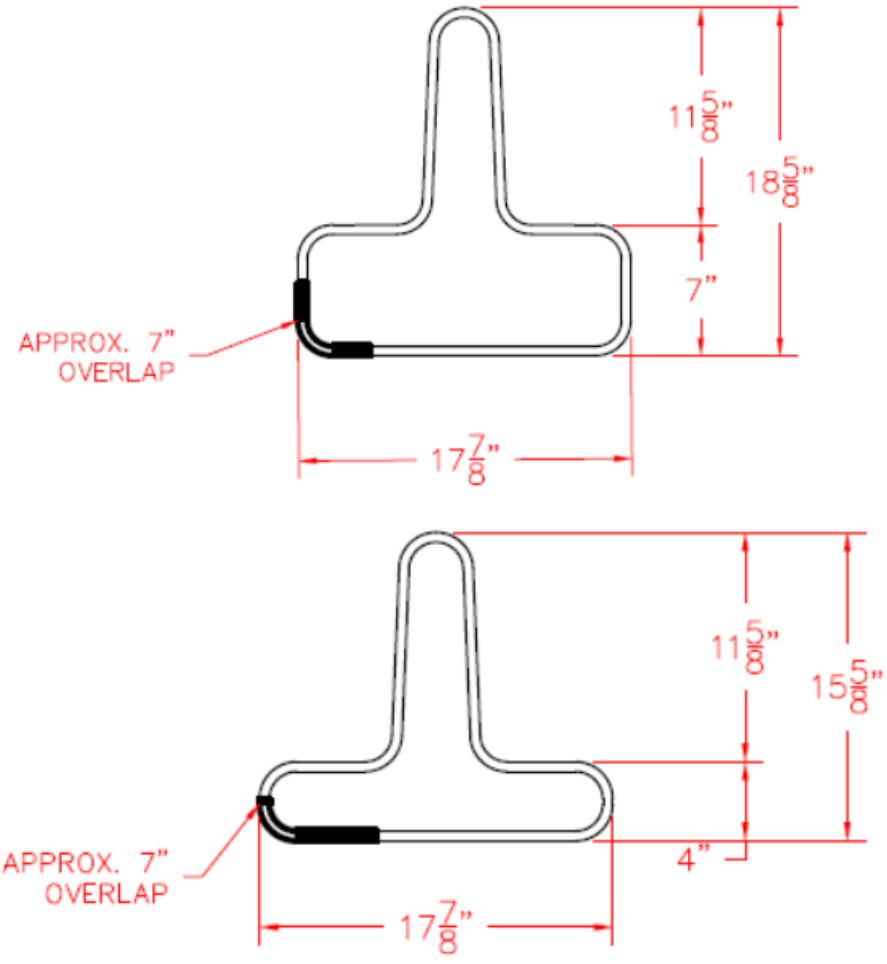

(b) Lower Stirrups

Figure 63. Alternative Stirrup Configurations

5.5 Other Considerations

A limited number of additional, relevant considerations were discussed during the development of the final staggered, interlocking PCB prototype. State DOTs noted some concern for thermal expansion or contraction of the barrier segments creating fitment issues in the field. The thermal expansion coefficient for concrete is 5.5x10-6 /F°. As such, thermal expansion for a 96-in. long segment with a 100-degree temperature change would be (5.5x10-6/F°)(100 deg. F)(96 in.) = 0.0528 in. of expansion/contraction. This is a very small change in segment length and was not anticipated to affect barrier gaps in a significant manner. As noted previously, simulation was performed on barriers with 1-in. wide gap during the concept development which indicated that small gaps posed no safety issues and minimal increase in deflection.

As noted previously, some end users may desire the use of longer barrier segments. There should not be concerns regarding the use of longer barrier segments as long as the structural reinforcement and capacity of the barrier segments is maintained as the segment length is increased. Longer barrier segments tend to reduce barrier deflection due to the increased mass and inertia of longer segments and the reduction of the number of joints in the barrier system. Thus, a staggered, interlocking PCB system with longer segment lengths would be expected to perform very similarly to a shorter segment length system with the exception of reduced dynamic deflection. It was noted that LS-DYNA could be used following full-scale crash testing to develop a fully validated model of the staggered, interlocking PCB system. This model could then be modified to estimate the dynamic barrier deflection of longer barrier segments without full-scale crash testing.

6 DESIGN DETAILS

Full details of the staggered, interlocking PCB were developed for the purpose of ordering prototypes for full-scale crash testing in a subsequent phase of the research. The staggered, interlocking PCB detail plans are shown in Figures 64 through 82, and photographs of the fabricated barrier segments are shown in Figures 80 through 83.

The barrier system test installation consisted of at 200-ft long PCB system comprised of 25 lower barrier segments, 24 upper barrier segments, and two end segments. The lower barrier segments are shaped like an inverted "T", while the upper barrier segments and end segments are shaped like and inverted U. The lower barrier segments are placed end to end, and the upper barrier segments are installed directly over the lower barrier segments such that the lower base segment protrusion extends into the interior cavity in the upper segment of the barrier. The upper and lower barrier segments are installed with a longitudinal offset of half of the barrier segment length. This staggering of the upper and lower barrier segments creates an interlocking of the barrier segments and provides shear and moment continuity for the barrier PCB system.

The lower barrier segment consisted of a 21½-in. wide by 21⅝-in. tall by 96-in. long precast concrete section in the shape of an inverted "T". The wide section of the inverted "T" was 10 in. tall by 21⅝ in. wide at the base, while the narrow vertical protrusion was 11⅝ in. tall by $6^{7}/_{16}$ in. wide at the top. The sides of the lower segment had a vertical draft of ½ in. over 12 in. Two 16-in. long by 3-in. tall drainage slots were located at the base of the barrier segment 16 in. from the ends of the barrier. Steel reinforcement of the lower barrier segment consisted of no. 4 stirrups at 6-in. spacing near the ends of the segment and at 10-in. spacing in the interior, and fourteen no. 4 longitudinal bars. The two lowest longitudinal bars incorporated vertical bends to allow them to pass continuously over the drainage slots in the segment. All reinforcing steel was ASTM A615 Grade 80. Two MeadowBurke DB-53 MB Dogbone Eye Anchors for lifting the barrier segment were anchored into the barrier with no. 3 ASTM A615 Grade 60 anchor bars.

The upper barrier segment consisted of a $20^{11}/_{16}$-in. wide by 22-in. tall by 96-in. long precast concrete section in the shape of an inverted "U". The wide section of the inverted "U" was 10 in. deep by $18^{27}/_{32}$ in. wide at the top, while the interior cavity was 12 in. deep by 7¼ in. wide at the top. The sides of the upper segment had a vertical draft of ½ in. over 12 in. Steel reinforcement of the upper barrier segment consisted of no. 4 stirrups at 6-in. spacing near the ends of the segment and at 10-in. spacing in the interior, and sixteen no. 4 longitudinal bars. Five V-shaped no. 5 rebar were placed near the ends of the segment that extended from the top into the outer legs of the segment in order to reduce damage and cracking of the outer legs. All reinforcing steel was ASTM A615 Grade 80. Two MeadowBurke DB-53 MB Dogbone Eye Anchors for lifting the barrier segment were anchored into the barrier with no. 3 ASTM A615 Grade 60 anchor bars.

The end barrier segment was identical in cross section to the upper barrier segment and consisted of a $20^{11}/_{16}$-in. wide by 22-in. tall by 48-in. long precast concrete section in the shape of an inverted "U". The wide section of the inverted "U" was 10 in. deep by $18^{27}/_{32}$ in. wide at the top, while the interior cavity was 12 in. deep by 7¼ in. wide at the top. The sides of the upper segment had a vertical draft of ½ in. over 12 in. Steel reinforcement of the upper barrier segment consisted of no. 4 stirrups at 6-in. spacing and sixteen no. 4 longitudinal bars. V-shaped no. 5 rebar were placed throughout the segment that extended from the top into the outer legs of the segment in order to reduce damage and cracking of the outer legs. All reinforcing steel was ASTM A615

Grade 80. Two MeadowBurke DB-53 MB Dogbone Eye Anchors for lifting the barrier segment were anchored into the barrier with no. 3 ASTM A615 Grade 60 anchor bars.

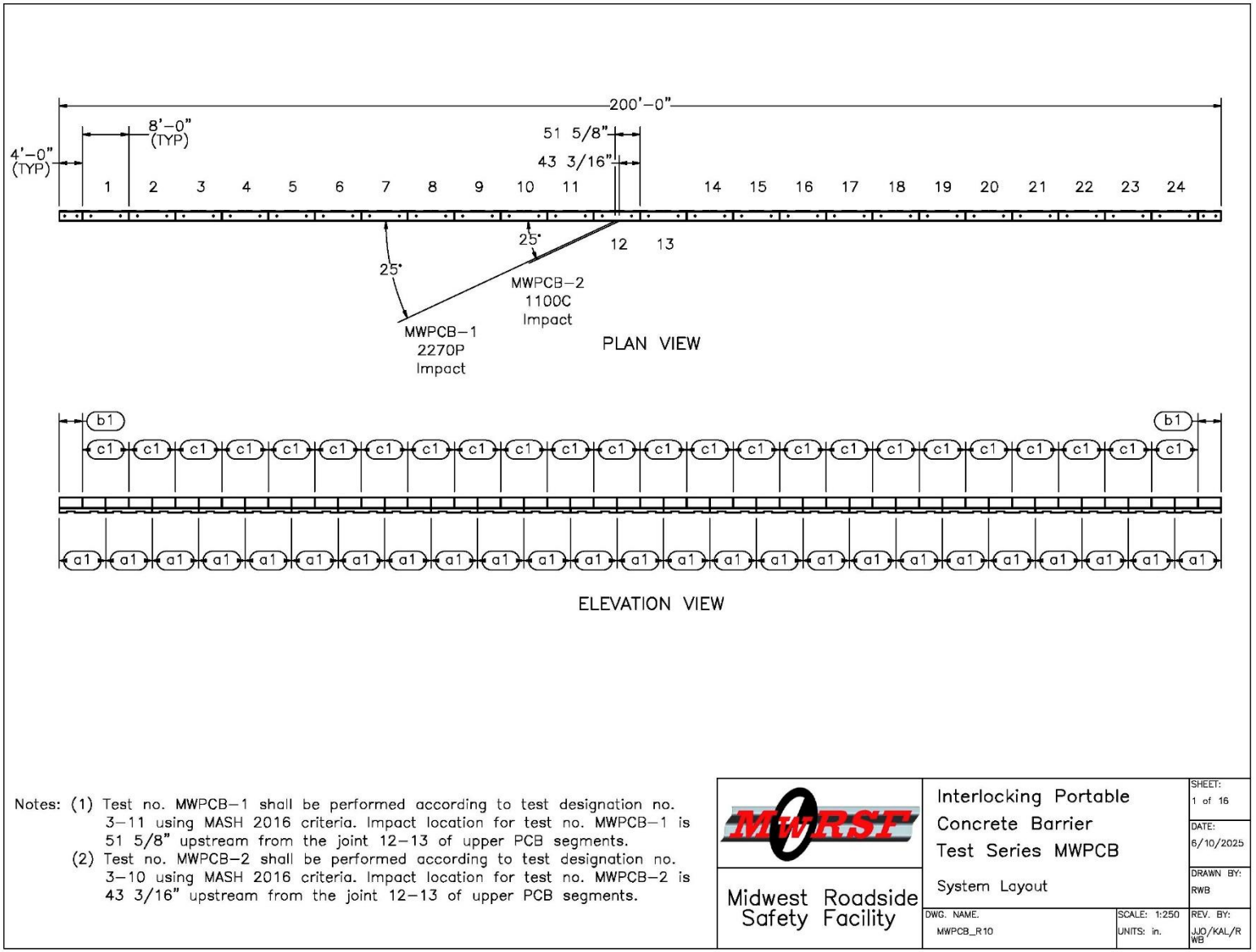

Figure 64. Staggered, Interlocking PCB Prototype, System Layout

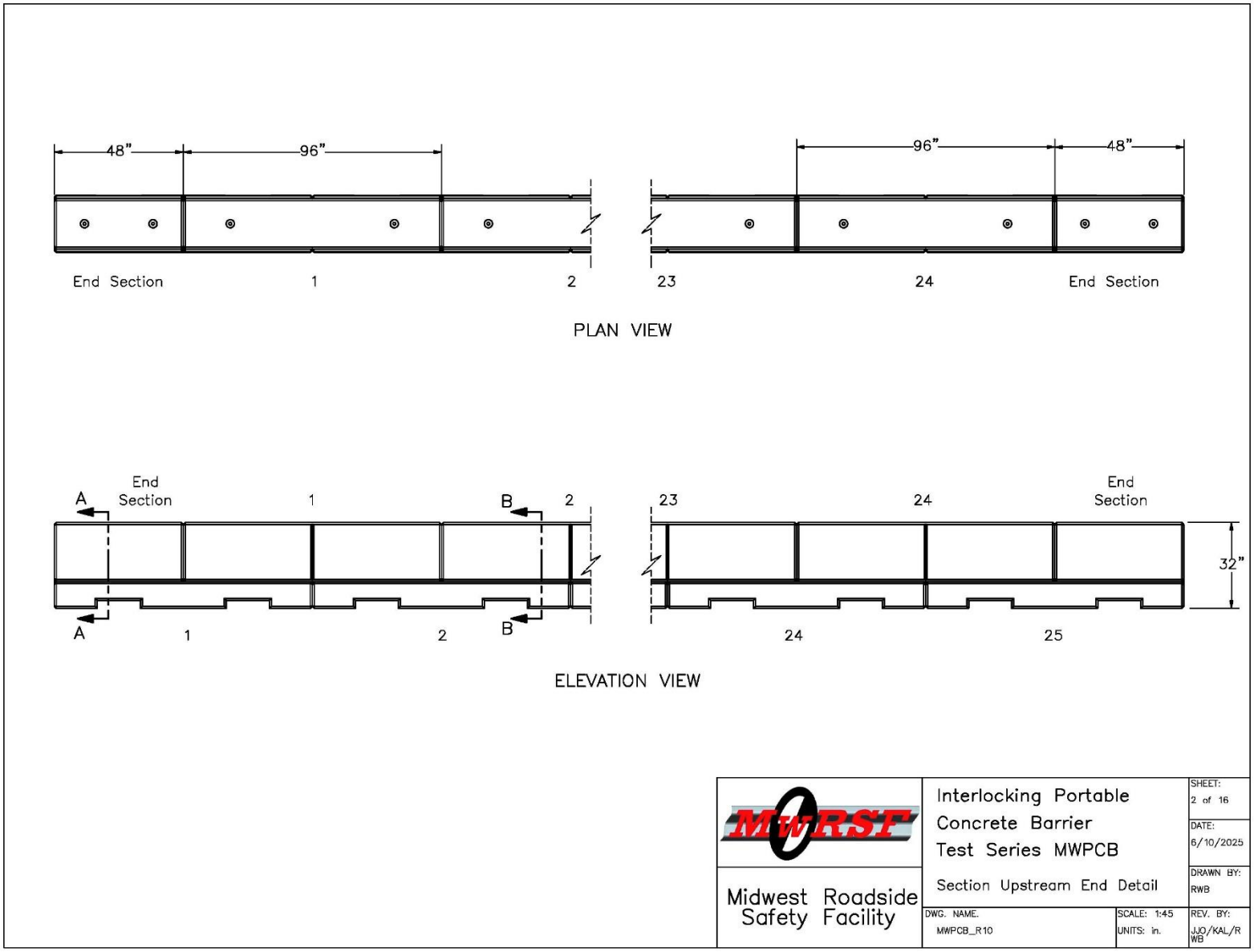

Figure 65. Staggered, Interlocking PCB Prototype , Upstream End Detail

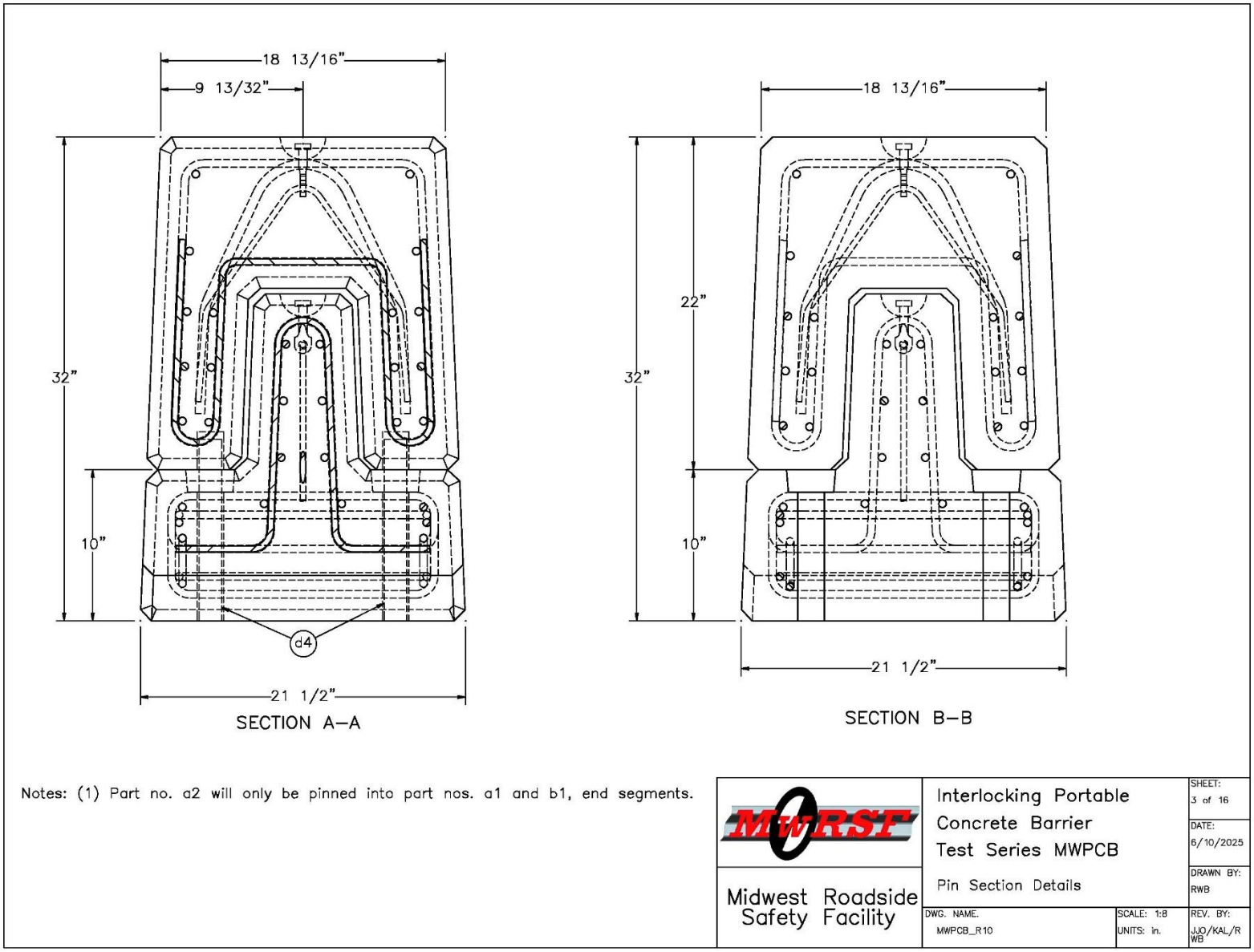

Figure 66. Staggered, Interlocking PCB Prototype, Pin Section Details

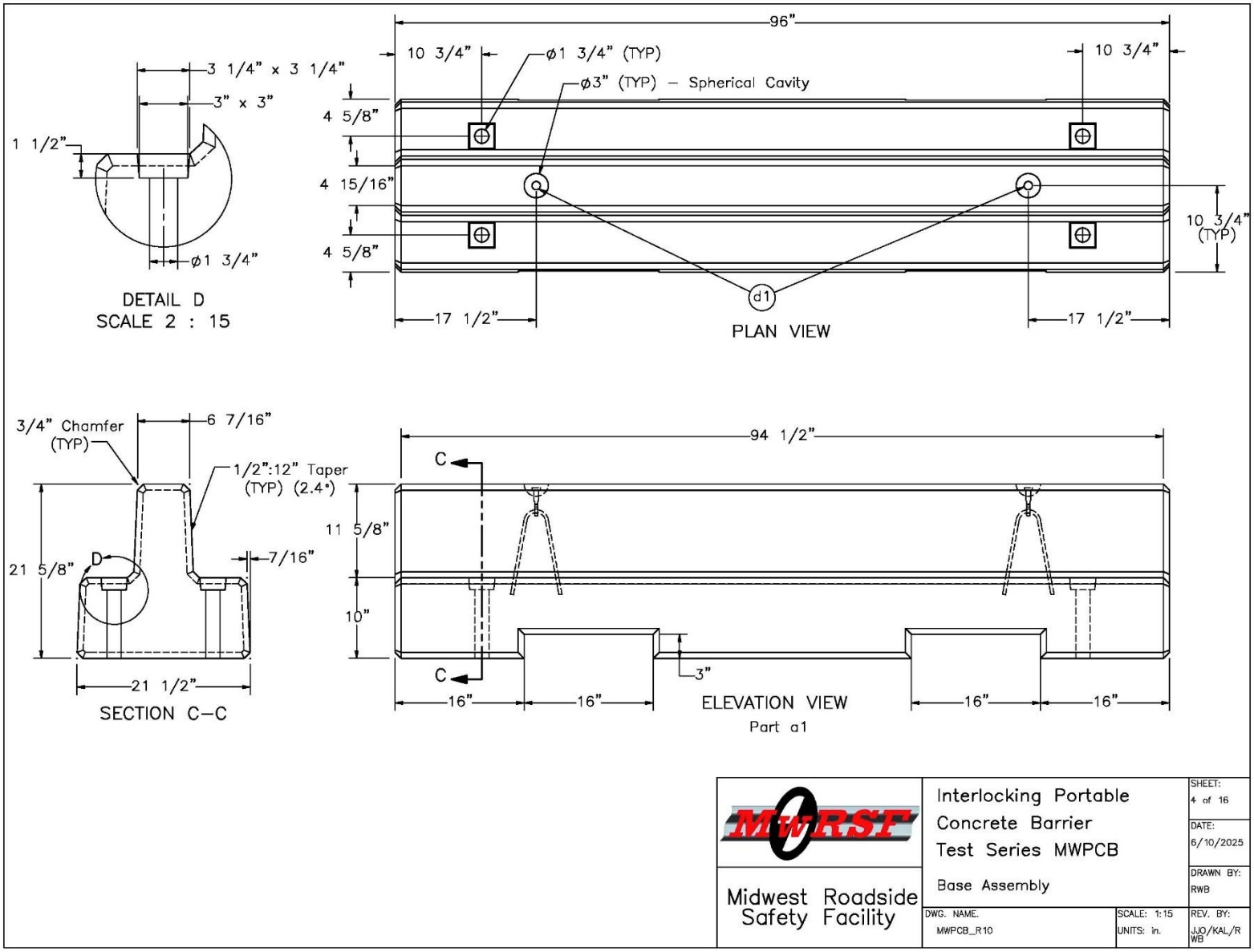

Figure 67. Staggered, Interlocking PCB Prototype, Base Assembly

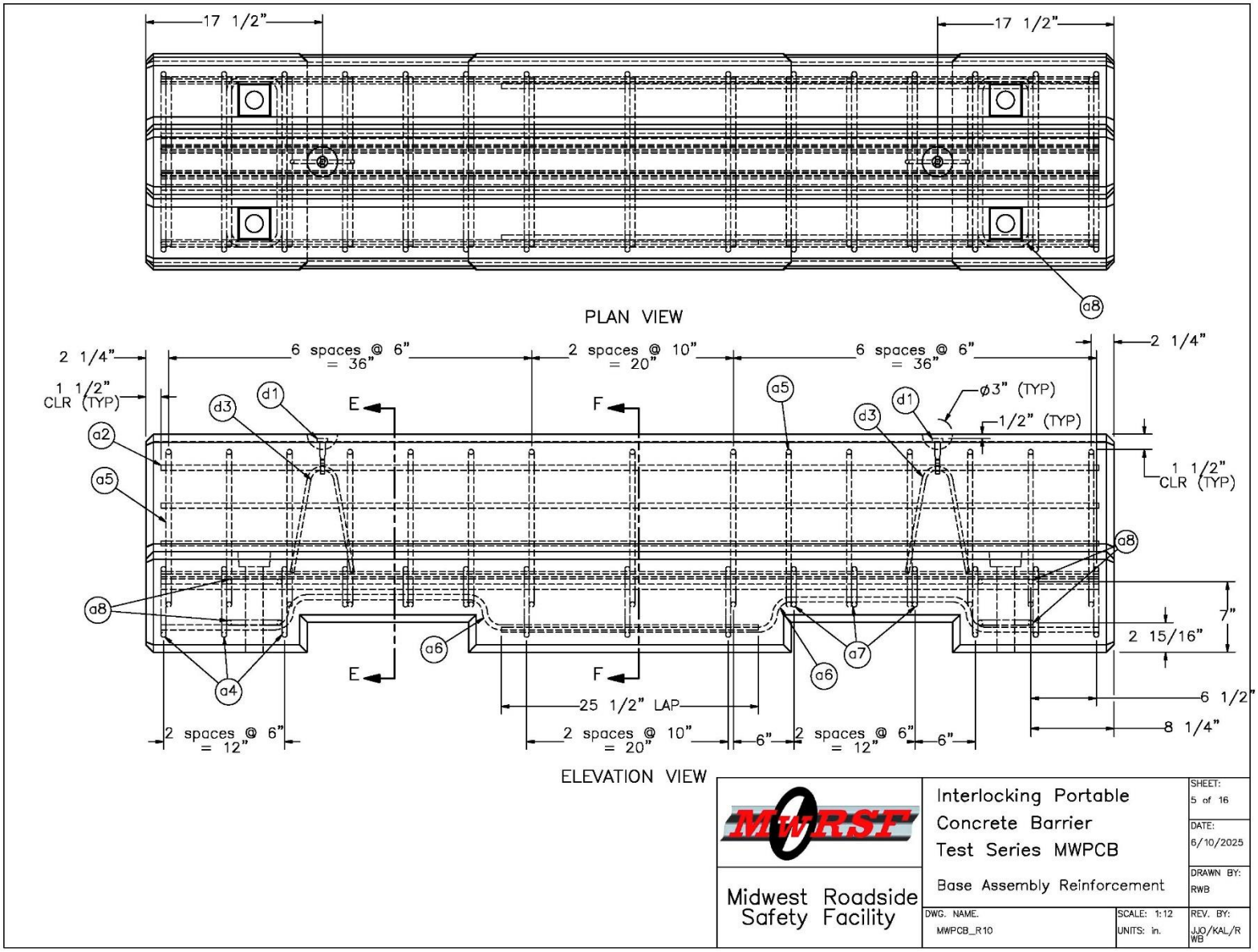

Figure 68. Staggered, Interlocking PCB Prototype, Base Assembly Reinforcement

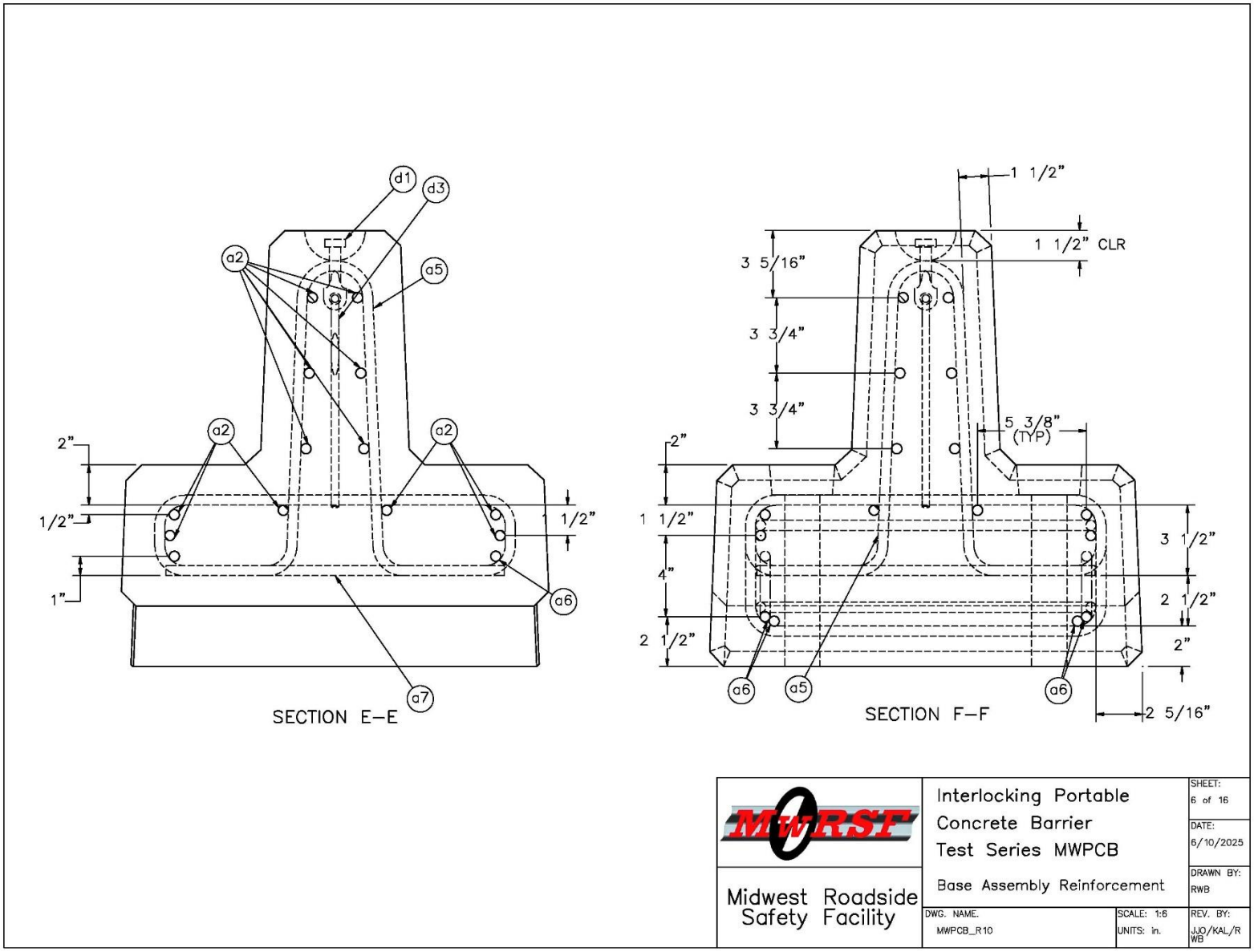

Figure 69. Staggered, Interlocking PCB Prototype, Base Assembly Reinforcement, Cont.

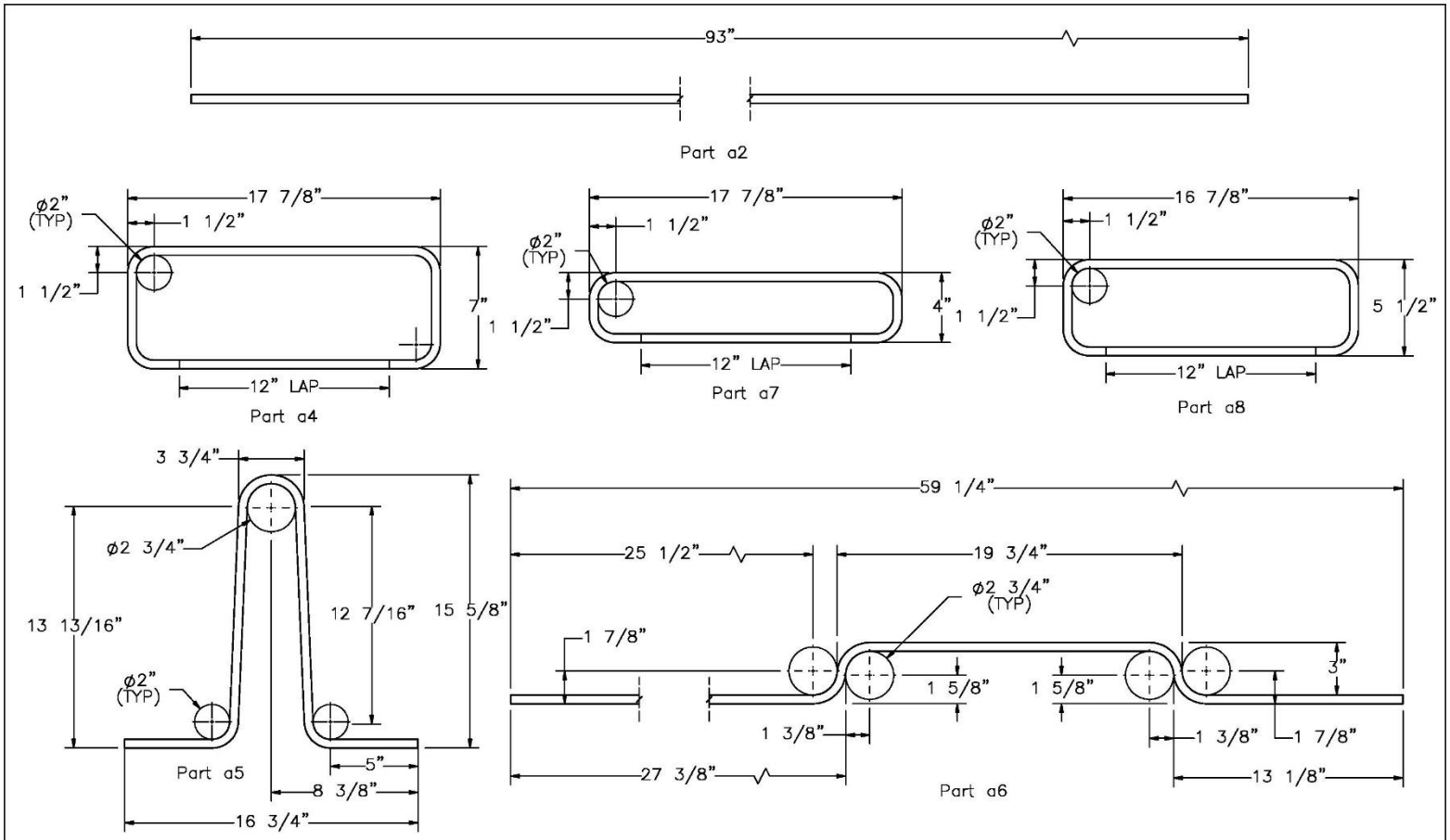

Bill of Bars					
Part No.	Bar No.	QTY.	Lap Length	Unbent Length	Material Specification
a2	#4	12	–	–	ASTM A615 Gr. 80
a4	#4	9	12"	59"	ASTM A615 Gr. 80
a5	#4	15	–	43 5/8"	ASTM A615 Gr. 80
a6	#4	4	25 1/2"	62 1/2"	ASTM A615 Gr. 80
a7	#4	6	12"	53"	ASTM A615 Gr. 80
a8	#4	4	12"	55 3/8"	ASTM A615 Gr. 80

Note: (1) Quantities in Bill of Bars represents one segment.

Midwest Roadside Safety Facility

Interlocking Portable Concrete Barrier
Test Series MWPCB
Rebar Details

SHEET: 7 of 16
DATE: 6/10/2025
DRAWN BY: RWB
DWG. NAME. MWPCB_R10
SCALE: 1:8
UNITS: in.
REV. BY: JJO/KAL/RWB

Figure 70. Staggered, Interlocking PCB Prototype, Rebar Details

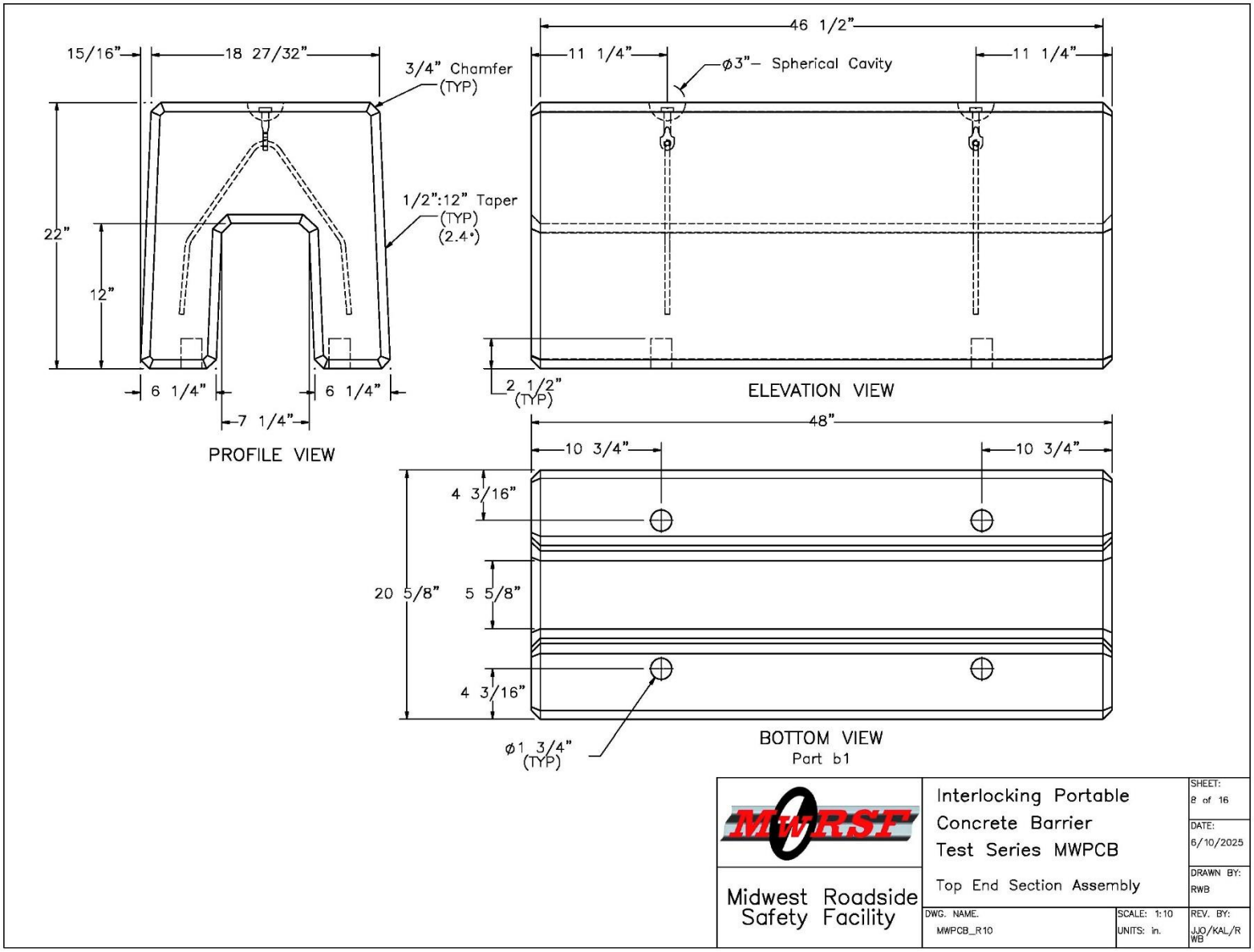

Figure 71. Staggered, Interlocking PCB Prototype, Top End Section Assembly

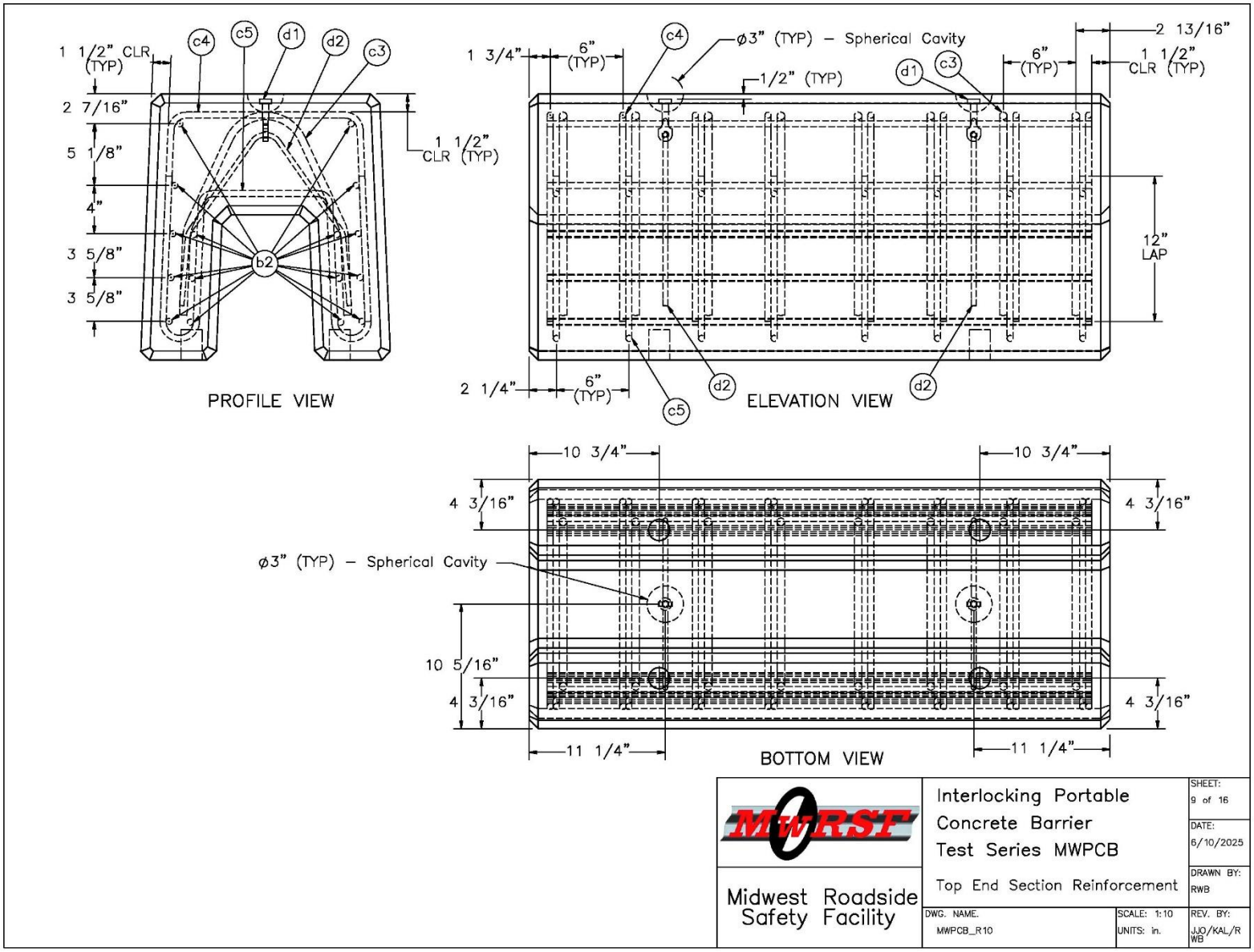

Figure 72. Staggered, Interlocking PCB Prototype, Top End Section Reinforcement

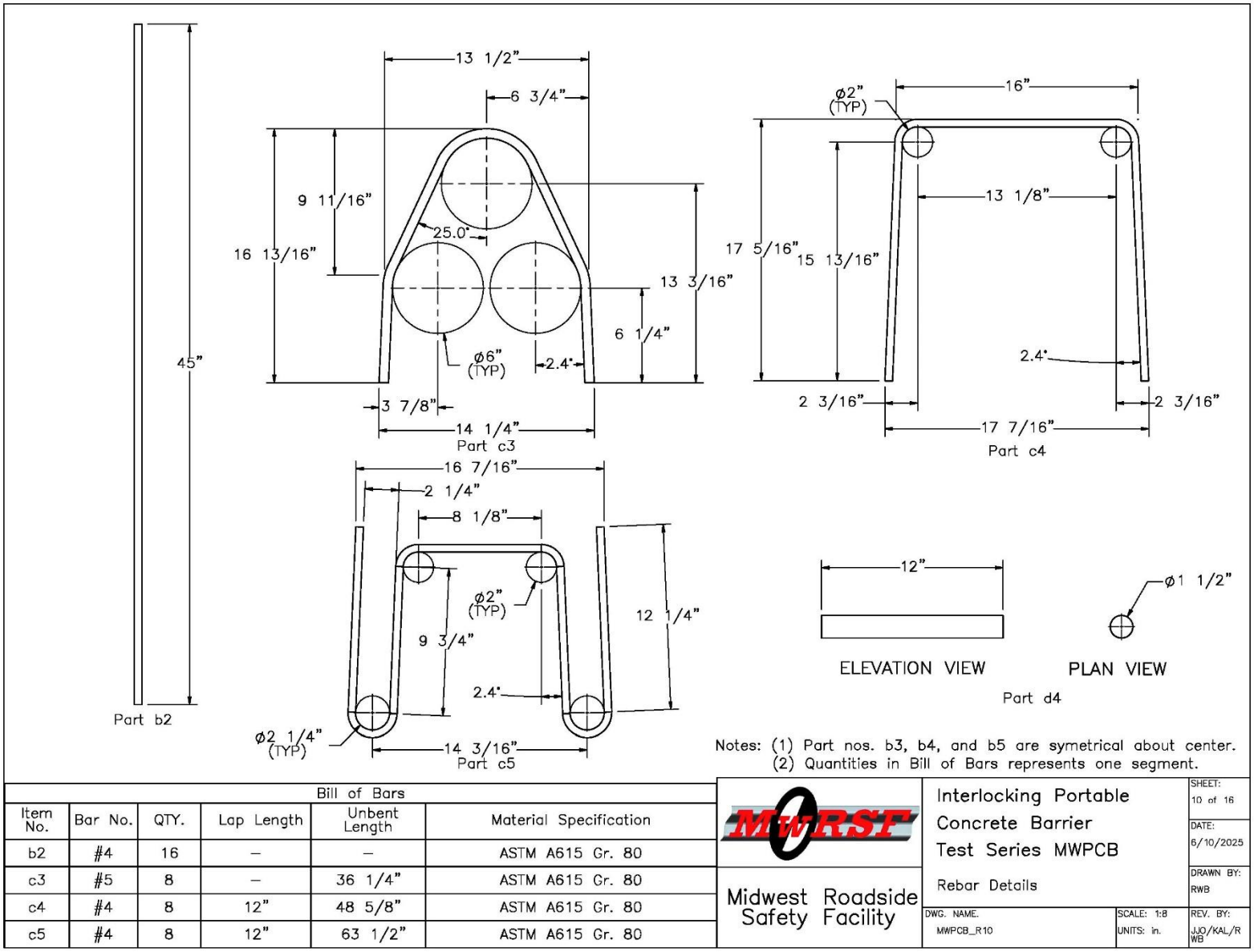

Bill of Bars

Item No.	Bar No.	QTY.	Lap Length	Unbent Length	Material Specification
b2	#4	16	–	–	ASTM A615 Gr. 80
c3	#5	8	–	36 1/4"	ASTM A615 Gr. 80
c4	#4	8	12"	48 5/8"	ASTM A615 Gr. 80
c5	#4	8	12"	63 1/2"	ASTM A615 Gr. 80

MwRSF

Midwest Roadside Safety Facility

Interlocking Portable Concrete Barrier
Test Series MWPCB
Rebar Details

SHEET: 10 of 16
DATE: 6/10/2025
DRAWN BY: RWB
DWG. NAME. MWPCB_R10
SCALE: 1:8
UNITS: in.
REV. BY: JJO/KAL/RWB

Figure 73. Staggered, Interlocking PCB Prototype, Rebar Details

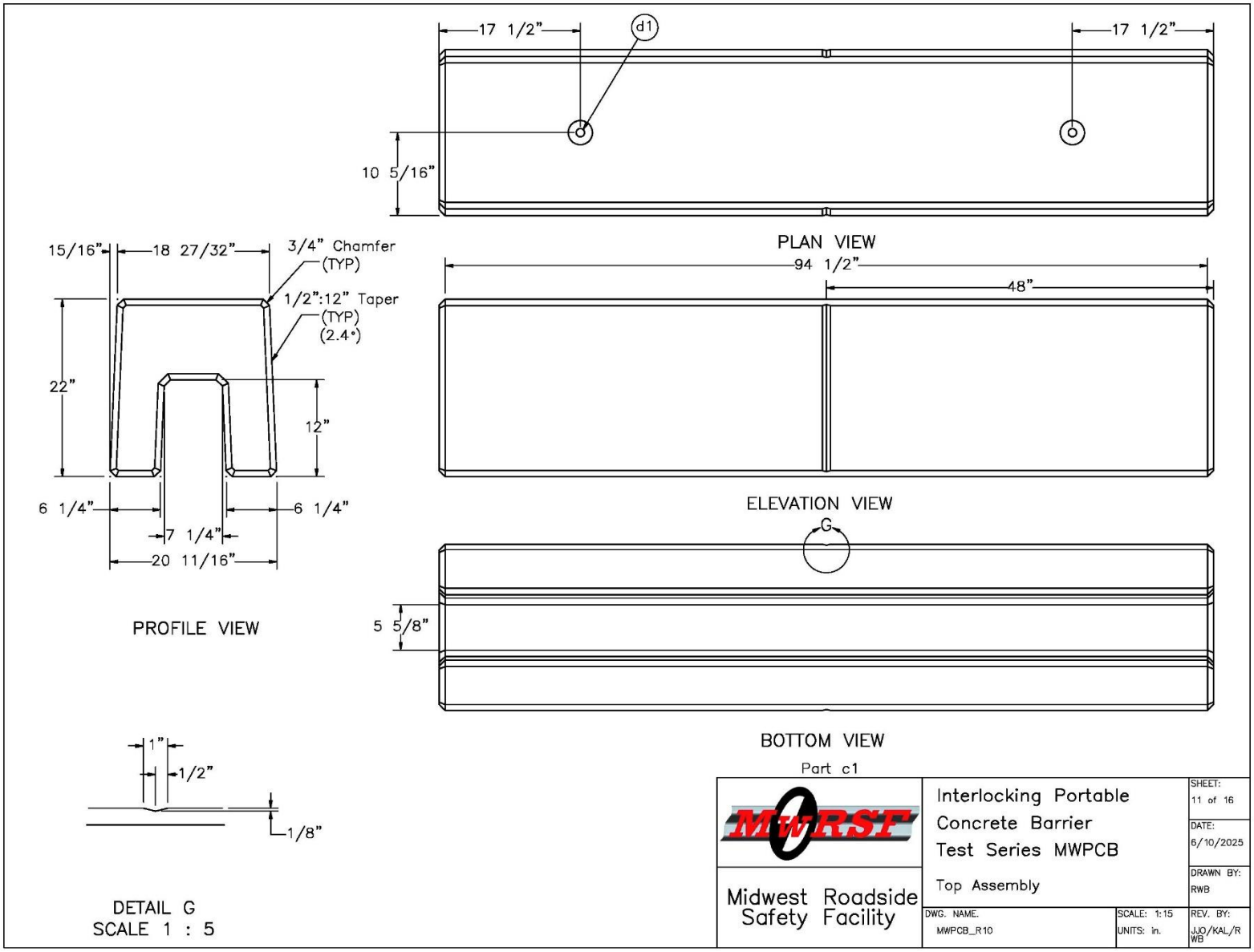

Figure 74. Staggered, Interlocking PCB Prototype, Top Assembly

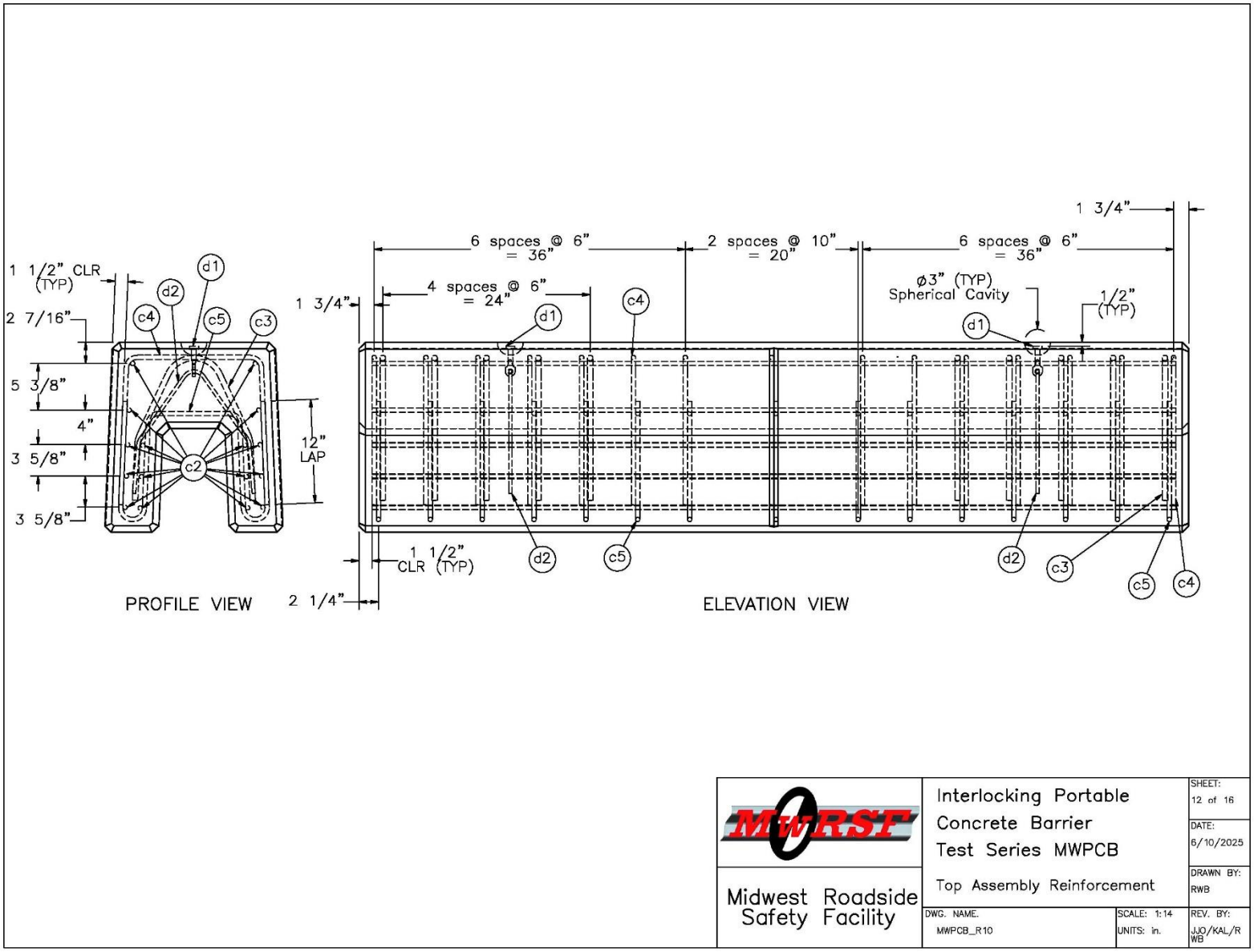

Figure 75. Staggered, Interlocking PCB Prototype, Top Assembly Reinforcement

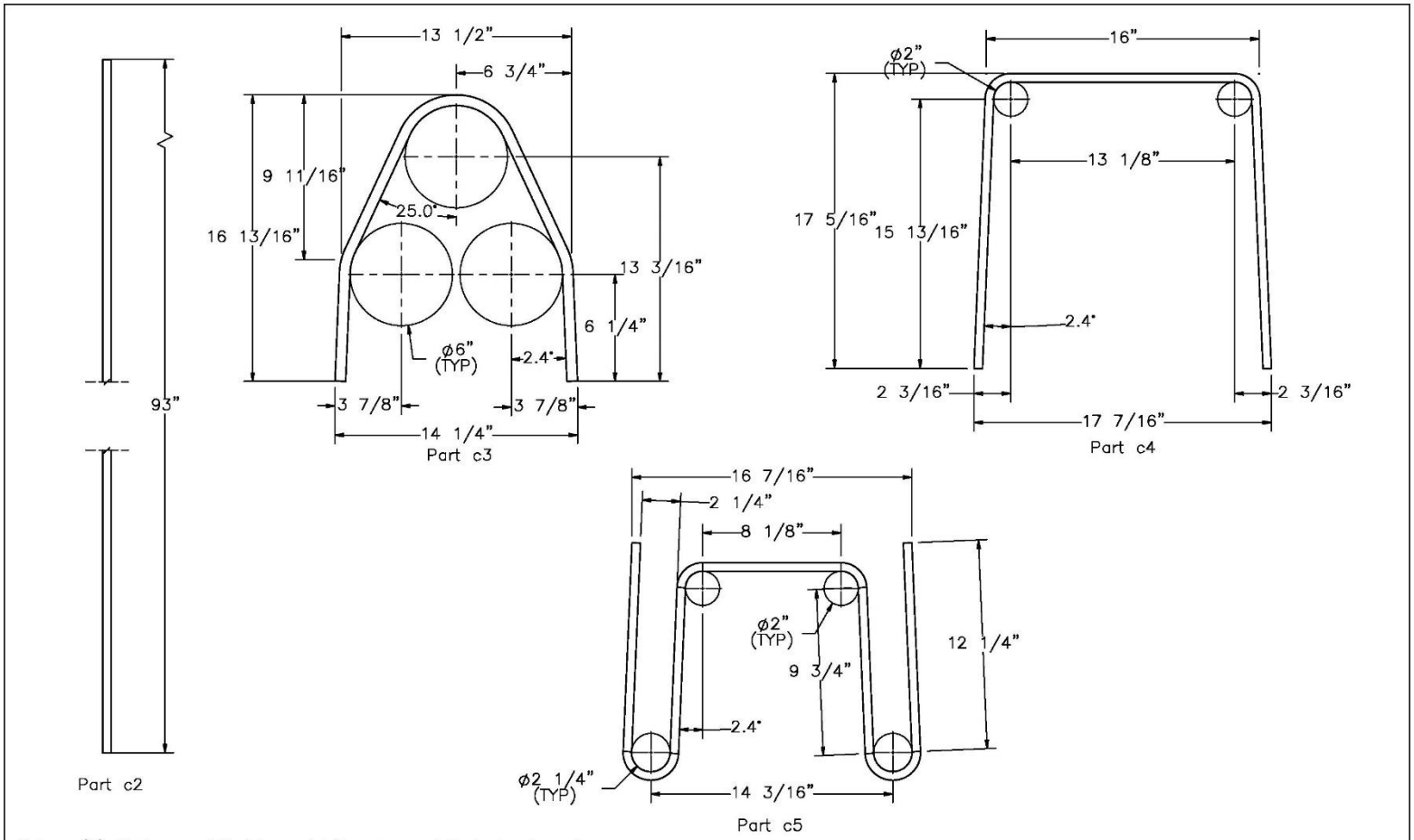

Notes: (1) Part nos. b3, b4, and b5 are symetrical about center.
(2) Quantities in Bill of Bars represents one segment.

Bill of Bars

Item No.	Bar No.	QTY.	Lap Length	Unbent Length	Material Specification
c2	#4	16	–	–	ASTM A615 Gr. 80
c3	#5	10	–	36 1/4"	ASTM A615 Gr. 80
c4	#4	15	12"	48 5/8"	ASTM A615 Gr. 80
c5	#4	15	12"	63 1/2"	ASTM A615 Gr. 80

MwRSF
Midwest Roadside Safety Facility

Interlocking Portable Concrete Barrier
Test Series MWPCB
Rebar Details

SHEET: 13 of 16
DATE: 6/10/2025
DRAWN BY: RWB
DWG. NAME. MWPCB_R10
SCALE: 1:8
UNITS: in.
REV. BY: JJO/KAL/RWB

Figure 76. Staggered, Interlocking PCB Prototype, Rebar Details

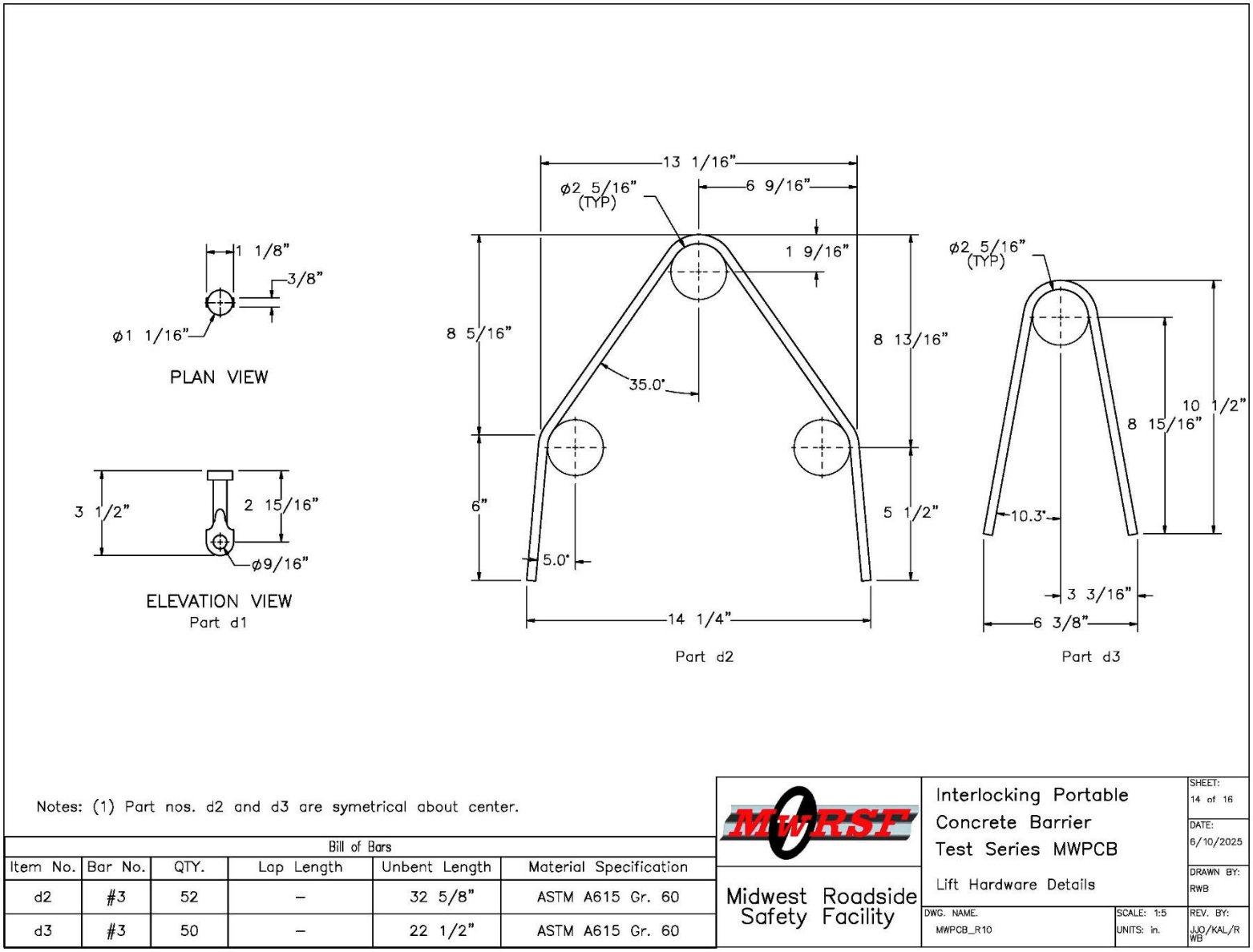

Figure 77. Staggered, Interlocking PCB Prototype, Lift Hardware Details

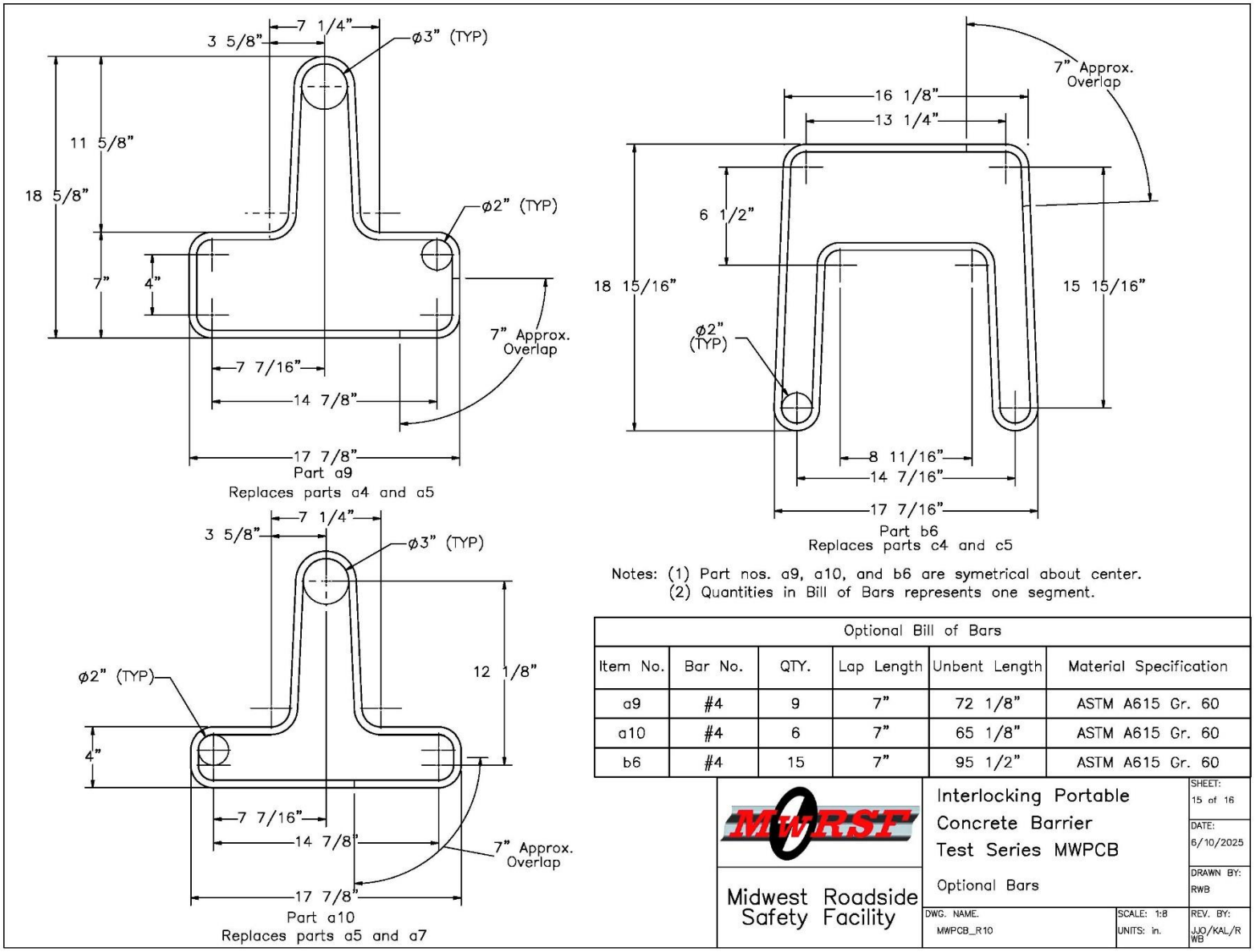

Optional Bill of Bars

Item No.	Bar No.	QTY.	Lap Length	Unbent Length	Material Specification
a9	#4	9	7"	72 1/8"	ASTM A615 Gr. 60
a10	#4	6	7"	65 1/8"	ASTM A615 Gr. 60
b6	#4	15	7"	95 1/2"	ASTM A615 Gr. 60

Figure 78. Staggered, Interlocking PCB Prototype, Optional Bars

Item No.	QTY.	Description	Material Specification	Treatment Specification
a1	25	Reinforced Concrete Bottom Assembly	Min f'c = 5,000 psi	–
a2	300	#4 Rebar, 93" Total Length	ASTM A615 Gr. 80	–
a4	225	#4 Rebar, 59" Total Unbent Length	ASTM A615 Gr. 80	–
a5	375	#4 Rebar, 43 5/8" Total Unbent Length	ASTM A615 Gr. 80	–
a6	100	#4 Rebar, 62 1/2" Total Unbent Length	ASTM A615 Gr. 80	–
a7	150	#4 Rebar, 53" Total Unbent Length	ASTM A615 Gr. 80	–
a8	100	#4 Rebar, 55 3/8" Total Unbent Length	ASTM A615 Gr. 80	–
b1	2	Reinforced Concrete End Section	Min f'c = 5,000 psi	–
b2	32	#4 Rebar, 45" Total Length	ASTM A615 Gr. 80	–
c3	16	#5 Rebar, 36 1/4" Total Unbent Length	ASTM A615 Gr. 80	–
c4	16	#4 Rebar, 48 5/8" Total Unbent Length	ASTM A615 Gr. 80	–
c5	16	#4 Rebar, 63 1/2" Total Unbent Length	ASTM A615 Gr. 80	–
c1	24	Reinforced Concrete Top Assembly	Min f'c = 5,000 psi	–
c2	384	#4 Rebar, 93" Total Length	ASTM A615 Gr. 80	–
c3	240	#5 Rebar, 36 1/4" Total Unbent Length	ASTM A615 Gr. 80	–
c4	360	#4 Rebar, 48 5/8" Total Unbent Length	ASTM A615 Gr. 80	–
c5	360	#4 Rebar, 63 1/2" Total Unbent Length	ASTM A615 Gr. 80	–
d1	102	Meadow Burke DB–53 Dogbone Eye Anchor	2–Ton	Hot–Dip Galvanized
d2	52	DB–53 Dogbone Rebar Reinforcing Pin – 2 Ton	ASTM A615 Gr. 60	–
d3	50	DB–53 Dogbone Rebar Reinforcing Pin – 2 Ton	ASTM A615 Gr. 60	–
d4	4	1 1/2" Dia., 12" Total Length Pin	ASTM A36	–

Midwest Roadside Safety Facility

Interlocking Portable Concrete Barrier
Test Series MWPCB
Bill of Materials

SHEET: 16 of 16
DATE: 6/10/2025
DRAWN BY: RWB
DWG. NAME. MWPCB_R10
SCALE: 1:768
UNITS: in.
REV. BY: JJO/KAL/RWB

Figure 79. Staggered, Interlocking PCB Prototype, Bill of Materials

Figure 80. Staggered, Interlocking PCB Prototype Photographs

Figure 81. Staggered, Interlocking PCB Prototype Photographs

Figure 82. Staggered, Interlocking PCB Prototype Photographs

Figure 83. Staggered, Interlocking PCB Prototype Photographs

7 SUMMARY AND CONCLUSIONS

This research effort focused on the development of a new MASH TL-3 portable barrier system that addressed issues with existing portable barriers in terms of excessive dynamic deflection and compromised vehicle stability. The new portable barrier design was also intended to allow for ease of installation and limit the use of additional connection hardware while providing durability and adequate service life.

The design effort began with a review of portable barrier concepts developed during an initial feasibility study and relevant design criteria for use in further development of preferred designs. Once the design criteria were firmly established, project sponsors were asked to provide input on the preferred barrier design for development into a functional barrier prototype. A near-vertical PCB comprised of staggered, interlocking barrier segments was selected for development based on its perceived ease of installation and its potential to significantly reduce dynamic barrier deflections under impact loading.

An initial design concept was configured based on the design criteria, and LS-DYNA computer simulation analysis was used to estimate the potential safety performance of the PCB and suggest design refinements. The simulation analysis investigated various reinforcement configurations, the effect of segment length on barrier performance, and evaluated if longitudinal gaps between barrier segments had an adverse consequence on barrier performance. The simulation effort determined that the staggered, interlocking PCB concept had the potential to meet MASH TL-3 while significantly lowering dynamic barrier deflections below 24 in. The computer simulation analysis was used to determine a structural reinforcement configuration for the barrier segments. Four reinforcement options were simulated and reviewed. The Option 1 reinforcement configuration with Grade 80 bars was selected for use in the design prototypes as that reinforcement configuration provided sufficient structural capacity to limit barrier damage during impact and provide adequate durability and robustness. A barrier segment length of 8 ft was selected for the final design based on a compromise between barrier dynamic deflection and a desire to accommodate reasonable horizontal curvatures in operation. It was noted that full-scale testing and evaluation of the barrier system with the shortest barrier segment length would represent the most critical barrier configurations, and the potential for the use of longer barrier segments would exist in the future if desired. End gaps between the barrier segments up to 1 in. long demonstrated no safety issues for the barrier system.

The proposed staggered, interlocking PCB design was further refined for implementation with consideration of drainage slots, lifting hardware, future anchorage options, and development of end barrier segments. Additionally, input from fabricators was incorporated into the design that aided in refinement of the structural reinforcement and other minor improvements.

Complete design details for the prototype barrier design were developed, the design was provided to a fabricator for construction, and design prototypes were received. A follow-on research effort funded by the Midwest Pooled Fund Program plans to conduct MASH test designation nos. 3-10 and 3-11 on the PCB design to evaluate its performance. The results of that testing and evaluation will be provided in a subsequent report.

8 REFERENCES

1. *Manual for Assessing Safety Hardware (MASH), Second Edition*, American Association of State Highway and Transportation Officials (AASHTO), Washington, D.C., 2016.

2. Ross, H.E., Sicking, D.L., Zimmer, R.A., and Michie, J.D., *Recommended Procedures for the Safety Performance Evaluation of Highway Features*, National Cooperative Highway Research Program (NCHRP) Report 350, Transportation Research Board, Washington, D.C., 1993.

3. Mak, K.K. and Sicking, D.L., *Rollover Caused by Concrete Safety Shaped Barrier Volume 1 – Technical Report*, Report No. FHWA-RD-88-219, Texas Transportation Institute (TTI), Texas A&M University, College Station, Texas, January 1989.

4. Strashny, A., *An Analysis of Motor Vehicle Rollover Crashes and Injury Outcomes*, Report No. DOT HS 810 741, National Center for Statistics and Analysis (NCSA), National Highway Traffic Safety Administration (NHTSA), Washington, D.C., March 2007.

5. Rosenbaugh, S.K., Sicking, D.L., and Faller, R.K., *Development of a TL-5 Vertical Face Concrete Median Barrier Incorporating Head Ejection Criteria*, Final Report to the Midwest State's Regional Pooled Regional Pooled Fund Program, Transportation Research Report No. TRP-03-194-07, Project No.: SPR-3(017), Project Code: RPFP-05-01 - Year 15, Midwest Roadside Safety Facility, University of Nebraska-Lincoln, December 10, 2007.

6. Bielenberg, R.W., Lingenfelter, J.L., Stolle, C.S., Ruskamp, R.J., and Pajouh, M.A., *Development of a New, MASH 2016 TL-3 Portable Barrier System – Phase I*, MwRSF Final Report No. TRP-03-460-22, TPF-5 (193) Supplement #137, Midwest Roadside Safety Facility, University of Nebraska – Lincoln, Lincoln, NE, April 19. 2022.

7. AASHTO, *AASHTO LRFD Bridge Design Specifications*, 9th Edition, Washington, D.C., 2020.

8. Polivka, K.A., Faller, R.K., Sicking, D.L., Rohde, J.R., Bielenberg, R.W., Reid, J.D., and Coon, B.A., *Performance Evaluation of the Free-Standing Temporary Barrier – Update to NCHRP 350 Test No. 3-11 with 28" C.G. Height (2214TB-2)*, Report No. TRP-03-174-06, Midwest Roadside Safety Facility (MwRSF), University of Nebraska-Lincoln, Lincoln, Nebraska, October 12, 2006.

9. Hallquist, J.O., *LS-DYNA Keyword User's Manual*, Livermore Software Technology Corporation, Livermore, California, 2007.

10. Loken, A.E., *Bridge Deck Overhang Design: Effective Vehicle Impact Loads, Ultimate Strength, and Implications on Bridge Rail Performance*, Dissertation, University of Nebraska Civil Engineering, Advisor: Dr. Joshua Steelman, December, 2024.

11. Steelman et al., *NCHRP Research Report 1078: MASH Railing Load Requirements for Bridge Deck Overhang*, National Academies of Science, Engineering, and Medicine, Washington, D.C., 2023.

12. Bligh, R.P., Sheikh, N.M., Menges, W.L., and Haug, R.R., *Development of Low-Deflection Precast Concrete Barrier*, Report No. 0-4162-3, Texas Transportation Institute, College Station, TX, January 2005.

13. Bielenberg, R.W., Quinn, T.E., Faller, R.K., Sicking, D.L., and Reid, J.D., *Development of a Retrofit, Low-Deflection, Temporary Concrete Barrier System*, Final Report to the Wisconsin Department of Transportation, Report No. TRP 03-295-14, Midwest Roadside Safety Facility, University of Nebraska-Lincoln, Lincoln, Nebraska, March 31, 2014.

14. Bielenberg, R.W., Meyer, D.T., Faller, R.K., and Reid, J.D., *Length of Need and Minimum System Length for F-Shape Portable Concrete Barrier*, Draft Report No. TRP-03-337-16, Midwest Roadside Safety Facility, UNL, Lincoln, Nebraska, November 2016.

15. *2018 Dodge Ram 1500 FE Detailed Mesh Model v3 Validation*, Center for Collision Safety and Analysis, George Mason University, Washington, D.C., model released May 2022. https://www.ccsa.gmu.edu/wp-content/uploads/2022/05/2018-dodge-ram-detailed-validation-v3.pdf

16. Bielenberg, R.W., Yoo, S., Faller, R.K., and Urbank, E.L., *Crash Testing and Evaluation of the HDOT 34-in. Tall, Aesthetic Concrete Bridge Rail: MASH Test Designation Nos. 3-10 and 3-11*, Final Report to the Hawaii Department of Transportation, Transportation Research Report No. TRP-03-420-19, Project Number 67167, Midwest Roadside Safety Facility, University of Nebraska-Lincoln, Lincoln, Nebraska, October 21, 2019.

17. Bielenberg, R.W., Dowler, N.T., Faller, R.K., and Urbank, E.L., *Crash Testing and Evaluation of the HDOT 42-in. Tall, Aesthetic Concrete Bridge Rail: MASH Test Designation Nos. 3-10 and 3-11*, Final Report to the Hawaii Department of Transportation, Transportation Research Report No. TRP-03-424-20, Project Number 67167, Midwest Roadside Safety Facility, University of Nebraska-Lincoln, Lincoln, Nebraska, January 9, 2020.

18. Bielenberg, R.W., Asselin, N.M., and Faller, R.K., *MASH TL-3 Evaluation of Concrete and Asphalt Tied-Down Anchorage for Portable Concrete Barrier*, Final Report to the Wisconsin Department of Transportation, Transportation Research Report No. TRP-03-386-19, Project No.: TPF(193) Supplement #114, Midwest Roadside Safety Facility, University of Nebraska-Lincoln, Lincoln, Nebraska, April 12, 2019.

19. Bielenberg, R.W., Hinojosa, M.A., Faller, R.K., and Bai, F., *Modification and MASH 2016 TL-3 Evaluation of the Asphalt Pin Tie-Down for F-Shape PCB*, Final Report to the Wisconsin Department of Transportation, Transportation Research Report No. TRP-03-428-21, Project No.: TPF-5(193) Supplement #136, Midwest Roadside Safety Facility, University of Nebraska-Lincoln, Lincoln, Nebraska, August 23, 2021.

20. Perry, B.J., Wilson, T.T., Bielenberg, R.W., and Faller, R.K., *Modification and Evaluation of the Asphalt Pin Tie-Down for F-shape PCB: Test No. WITD-4*, Final Report to the Midwest Pooled Fund Program, Transportation Research Report No. TRP-03-488-24, Project No.: TPF-5(430) Supplement #16, Midwest Roadside Safety Facility, University of Nebraska-Lincoln, Lincoln, Nebraska, December 17, 2024.

END OF DOCUMENT